LUND UNIVERSITY

Advancing the understanding of pilot ignition in dual fuel engines

Experimental and conceptual studies

Merts, Menno

2022

Link to publication

Citation for published version (APA):
Merts, M. (2022). *Advancing the understanding of pilot ignition in dual fuel engines: Experimental and conceptual studies*. Division of Combustion Engines, Lund Institute of Technology.

Total number of authors:
1

General rights
Unless other specific re-use rights are stated the following general rights apply:
Copyright and moral rights for the publications made accessible in the public portal are retained by the authors and/or other copyright owners and it is a condition of accessing publications that users recognise and abide by the legal requirements associated with these rights.
- Users may download and print one copy of any publication from the public portal for the purpose of private study or research.
- You may not further distribute the material or use it for any profit-making activity or commercial gain
- You may freely distribute the URL identifying the publication in the public portal

Read more about Creative commons licenses: https://creativecommons.org/licenses/

Take down policy
If you believe that this document breaches copyright please contact us providing details, and we will remove access to the work immediately and investigate your claim.

LUND UNIVERSITY

PO Box 117
221 00 Lund
+46 46-222 00 00

Advancing the understanding of pilot ignition in dual fuel engines

Experimental and conceptual studies

MENNO MERTS | DIVISION OF COMBUSTION ENGINES
DEPARTMENT OF ENERGY SCIENCES | LUND UNIVERSITY, 2022

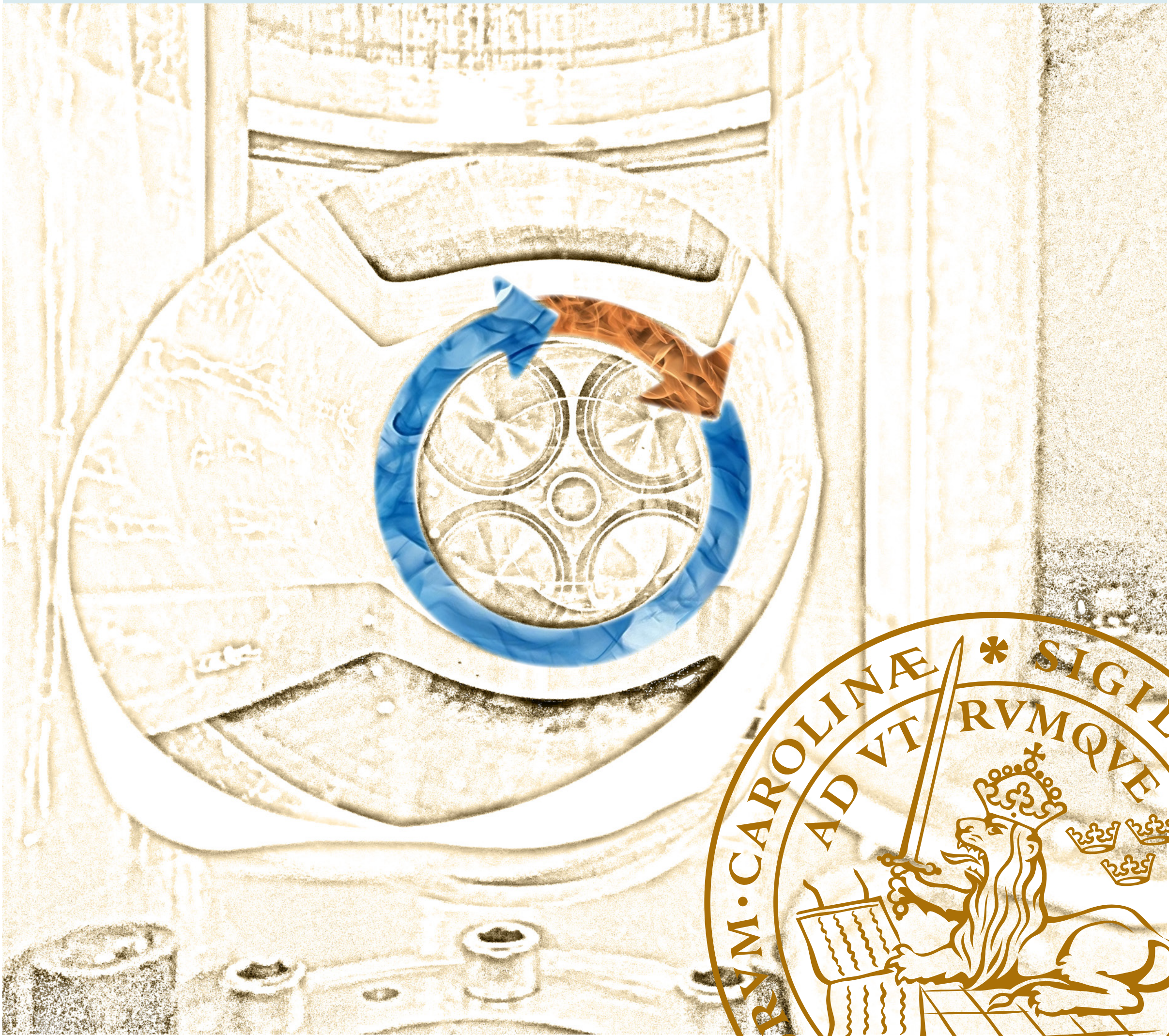

Advancing the understanding of pilot ignition in dual fuel engines

Advancing the understanding of pilot ignition in dual fuel engines

Experimental and conceptual studies

by Menno Merts

DOCTORAL DISSERTATION

Doctoral dissertation for the degree of Doctor of Philosophy (PhD) at the Faculty of Engineering at Lund University to be publicly defended on 15th of June 2022 at 10.15 in KC:A Hall, Department of Chemistry, Naturvetarvägen 18 Lund

Faculty opponent
Dr. Cinzia Tornatore

Organization
LUND UNIVERSITY

Department of Energy Sciences
Box 188
SE-221 00 Lund

Author
Menno Merts

Document name
Doctoral Dissertation

Date of disputation
2022-06-15

Sponsoring organizations
KCFP Engine Research Center
Interreg Deutschland Nederland
HAN University of Applied Sciences

Title and subtitle Advancing the understanding of pilot ignition in dual fuel engines:
Experimental and conceptual studies

Abstract

The energy transition is looking for new technologies to reduce CO_2 emissions. One of the promising options is the dual fuel engine. In this concept, based on a diesel engine, a small pilot diesel injection is used to ignite a second fuel. This second fuel can be a low carbon or renewable high-octane fuel, that otherwise could not be applied in a diesel engine. Good results on emissions and efficiency are reported for this concept, but there is still room for improvement. This study worked on advancing the understanding of the dual fuel engine

Research on a dual fuel truck engine showed what could be achieved, and where limitations are seen. One of the limitations, cylinder to cylinder variation, was investigated. It could be explained making use of experiments and 1D simulations. The cause was found in exchange of injected fuel in the intake port, through the manifold. This resulted in enrichment of downstream cylinders, with fuel from the cylinders at the begin of the intake manifold.

In a next stage, optical research was performed on a dual fuel marine engine. Here it was shown how the combustion could run in two different modes, Conventional Dual Fuel (CDF) and Reactivity Controlled Compression Ignition (RCCI). A fundamental difference in control mechanism was found between the two modes, where advancing the pilot results in earlier combustion in CDF mode, and in later combustion in RCCI mode. Initiated by a different pilot injection timing, a significant difference in dilution of the pilot fuel was seen in RCCI. This results in a more graduate heat release, which is known to create lower NO_x emission.

Since the optical campaign did not allow emission measurements, a second campaign was performed on a standard configuration. This indeed showed that with the RCCI combustion, created by a very early pilot timing, extremely low NO_x emissions could be achieved. However, this reduction of polluting emissions came with an increase in the emission of uncombusted methane, which is a strong greenhouse gas. An optimum was found at late RCCI combustion, close to the transition to CDF, combining low emissions with a high efficiency.

The position of the found optimum, and the limited availability of explanation of the operational differences between the combustion modes led to the creation of a conceptual model. It describes how the start of combustion is related to the pilot injection timing. It explains how in CDF mode the combustion can start after a short ignition delay, in which the liquid pilot fuel is diluted just enough to be ignitable. This gives an almost constant relation between the injection timing and the start of combustion. In RCCI mode the pilot fuel is injected much earlier, resulting in a much higher dilution. As a consequence, a higher temperature and pressure are required to start combustion. This explains why advancing the injection in this mode results in a later start of combustion and vice-versa. The higher dilution created by earlier injection requires ignition conditions that occur later in the engine cycle.

All in all, the found optima and insights should help to run engines effectively in dual fuel mode. This allows the usage of renewable high-octane fuels in widely available diesel engines. In this way the transition towards sustainable transport can be strongly accelerated, without the need for high investments in electric infrastructure, depleting the world's rare minerals and replacing the complete engine ecosystem.

Key words
Combustion engines, Dual fuel, RCCI, Pilot injection, Renewable fuels, Conceptual model, LTC, Heavy duty, Marine, Start of combustion, Optical engine research.

Classification system and/or index terms (if any)

Supplementary bibliographical information	**Language** English
ISSN and key title 0282-1990	**ISBN** 978-91-8039-257-0 (electronic) 978-91-8039-258-7 (print)

Recipient's notes	**Number of pages** 180	Price
	Security classification	

I, the undersigned, being the copyright owner of the abstract of the above-mentioned dissertation, hereby grant to all reference sources permission to publish and disseminate the abstract of the above-mentioned dissertation.

Signature

Date 2022-05-05

Advancing the understanding of pilot ignition in dual fuel engines

Experimental and conceptual studies

by Menno Merts

LUND
UNIVERSITY

A doctoral thesis at a university in Sweden takes either the form of a single, cohesive re-search study (monograph) or a summary of research papers (compilation thesis), which the doctoral student has written alone or together with one or several other author(s).

In the latter case the thesis consists of two parts. An introductory text puts the research work into context and summarizes the main points of the papers. Then, the research publications themselves are reproduced, together with a description of the individual contributions of the authors. The research papers may either have been already published or are manuscripts at various stages (in press, submitted, or in draft).

Cover illustration: a view inside the optical engine in TC12 at Lund University. Arrows representing circularity and the combustion of high-reactivity fuel and natural gas.

© Menno Merts

Faculty of Engineering, Department of Energy Sciences

ISBN: 978-91-8039-258-7 (print)
ISBN: 978-91-8039-257-0 (electronic)
ISRN: LUTMDN/TMHP-22/1168-SE
ISSN: 0282-1990

Printed in Sweden by Media-Tryck, Lund University
Lund 2022

NORDIC SWAN ECOLABEL
Printed matter
3041 0903

Media-Tryck is a Nordic Swan Ecolabel
certified provider of printed material.
Read more about our environmental
work at www.mediatryck.lu.se

MADE IN SWEDEN

Keep the engine, change the fuel

Acknowledgements

This PhD journey was an interesting journey. It took time, it took effort, it took attention and a fair bit of ‘normal’ life, but it was worth it. Looking back at the start, I think I’ve evolved in knowledge, skills and mentality. Improving myself was the reason to start, so I can only be satisfied and grateful. During this trajectory it became more and more clear what an interesting era to work with combustion engines this is. One part of the world is convinced engines are a dying breed, while another part knows that we are in need for knowledge and manpower to make them cleaner, more efficient, and is fighting to have them run on renewable fuels. I’m part of the second group, and greedy to boost the development that is still ahead of us. Hopefully this PhD added a piece to it.

I want to thank Sebastian Verhelst, for making this PhD possible. It was a great move that you pointed me to Lund University, and I’m thankful for how you guided me into the advanced engine research world. I strongly appreciate the room you always gave me, to play around with my own ideas. You were always available for a discussion, but left it to me to conclude whether they were good (a few) or bad (a few more) ideas. This approach was not only inspirational and effective for my PhD research, but also turned me into another type of supervisor for my own students. I appreciate your knowledge, liked the chats on motorcycles, combustion, engines and cars, and am still deeply impressed by your spot-on questions and comments. You made Relevance into an art!

Thanks to everyone at the Combustion Engine division of Lund University. Marcus, you always made me feel welcome, and thanks for all the support, planning and fun, within and outside of the university. Nhut, thanks for making my research stay convenient by showing me the way in the university, and in Sweden in general. André, thanks for our fruitful Friday night biofuel meetings, one day we will have one in the Netherlands. Anders, thanks for all the hard and though work on TC12. This wasn’t the most easy engine around, but with your support so much was achieved. That engine brings me to Wärtsilä. The cooperation with Jari Hyvönen, Henrik Back and Jussi Sievänen was always nice and effective, a big thanks for making the medium speed work possible.

Without the support I received at HAN Automotive Research this whole PhD work would not even have started. Thanks Bram for pushing and allowing me, Peter Mesman for the LNG Pilots project and the guidance during the journey. A big thanks for Quintin, for our awesome engine activities, the clever discussions, and the always motivating cooperation we had. The rest of the people I worked with in the ARLA lab, within the research and within the educational department, thanks for your cooperation and taking tasks, allowing me to distribute my effort and attention.

Thanks for the friends and family who supported me. Whether it was by visiting me in Sweden, giving me feedback, or by coping with my lack of attention for everything not-PhD, it was highly appreciated. Much further goes what I feel for Maureen, and about her role during the last four years. Your support and the room you gave me was incredible. You gave me so much motivation, joy, and confidence; hartje ☺ .

Let’s finish this reflection with a few words about the Roaring Twenties in which I did most of my PhD. They started with a small cough resulting in a big impact on society. They brought a lot of misery and significantly limited possibilities. But this also made me realize that these were not the worst conditions for spending time in the engine lab and running Matlab at my desk like forever. And the working from home situation was not the worst condition to travel the PhD journey. Let’s see where the next journey goes…

Table of Contents

Acknowledgements .... **viii**

Popular scientific summary .... **xii**

Populärvetenskaplig sammanfattning .... **xiv**

Publiekssamenvatting .... **xvi**

Nomenclature .... **xviii**

List of publications .... **xxi**

1. Introduction **1**
- 1.1. Fuelling the climate change 1
- 1.2. Scope; Application of renewable fuels 6
- 1.3. Thesis contributions 7
- 1.4. Thesis outline 8

2. Combustion concepts for high-octane fuels **9**
- 2.1. Combustion modes 9
- 2.2. Running on high-octane fuel 12
- 2.3. Dual Fuel 15
- 2.4. Research motivation 20

3. Experimental studies **25**
- 3.1. Dual fuel on a heavy-duty engine 25
- 3.2. Cylinder to cylinder variations in a heavy-duty dual fuel engine ... 29
- 3.3. Optical campaign on Wärtsilä W20DF 34
- 3.4. Metal campaign on W20DF 48

4. Conceptual model **55**
- 4.1. From assumption to concept 55
- 4.2. Verification of the assumptions 60
- 4.3. Expanding on the conceptual model 66

5. Summary and conclusions **71**

5.1. Contributions 71
5.2. Outlook 72
References 75
Scientific publications 82

Popular scientific summary

The energy transition is looking for new technologies to reduce CO_2 emissions. One of the promising options is the dual fuel engine. In this concept, based on a diesel engine, a small pilot diesel injection is used to ignite a second fuel. This second fuel can be a low-carbon or renewable fuel, that otherwise could not be applied in a diesel engine. Because of the high availability of diesel engines, making them run on a renewable fuel has a high impact on sustainability. Good results on emissions and efficiency are reported for this concept, but there is still room for improvement. Hence, this study worked on advancing the understanding of the pilot ignition in the dual fuel engine. The goal is to come to a dual fuel engine with a minimum of pollutant and greenhouse gas emissions.

This PhD study started with the conversion of a truck engine to dual fuel. Research on this engine showed what could be achieved with dual fuel, and where limitations are seen. The gained experience paved the road to the next stage; doing research on a dual fuel marine engine. Where dual fuel for road transport is rather exotic, it is commercially available technology for large marine engines. This makes the further improvement of one of its benefits, low emissions, a relevant research topic.

The research work on this diesel / natural gas marine engine consisted out of three parts. The first part, doing optical research, was the most complicated to perform. Although the engine was already prepared for it, the complex setup that was needed for this research required a lot of dedication. It confirmed why optical research on large bore engines is such a novelty. Making use of a high-speed camera and a glass piston crown, it was possible to actually see how the dual fuel process develops in the combustion chamber. The campaign made clear that this combustion could be done in two different modes. The first one is known as Conventional Dual Fuel (CDF), where the start of combustion is highly similar to diesel ignition. The other one, Reactivity Controlled Compression Ignition (RCCI), a so-called low temperature combustion concept, is a hot topic in the engine research world. It aims at a low combustion temperature, to reach very low emissions. The optical campaign showed that the biggest difference is seen in the dilution of the pilot diesel injection. The parameter used to create one or the other mode was the timing of the pilot injection. The result was also measurable in the heat release of the combustion. In CDF combustion a strong initial peak from the pilot fuel is seen, which is known to create high NO_x emission. In RCCI mode this peak was absent.

Since the optical measurements did not allow emission measurements, a second campaign was performed. Here the engine was converted back to a standard configuration, in which emissions could be measured. A campaign was performed where, besides other parameters, the timing of the pilot injection was varied. This indeed showed that with the RCCI combustion, created by a very early pilot timing, extremely low NO_x emissions could be achieved. Unfortunately, this reduction of polluting emissions came with an increase in the emission of uncombusted methane, which is a very strong greenhouse gas. An optimum was found at late RCCI combustion, close to the transition to CDF, combining low emissions with a high efficiency.

The position of this found optimum, and the limited availability of explanation of the operational differences between the two combustion modes led to the creation of a conceptual model. It describes how the start of combustion is related to the injection timing. It explains how in CDF mode the combustion can start after a short ignition delay, in which the liquid pilot fuel is diluted just enough to be ignitable. This gives an almost constant relation between the injection timing and the start of combustion. In RCCI mode however, the pilot fuel is injected much earlier, resulting in a much higher dilution. As a consequence, a higher temperature and pressure are required to start combustion. This explains why advancing the injection in this mode results in a later start of combustion and vice-versa. The higher dilution created by earlier injection requires ignition conditions that occur later in the engine cycle.

All in all, the found optima and insights should help to run engines effectively in dual fuel mode. This allows the usage of renewable high-octane fuels in widely available diesel engines. In this way the transition towards sustainable transport can be strongly accelerated, without the need for high investments in electric infrastructure, depleting the world's rare minerals and replacing the complete engine ecosystem.

Populärvetenskaplig sammanfattning

Energiomställningen letar efter ny teknik för att minska CO_2-utsläppen. Ett lovande alternativ är dubbelbränslemotorn, dvs. dual fuel. I detta koncept, som utgår ifrån dieselmotorns principer, används en liten dieselinsprutning för att antända ett andra (högoktanigt) bränsle, som annars inte skulle kunna användas i en dieselmotor. Detta andra bränsle kan vara ett bränsle med lågt kolinnehåll, som i sin tur ger ett lågt koldioxidutsläpp eller det kan vara ett förnybart bränsle.. På grund av den höga tillgängligheten av dieselmotorer har det en stor inverkan på miljön att de kan drivas med ett förnybart bränsle. Dubbelbränslemotorn har visat goda resultat på utsläpp och effektivitet, men det finns fortfarande utrymme för förbättringar. Denna studie fokuseras på att förbättra förståelsen av antändningsprocessen i dubbelbränslemotorn. Det övergripande målet är att utveckla en dubbelbränslemotor med minimalt utsläpp av föroreningar och växthusgaser.

Denna doktorandstudie började med konvertering av en lastbilsmotor till att drivas på dubbla bränslen. Forskningen på denna motor visade vad som kan uppnås med dubbelbränslekonceptet, och vad begränsningar kan vara. Erfarenheterna från detta banade vägen till nästa steg; forskning på en marinmotor med två bränslen. Då dubbelbränsle för vägtransporter är ganska exotiskt, är det en kommersiellt tillgänglig teknik för stora marinmotorer. Detta gör den ytterligare förbättringen av en av dess fördelar, låga utsläpp, till ett relevant forskningsämne.

Forskningsarbetet på denna diesel/naturgas marinmotor bestod av tre delar. Den första delen, tillika den mest tidskrävande delen var att göra optiska mätningar. Det bekräftade varför optisk forskning på motorer med stora borrhål är en sådan nyhet. Med hjälp av optiska mötningar i kombination med en höghastighetskamera och en kolvkrona av glas var det möjligt att faktiskt se hur förbränningsprocessen utvecklas i förbränningskammaren. Kampanjen klargjorde att dubbelbränsleförbränning kunde göras i två olika lägen. Den första är känd som Conventional Dual Fuel (CDF), där förbränningsstarten i hög grad liknar dieseltändning. Den andra, Reactivity Controlled Compression Ignition (RCCI), ett så kallat lågtemperaturförbränningskoncept, som syftar till en låg förbränningstemperatur, för att nå mycket låga utsläpp av kväveoxider (NO_x). Parametern som användes för att skapa det ena eller andra läget var tidpunkten för pilotinsprutningen. Den optiska kampanjen visade att den största skillnaden mellan lägena syns i utspädningen av dieselinsprutningen. Resultatet var även mätbart i förbränningens värmeavgivningsprofil, vid CDF-förbränning ses en stark initial topp från dieselbränslet, vilket är känt för att skapa höga NO_x-utsläpp. I RCCI-läget saknades denna topp.

Eftersom de optiska mätningarna inte tillät avgasmätningar genomfördes en andra kampanj. Här konverterades motorn tillbaka till en standardkonfiguration, där utsläppen kunde mätas. En kampanj genomfördes där, primärt tidpunkten för dieselinjektionen varierades. Detta visade verkligen att med RCCI-förbränningen, skapad av en mycket tidig dieselinsprutning, kunde extremt låga NO_x-utsläpp uppnås. Tyvärr kom denna minskning av utsläpp med en ökning av utsläpp av oförbränd metan, som är en mycket stark växthusgas. Ett optimum hittades nära övergången från RCCI-förbränning till CDF, som kombinerar låga utsläpp med hög verkningsgrad. I detta skede saknades dock en förklaring till varför detta optimum fungerar bra, likaså saknades en beskriver som förklarar skillnaderna mellan de två förbräningslägena.

I försök att förklara detta skapandes en konceptuell modell, som beskriver hur förbränningsstarten är relaterad till insprutningstiden. Modellen visar hur förbränningen i CDF-läget kan starta efter en kort fördröjning från insprutning, där det flytande pilotbränslet späds ut precis tillräckligt för att vara antändbart. Detta ger ett nästan konstant förhållande mellan insprutningstidpunkten och förbränningens start. I RCCI-läget sprutas dock dieselbränslet in mycket tidigare, vilket resulterar i en mycket högre utspädning. Som en konsekvens krävs högre temperatur och tryck för att starta förbränningen. Detta förklarar varför en tidigareläggning av insprutningen i detta läge resulterar i en senare start av förbränning och vice versa. Dvs. den högre utspädningen som skapas av tidigare insprutning kräver antändningsförhållanden som inträffar senare i motorns cykel.

Sammantaget kan de funna insikterna hjälpa till att köra motorer effektivt i ett dubbelbränsleläge. Detta möjliggör användningen av förnybara högoktaniga bränslen i allmänt tillgängliga dieselmotorer. På så sätt kan övergången till hållbara transporter påskyndas kraftigt, utan att det krävs stora investeringar i infrastruktur.

Publiekssamenvatting

De energietransitie vraagt om nieuwe technologieën om de uitstoot van CO_2 te verminderen. Een van de veelbelovende opties is de dual fuel motor. In dit concept, gebaseerd op een dieselmotor, wordt een kleine pilot dieselinjectie gebruikt om een tweede brandstof te ontsteken. Deze tweede brandstof kan een koolstofarme of hernieuwbare brandstof zijn, die anders niet in een dieselmotor toegepast zou kunnen worden. Door het grote aantal dieselmotoren in industrie en transport heeft het toepassen van een hernieuwbare brandstof hierin een grote impact op duurzaamheid. Voor dit concept worden goede resultaten gerapporteerd op het gebied van emissies en efficiëntie, maar er is nog ruimte voor verbetering. Daarom is deze studie naar een verbeterd begrip van de pilot ontsteking in de dual fuel motor uitgevoerd. Het doel is om te komen tot een dual fuel motor met een minimum aan uitstoot van schadelijke emissies en broeikasgassen.

Dit promotieonderzoek begon met de ombouw van een vrachtwagenmotor naar dual fuel. Onderzoek naar deze motor liet zien wat er met dual fuel kan worden bereikt en waar de beperkingen liggen. De opgedane ervaring effende de weg naar de volgende fase; onderzoek doen naar een dual fuel scheepsmotor. Waar dual fuel voor het wegvervoer enigszins exotisch is, is het een commercieel beschikbare technologie voor grotere scheepsmotoren. Dit maakt het verder verbeteren van een van de voordelen, lage emissies, een relevant onderzoeksthema.

Het onderzoekswerk aan deze diesel/aardgas scheepsmotor bestond uit drie delen. Het eerste deel, optisch motor onderzoek, was het meest ingewikkeld om uit te voeren. Hoewel de motor er al op voorbereid was, vergde de complexe setup die nodig was voor dit onderzoek veel toewijding. Het bevestigde waarom optisch onderzoek in motoren met grote boring zo uniek is. Met behulp van een high-speed camera en een glazen zuigerbodem was het mogelijk om daadwerkelijk in de verbrandingskamer te kijken hoe het dual fuel proces verloopt. De metingen maakten duidelijk dat deze verbranding op twee verschillende manieren kan verlopen. De eerste staat bekend als Conventional Dual Fuel (CDF), waarbij het begin van de verbranding sterk lijkt op dieselverbranding. De andere, Reactivity Controlled Compression Ignition (RCCI), een zogenaamd lage temperatuur verbrandingsconcept, is een hot topic in de motoronderzoekswereld. Het concept streeft naar een lage verbrandingstemperatuur, om daarmee zeer lage emissies te bereiken. Uit de optische meetcampagne bleek dat het grootste verschil zit in de verdunning van de pilot dieselinjectie. De parameter die werd gebruikt om de ene of de andere modus te creëren, is de timing van de pilot injectie. Het resultaat was ook meetbaar in de warmtevrijstelling van de verbranding. Bij CDF-verbranding is een sterke initiële piek van de pilot brandstof te zien, waarvan bekend is dat deze een hoge NO_x emissie veroorzaakt. In de RCCI-modus was deze piek afwezig.

Omdat in optische configuratie geen emissiemetingen mogelijk waren, werd een tweede meetcampagne uitgevoerd. Hiervoor is de motor weer omgebouwd naar een standaardconfiguratie, waarin emissies gemeten konden worden. Er werd een campagne uitgevoerd waarbij, naast andere parameters, de timing van de pilot-injectie werd gevarieerd. Dit toonde inderdaad aan dat met de RCCI-verbranding, gecreëerd door een zeer vroege pilot timing, extreem lage NO_x emissies bereikt kunnen worden. Helaas ging de vermindering van deze emissies gepaard met een toename van de uitstoot van onverbrand methaan, een zeer sterk broeikasgas. Een optimum werd gevonden bij de late RCCI-verbranding, dicht bij de overgang naar CDF, waarbij lage emissies worden gecombineerd met een hoog rendement.

De ligging van het gevonden optimum, en de beperkte beschikbaarheid van verklaringen voor de operationele verschillen tussen de twee verbrandingsmodi waren de aanleiding voor het ontwikkelen van een conceptueel model. Dit model beschrijft hoe de start van de verbranding gerelateerd is aan de injectie timing. Het legt uit hoe in CDF-modus de verbranding na een korte ontstekingsvertraging start, waarbij de geïnjecteerde pilot brandstof net genoeg wordt gemengd om ontvlambaar te zijn. Dit geeft een vrijwel constante relatie tussen het inspuitmoment en het begin van de verbranding. In RCCI-modus wordt de pilot brandstof echter veel eerder geïnjecteerd, wat resulteert in een veel sterkere verdunning. Als gevolg hiervan zijn een hogere temperatuur en druk nodig om de verbranding te starten. Dit verklaart waarom het vervroegen van de injectie in deze modus resulteert in een latere start van de verbranding en vice versa. De hogere verdunning die wordt gecreëerd door vroegere injectie, vereist voor ontsteking omstandigheden die later in de cyclus optreden.

Al met al moeten de gevonden optima en inzichten helpen om motoren effectief in dual fuel modus te laten draaien. Dit maakt het gebruik van hernieuwbare brandstoffen met een hoog octaangetal mogelijk in dieselmotoren. Op deze manier kan de transitie naar duurzaam vervoer sterk worden versneld, zonder dat er hoge investeringen in elektrische infrastructuur nodig zijn, de zeldzame mineralen wereldwijd worden uitgeput, en de complete motoren bedrijfssector vervangen hoeft te worden.

Nomenclature

aTDC	-	After Top Dead Centre
aTDC-F	-	After Top Dead Centre – Firing
BDC	-	Bottom Dead Centre
bTDC	-	Before Top Dead Centre
BEV	-	Battery Electric Vehicle
BMEP	-	Brake Mean Effective Pressure
CA50	-	Crank Angle at 50% heat release
CAD	-	Crank Angle Degree
CDC	-	Conventional Diesel Combustion
CDF	-	Conventional Dual Fuel
CFD	-	Computational Fluid Dynamics
CI	-	Compression Ignition
CO_2	-	Carbon dioxide
CNG	-	Compressed Natural Gas
DI	-	Direct Injection
ECU	-	Electronic Control Unit
EGR	-	Exhaust Gas Recirculation
EHVA	-	Electro Hydraulic Valve Actuation
EVC	-	Exhaust Valve Closed
EVO	-	Exhaust Valve Opened
FIE	-	Fuel Injection Equipment
FPGA	-	Field Programmable Gate Array
GER	-	Gas Energy Ratio
GHG	-	Green House Gas
GWP	-	Global Warming Potential
HCCI	-	Homogeneous Charge Compression Ignition
HRF	-	High-Reactivity Fuel
IMEP	-	Indicated Mean Effective Pressure
ICE		Internal Combustion Engine
IMO	-	International Maritime Organization
IVO	-	Inlet Valve Opening
IVC	-	Inlet Valve Closing
LRF	-	Low-Reactivity Fuel
LPG	-	Liquefied Propane Gas
LTC	-	Low-Temperature Combustion

NO_x	-	Nitrogen Oxides
PPC	-	Partly Premixed Combustion
PM	-	Particulate Matter
RCCI	-	Reactivity Controlled Compression Ignition
RDE	-	Real Driving Emissions
SACI	-	Spark Assisted Compression Ignition
SOC	-	Start of Combustion
SOI	-	Start Of Injection
STP	-	Standard Temperature and Pressure
TDC	-	Top Dead Centre
TTW	-	Tank To Wheel
uHC	-	Uncombusted HydroCarbons
WTW	-	Well To Wheel
γ	-	Ratio of specific heat capacities
λ	-	Air / fuel equivalence ratio
ϕ	-	Fuel / air equivalence ratio

List of publications

This thesis is based on the following publications, referred to by their Roman numerals:

I **Cylinder to Cylinder Variation Related to Gas Injection Timing on a Dual Fuel Engine**

M. Merts, Q. Pet, P. Mesman, and S. Verhelst
Published: SAE Technical Paper, 2019-01-1162

II **Literature Review on Dual Fuel Combustion Modelling**

M. Merts and S. Verhelst
Published: SAE Technical Paper 2019-24-0120

III **An optical investigation of dual fuel and RCCI pilot ignition in a medium speed engine**

M. Merts, S. Derafshzan, J. Hyvönen, M. Richter, M. Lundgren, and S. Verhelst
Published: Fuel Communications, vol. 9, p. 100037, 2021

IV **Conceptual model for the start of combustion timing in the range from RCCI to conventional dual fuel**

M. Merts, A. Fogué Robles, J. Monsalve-Serrano, A. Garcia, M. Lundgren, and S. Verhelst
Published: SAE Technical Paper 2022-01-0468

V **Experimental optimization of a medium speed Dual Fuel engine towards RCCI operation**

M. Merts, J. Hyvönen, B. Veenhuizen, M. Lundgren, and S. Verhelst,
Paper accepted for publication at Thiesel 2022, Valencia, Spain

1. Introduction

1.1. Fuelling the climate change

One of the biggest challenges of the 21st century is climate change. During the last decades this topic moved from a debated suspicion to a recognized reason for concern [1]. The main driver for the current global warming is the concentration of greenhouse gases in the atmosphere. Multiple biogenic and anthropogenic gases with a significant Global Warming Potential (GWP) play a role [2], but most attention goes to the increasing concentration of anthropogenic CO_2, as shown in Figure 1. The focus in mitigating climate change is on the reduction of CO_2 emissions. Energy-use related CO_2 emission is the largest contributor to climate change.

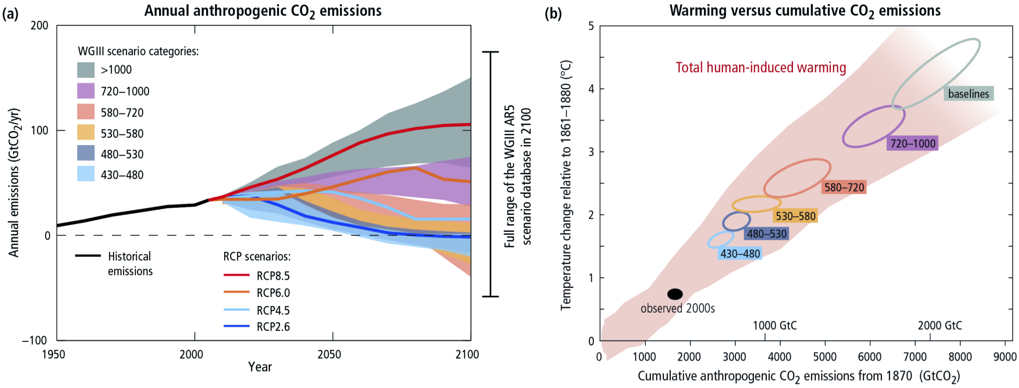

***Figure 1** CO2 emissions and global warming; historical evolution and future prediction. [3]*

The emission of CO_2 comes from a wide range of energy sources, where fossil fuels predominate. The continuous growth of earth's population and the increasing welfare of this population result in an ongoing increase of energy use. Figure 2 shows that fossil fuels (coal, natural gas, oil) are still dominant in worldwide energy supply. Also, the relation with (economic) welfare can be recognized by the only two dips in the development of total energy consumption. They can be attributed to the financial crisis in 2008 and the Corona crisis in 2020.

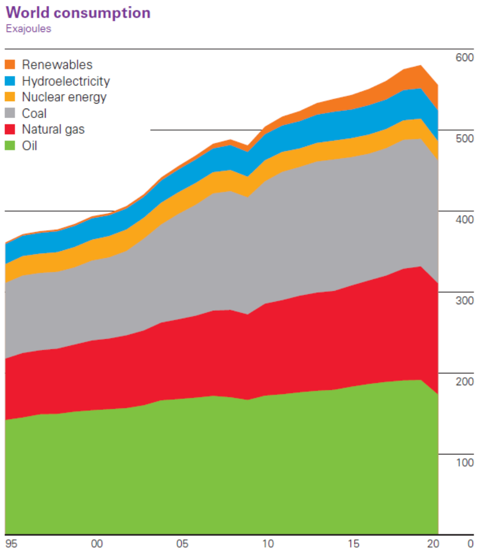

Figure 2 *Sources for world energy consumption. [4]*

There is a large difference in CO_2 output between the different available energy sources. Renewables and hydroelectricity are not adding new carbon to the global CO_2 cycle, while coal energy consists almost entirely of the conversion from carbon to CO_2. From the available fossil sources, natural gas is the least CO_2 intensive. The wide range of specific CO_2 emissions from the different sources makes the choice of preferred energy sources a dominant parameter in the climate transition topic.

Leaving possible socio-economic measures out of the scope of this work, we look at technological paths that can lead to lower global carbon emissions. Propulsion, i.e. the transport sector, has a share of 22% in the worldwide CO_2 production [5], and will be the topic of this study. Historically this sector is, besides a small share of LPG and natural gas, mainly driven by gasoline- and diesel-powered Internal Combustion Engines (ICE). In the light of climate change the goal can be formulated to phase out the net emission of CO_2 coming from the application of fossil fuels in this sector.

Besides the climate impact, there is another reason why society is interested in the replacement of fossil fuels. The future availability of these fuels is a concern. Although its predicted availability is still significant and depletion is not expected in the short term [6], the limitedness of availability and the origin from often politically sensitive areas is another driver for the energy transition. Unfortunately this topic became very relevant again in 2022.

One of the pathways that gets much attention from policymakers is electrification. For light duty, most manufacturers are offering Battery Electric Vehicles (BEV), and in Western Europe sales are increasing. Electrification of light duty vehicles increases efficiency, thus reducing primary energy demand, and solves the issue of local emissions. It has to be noted that this does not automatically mean that BEVs do not contribute to global warming. Besides the impact of production, this is dependent on the source of electricity used to charge batteries. The percentage of renewable or carbon-free electricity in a national grid defines the actual well to wheel CO_2 emission of electrified transport. Although the availability of renewable energy is strongly increasing in Western Europe, Figure 3 shows that fossil fuels still play a dominant role in electricity production, having a share of 63% in 2019. It is expected that new sales of passenger cars with an Internal Combustion Engine in Europe will be banned in 2035 [7] .

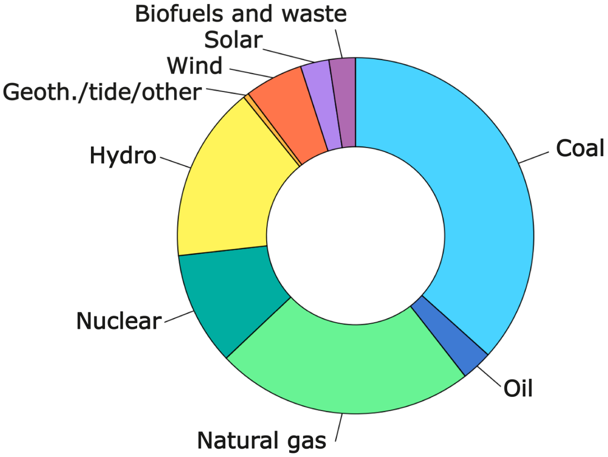

Figure 3 *World gross electricity production by source in 2019. Reproduced from [8]*

Taking the average lifetime of a vehicle into account, this means that the bulk of the fleet will consist of electric vehicles by 2050. With the current pace of electrification, and the renewable share in electric energy, the Renewable Energy Directive (REDII) target for 2030, which states that 14% of the energy in transport should come from renewable sources, seems unachievable by electrification only.

A faster scaling-up is limited by costs, availability of rare earth materials and green electricity, and a limited grid capacity. When looking at transport sectors beyond light duty, where large energy amounts are consumed, the low energy density of batteries is problematic and prevents mass-electrification.

Another route towards defossilizing transport is through the application of renewable fuels in combustion engines. This approach stands out for the following characteristics:

- The engines are already there, so the transition can be made fast.
- They are made of abundantly available, well recyclable materials.
- By using current engines, or slightly modified engines, limited investments are required.
- Energy density of fuel is high, which makes this route feasible for sectors where large amounts of energy are used.
- Right-sized engines at high loads can demonstrate a proper efficiency.
- Infrastructure and logistics are not a concern.

This approach, which can be summarized as: “keep the engine, change the fuel” [9] requires the transition to a low- or no-carbon fuel. Fundamentally this can be done with three different types of fuel:

- A fuel without CO_2 formation during combustion.
- A fuel that uses carbon that was already a part of earth’s short-term carbon cycle; biogenic carbon.
- A fuel that is based on carbon which is obtained from already emitted CO_2.

A wide range of sources, processes and fuels are able to provide one of these three options. An overview can be seen in Figure 4. Also, the fossil sources and common transportation fuels are shown here. It has to be noted that the dominant fuels for road transport in Europe, gasoline and diesel, are already partly of renewable nature, through the blending of biofuels as prescribed by European Directive 2009/30/EC. In petrol this is done with up to 10% bioethanol in E10 fuel, in diesel it is done with maximum 7% biodiesel in B7 fuel. With limited percentages, but a large total fuel quantity in the market, this approach already has a significant contribution to the reduction of CO_2, but further actions are needed to increase the impact [10]. The European climate law [7] recognizes the potential of renewables, and puts them forward as only realistic option for aviation and marine transport.

Before focusing on the available fuels themselves, it should be clear which requirements should be met, to make a fuel suitable as a renewable fuel for transport. We follow the triple S criteria [9] for this. A fuel should be:

- Sustainable. The fuel should have a minimal well to wheel climate impact.
- Scalable. The fuel has to be made available in very large quantities, at reasonable costs.
- Storable. The fuel should have an energy density meeting the needs of the application.

Alternative fuels that are getting much attention nowadays are methane [11], hydrogen [12], ammonia [13] and methanol [14]. When we combine these candidates with the criteria mentioned above, a few conclusions can be drawn. Methane has to be liquefied to fulfil the Storable-criterion, at least for heavy duty transport. Its source has to be biological or from renewable electricity [15], [16] to fulfil the Sustainability-criterion. As natural gas it has the lowest specific CO_2 emissions of all fossil fuels [17] but it is not renewable. Alarming however, is the recent insight on direct emissions of methane to the atmosphere during the processing of natural gas [18], which has, with its high Global Warming Potential, a significant contribution to global warming. Hydrogen is struggling to match the Storable-criterion, but has the "political advantage" that it is not only potentially low carbon on a Well to Wheel (WTW) level but that is zero carbon on a Tank to Wheel (TTW) level. The same goes for ammonia, but this has the disadvantage that it is difficult to combust, and its safe storage and handling requires attention. On the storage criterion, methanol has the clear advantage that it is liquid under STP conditions. As shown in Figure 4 it can originate from all possible sources, which ensures the availability. It does need to be produced from a biogenic or renewable electricity source, to match the sustainability criterion.

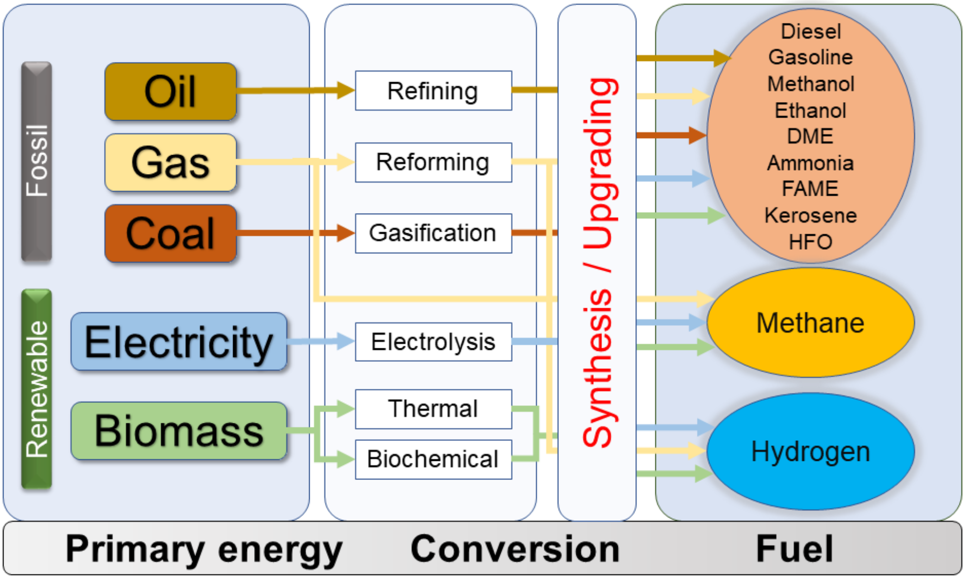
Fossil
Oil
Gas
Coal
Renewable
Electricity
Biomass
Refining
Reforming
Gasification
Electrolysis
Thermal
Biochemical
Synthesis / Upgrading
Diesel
Gasoline
Methanol
Ethanol
DME
Ammonia
FAME
Kerosene
HFO
Methane
Hydrogen
Primary energy
Conversion
Fuel

***Figure 4** Energy sources, conversion pathways and fuels. Reproduced from [19]*

All in all, it can be concluded that multiple fuel candidates are available, that can contribute to the reduction of greenhouse gases in a favourable way. This raises the question what the best way is, to apply such fuels.

Besides energy source- and climate-issues, and the closely related engine efficiency, another relevant engine aspect is tailpipe emissions. Although historically large improvements have been made, we globally still see issues with local air quality. In road transport the actual Euro 6 and VI limits, and upcoming 7 and VII limits are approaching Near to Zero emissions. Motivated by Dieselgate [20], legislation from Euro 6d and onwards guarantees that the clean emissions are also achieved in daily usage, through Real Driving Emissions (RDE) regulations. We see that other sectors, and other regions worldwide are following the EU limits. Stage V legislation for Non-road and marine is moving towards the same low emission levels as used for road transport. Nevertheless, when looking at alternative fuels and engine concepts, emissions are still very relevant and for that reason emissions are a significant part of this work.

1.2. Scope; Application of renewable fuels

What all the here mentioned alternative fuels - methane, methanol, hydrogen and ammonia - have in common is that they are high-octane fuels. This is closely related to their low cetane number. This makes them very suitable for Spark Ignited (SI) engines. Some of their relevant properties as engine fuel are shown in Table 1.

Table 1 *Properties of various renewable fuels, including gasoline and diesel fuel as references.*

		Gasoline	**Methane**	**Methanol**	**Hydrogen**	**Ammonia**	**Diesel**
Chemical formula		$C_4 - C_{12}$	CH_4	CH_3OH	H_2	NH_3	C_8-C_{25}
Lower heating value	[MJ/kg]	43.3	49.7	19.5	120	18.5	43.1
Density @ STP	[kg/m3]	720	0.65	790	0.08	0.86	820
Liquid density	[kg/m3]	720	717	790	71	696	820
Phase @ STP		Liquid	Gaseous	Liquid	Gaseous	Gaseous	Liquid
Storage phase		Liquid	Gas / liquid	Liquid	Gas / liquid	Liquid	Liquid
Viscosity	[10^{-6}Pa s]	380	18.8	560	13.7	20.6	2400
Octane number	RON	95-98	120	109	120	130	<20
Cetane number	CN	15-20	0	5	<5	0	51-54

Because of their high efficiency, reliability, and long lifetime, the world of marine, heavy duty, and industrial powertrains almost completely consists of diesel engines. These engines require a fuel with a high cetane number. Replacing all these engines with SI engines is not feasible because of costs, sustainability, specific torque, and engine efficiency. For this reason, we are interested in applying a high-octane fuel in a compression ignition engine. One of the possible ways to do this, is by applying the dual fuel concept. In this engine concept a high-reactivity fuel is used to ignite a high-octane fuel.

Two different approaches are seen in the application of this dual fuel concept; Conventional Dual Fuel (CDF), and Reactivity Controlled Compression Ignition (RCCI). Both have different backgrounds and different goals, and a different Technology Readiness Level [21]. A discriminating parameter between both approaches is not very well defined. Since knowledge on such a parameter and overview on the behavioural differences between both approaches are far from complete, as will be described in more detail in Chapter 2.4, this work focusses on the behaviour of both concepts in dual fuel engines and specifically on the transition area in between them.

1.3. Thesis contributions

Several experimental and theoretical studies were performed to develop an understanding of the combustion and emission formation process in dual fuel combustion engines. Before starting the experimental campaigns, the initial plan was to develop a predictive phenomenological combustion model for dual fuel operation, suitable for real-time control. To get a clear view on the current state of art of dual fuel combustion modelling a literature review was performed. Also multiple experimental campaigns were performed, to create insight in dual fuel operation and to generate relevant measurement data for modelling. During these activities, when the experimental campaign moved from conventional dual fuel to RCCI, a more specific knowledge gap showed up. A clear and simple description of the relation between injection timing and start of combustion in both modes was not available. A thorough understanding was still lacking on the behaviour of the pilot injection and how it ignites the mixture, over the complete operating range from RCCI to CDF. To fill this knowledge gap, a conceptual model was developed. In line with the initial goal, this is not a complex, computationally heavy model but it focusses on a fundamental explanation at low computational cost to enable future implementation in an engine controller.

The main activities executed are the following:

- A heavy-duty engine was converted to dual fuel operation at the applied research lab of HAN Automotive. The engine was assessed on emissions and performance. One specific topic was investigated in detail: cylinder to cylinder variations. In a combination between experiments and simulations the causes and possible solutions were found.
- A literature study was conducted to create an overview of the current state of art on combustion modelling for dual fuel engines. Models with different

levels of detail were assessed, paying attention to the various stages of the combustion process. A trade-off was found between model precision and computational cost, which limits the possibilities for predictive control-oriented models.

- An optical campaign was performed on a medium speed marine engine at Lund University. The goal of this research was to increase the understanding of how the pilot injection ignites the premixed fuel under different conditions. A strong influence of the injection timing on the amount of premixing of the pilot fuel was observed. The different behaviour between CDF and RCCI combustion mode was made visible.
- To extend the optical measurements with emission results, and to define preferred operating conditions for further optical experiments, a measurement campaign on the same medium speed marine engine, albeit in metal configuration, was carried out. Optimal results were achieved at a global lambda value of 2, using late RCCI injection timing. Data was created for the next step, development of the conceptual model.
- The behaviour of the start of combustion in relation to pilot injection timing was analysed. To create a phenomenological understanding of this behaviour, a conceptual model was developed. Based on in-cylinder conditions, spray mixing, and a kinetic scheme, the model can confirm and predict how the longer premixing from an earlier pilot injection results in a later start of combustion.

Because of availability and market maturity all work was done on diesel-natural gas dual fuel, but the main findings should also be transferable to the high-octane renewable fuels discussed earlier.

1.4. Thesis outline

This thesis contains 5 chapters, including the introduction chapter. The second chapter gives an overview of combustion methods and engine technologies. They will be assessed on their usability for high-octane fuels. Subsequently the dual fuel technology is explained, including a comparison of the CDF and the RCCI variant with their specific pros and cons. This leads to the research goal of this work. All involved experimental campaigns are reported in chapter 3. The created conceptual model that was based on these investigations is presented in chapter 4. Finally, chapter 5 provides the summarizing conclusions of this doctoral study.

2. Combustion concepts for high-octane fuels

As explained in the previous chapter, there is a need for concepts that allow to burn a high-octane fuel in a compression ignition engine. Therefore, this chapter starts with a short overview of combustion principles. As a next step, common engine concepts will be reviewed on their usability for high-octane fuels. The dual fuel option will be explained more in detail, with attention to the CDF and the RCCI approach. After going through limitations and differences, it will be discussed how these can challenge the application of dual fuel. Based on this, a solution route will be outlined resulting in a more detailed formulation of the research questions addressed in this work.

2.1. Combustion modes

Engine concepts can be classified along different criteria, like the way the fuel is introduced into the engine, the properties of its used fuel, the way the combustion is initiated, or the way in which the combustion process develops. The last aspect is strongly dependent on the before mentioned fuel related parameters, and is of crucial influence on the power, emissions and efficiency delivered by the engine. Three different principal mechanisms controlling this combustion process development can be recognized: flame propagation, mixing controlled combustion and kinetically controlled combustion [22]. Each of these is explained in the following sections.

Flame propagation

This is the common type of combustion in Otto engines [23]. The usually homogeneous premixed air/fuel mixture is spark ignited just before top dead centre. Combustion starts as a small flame kernel at the spark plug. This kernel subsequently increases in size as a developing flame front that is propagating through the combustion chamber. Ideally combustion will end when the flame front reaches the edges of the combustion chamber and has consumed all air/fuel mixture that was available in the cylinder. The speed at which the flame front travels through the combustion chamber defines the combustion speed. This flame propagation speed is influenced by the laminar flame speed of the air fuel mixture, but mainly by the amount of turbulence that wrinkles and stretches the flame front. In Figure 5 an example of the progress of turbulent flame propagation from a central ignition location is shown by schlieren images, recorded in a high-pressure vessel.

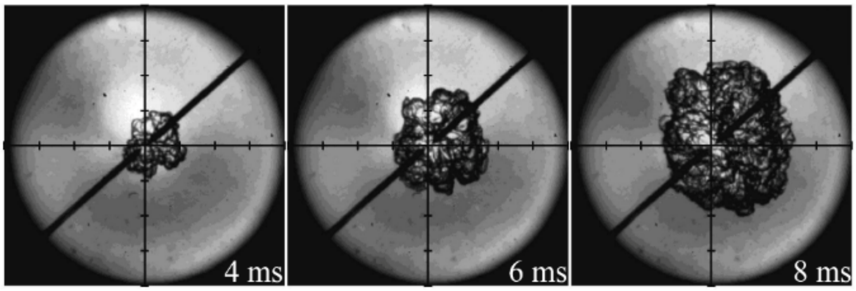

Figure 5 *Turbulent flame propagation of a methane flame. Schlieren optical images recorded in a high-pressure chamber. Reproduced from [24]*

Mixing controlled combustion

This is the type of combustion typically seen in a diesel engine. In this compression ignited engine the intake air is compressed to such a high pressure, that the resulting temperature is high enough to ignite a high-reactivity fuel shortly after its injection. The timing of the injection can directly be used to control the start of combustion. After spray formation, mixing with air, and a first very rich reaction step, full oxidation of the fuel takes place as a diffusion flame under stoichiometric conditions. A schematic presentation of the combustion, based on insights from various optical measurement results and chemical kinetic calculations, is shown in Figure 6. The diffusion flame outlined around the jet is indicating the location where the bulk of the heat release takes place. The speed of combustion is controlled by how fast the injected fuel can evaporate and how fast combustion air can entrain in the fuel spray. Combustion will end when practically all injected fuel is consumed, which is later than the end of the injection.

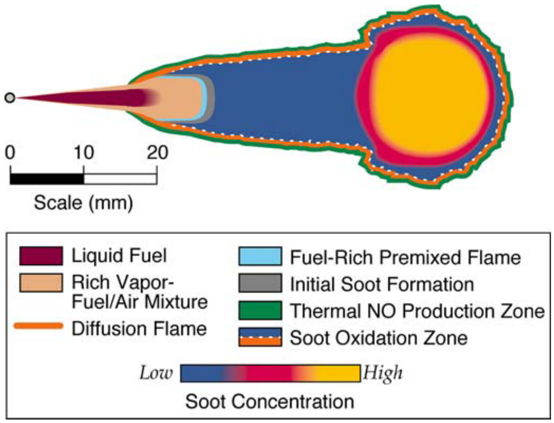

Figure 6 *Schematic of mixing controlled combustion. [25]*

Kinetically controlled combustion

In this combustion concept, which is not common in commercially available engines, both the start of the combustion and the combustion speed are defined by the chemical reaction rate of the air-fuel mixture. This reaction rate is, for the species present in the combustion chamber, dependent on local temperature, pressure, and air-fuel ratio. The fuel can be either fully or partially premixed, affecting local air-fuel ratio. Dependent on the timing of the fuel injections, the mixture is or is not homogeneous. This can be used as a parameter to obtain a required start and rate of combustion, by controlling the mixture stratification. Also EGR can be used to push the combustion process towards a desired behaviour (e.g. slowing down burn rates).

An unwanted limit-case of kinetically controlled combustion is the occurrence of knock in Otto engines. Here temperature and pressure result in an unwanted, uncontrolled very high reaction rate of the air-fuel mixture. However, when properly controlled, kinetically controlled combustion can have desirable features which make it an intensely researched topic in the last decades. The research on the kinetically controlled combustion concept started with the development of Homogenous Charge Compression Ignition (HCCI) [26]. The goal of this concept was to achieve the high efficiency of a diesel engine, but without its high NO_x production that is inherent of locally near-stoichiometric diffusive combustion at high temperature. Because of the absence of this high temperature zone, the concepts using kinetically controlled combustion are summarized by the term LTC, Low-Temperature Combustion. Ultimately the lower peak temperature during combustion results in lower heat losses and thus a higher engine efficiency. A complexity is introduced by the fact that the start of combustion is not triggered by a controllable discrete event like the timing of a spark or the start of an injection. Instead, the main driver is temperature, which is per definition a slowly changing variable. This makes the control of this type of combustion cumbersome. Consequently, the HCCI concept was never brought to market. Currently the research world is investigating variants of this concept, like PPC, PCCI and RCCI. How these concepts are positioned in relation to the different combustion modes is seen in Figure 7. The common goal of all investigated new concepts is to have a well controllable engine with high efficiency and low emissions.

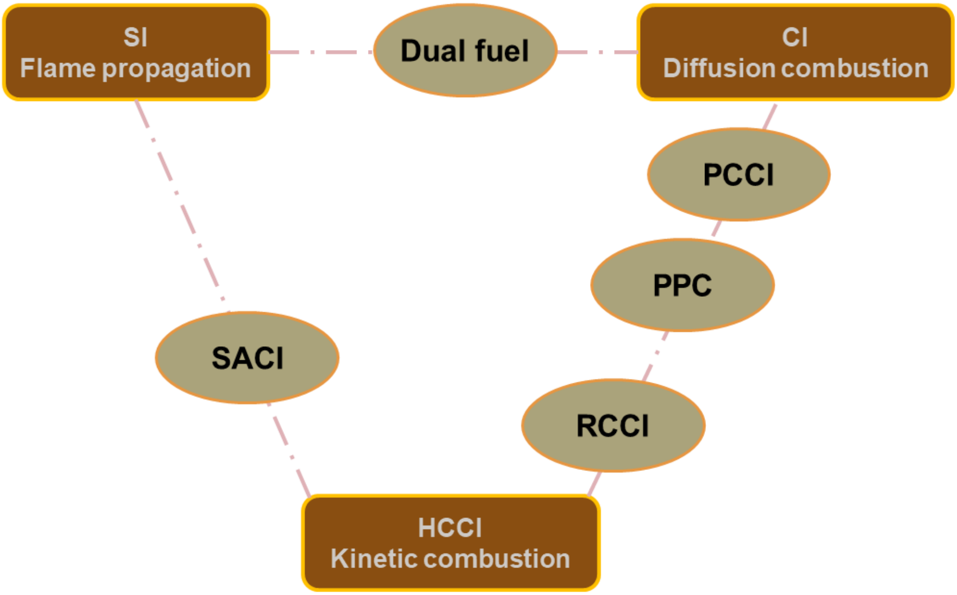

***Figure** 7 Combustion modes and engine concepts. Reproduced from [27]*

With the different combustion modes in mind, the next section will discuss in which way we can apply a high-octane fuel in a combustion engine.

2.2. Running on high-octane fuel

High-octane fuels can be used in different ways in different engine types. In this section, the available engine concepts suitable for the application of high-octane fuels will be reviewed. Based on market situations and the strong and weak points of the combustion mode, their feasibility will be assessed.

Otto engines

An engine type designed to use a high-octane fuel is the Otto or Spark Ignited engine. In this concept the combustion should start by spark ignition and not by auto-ignition during compression. This requires a fuel with sufficient knock resistance, represented by the octane number. After ignition the combustion proceeds by flame propagation.

In light duty applications almost all Otto engines are petrol engines [28]. In heavy duty and industry, the engines that are available with spark ignition are mainly natural-gas engines. For both petrol and gas engines it is not very complex to convert them to another high-octane fuel. Such conversions usually boil down to changing injection hardware, injection control and eventually spark control. An example of the conversion from natural gas to methanol is given in [29]. Further optimization can be achieved by also optimizing parameters like compression ratio and valve timing for a new fuel. Besides the required technical effort, the most important factor limiting the usage of sustainable high-octane fuels in SI engines is the availability of such engines in heavy duty, marine and industry, which is very low. Because of the SI engines' lower efficiency, torque density and increasing knock sensitivity at larger bore size, these sectors consist mainly of diesel engines.

Diesel to Otto conversions

Taking the widely available diesel engine as a starting point, it is not a small step to convert it into a spark ignited engine. The most obvious problem is the absence of an ignition system. It is feasible to add the electrical hardware, but the placement of a spark plug in the cylinder head can be challenging. In cases where this is done, often the diesel-injector is removed, and its mounting hole is used to install the spark plug [30]. A bigger complication is that almost all combustion-relevant engine parameters, like compression ratio, combustion chamber design, valve timing, thermal management and sizing of the turbocharger are optimized for a diesel engine and far from optimal for an SI engine. Although successful conversions are seen, the combination of high effort and suboptimal end results makes that this route is not per definition favourable.

Diesel engines

In a diesel engine, the injected fuel should auto-ignite when it is injected into the cylinder close to top dead centre. A diesel engine can function properly by the grace of the high reactivity of the diesel fuel. This high reactivity, expressed in the cetane number of a fuel, enables its auto-ignition shortly after injection in the hot combustion chamber. When injecting a high-octane fuel instead, the fuel will be very hard to auto-ignite. Per definition a fuel that has a high-octane number has a low cetane number, as illustrated by Figure 8. This makes the standard diesel engine, dependent on the high cetane number of its fuel, not fit to run on high-octane fuel.

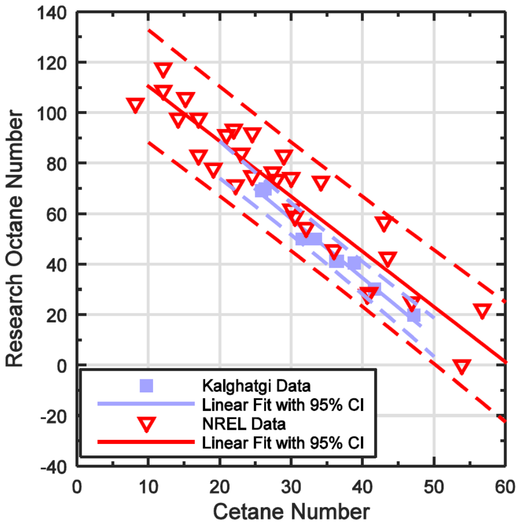

Figure 8 *Octane and cetane numbers for blends of n-heptane, iso-octane and toluene. [31]*

Applications are seen where engine hardware is changed such that the compression end temperature increases significantly. This allows the auto-ignition of a direct injected high-octane fuel, when this is blended with a few percent of ignition improver to increase its cetane number. This approach is successfully demonstrated with ethanol and methanol in the ED95 and MD95 concepts [32]. Here a compression ratio of 1:28 was applied. The fact that these concepts require significant hardware changes and an additive to the fuel are limiting factors for a large-scale market dominance.

Pilot ignition in a diesel engine

Another way to apply high-octane fuel in a diesel engine is found in the dual fuel concept [33]. It makes use of a combination of a high-reactivity and a high-octane fuel at the same time in one engine. The high-reactivity fuel is supplied through the diesel injection system to create a small, so-called “pilot” injection. This directly injected high-reactive fuel is able to auto-ignite at the end of the compression phase, and acts as an ignition source for the separately supplied, usually premixed, high-octane fuel. In this way a high-octane fuel, that would not be able to ignite on its own, can be combusted in a diesel engine. By limiting the pilot fuel amount as much as possible, the bulk of the energy can be supplied by the high-octane fuel. Although strongly dependent on the exact requirements, dual fuel is often seen as the most feasible way to apply a high-octane renewable fuel in a diesel engine [34]. This concept will be discussed in more detail in the next section.

2.3. Dual Fuel

Running a high-octane and a high-reactivity fuel in one combustion chamber can be done in various modes. This depends on the applied fuels and on the way in which the fuels are introduced in the engine. We can distinguish these as Conventional Dual Fuel, Reactivity Controlled Compression Ignition, and dual fuel with direct injection of both fuels (Dual DI). After a short description of their important characteristics, attention is paid to dual fuel limitations that were relevant during the executed experimental campaigns as reported in chapter 3.

Dual fuel modes

Conventional Dual Fuel

In a CDF engine the high-octane fuel is supplied in the inlet trajectory and admitted to the cylinder as a premixed air/fuel mixture. The pilot fuel is injected close to top dead centre. The Start of Injection (SOI) timing is comparable to a conventional diesel engine, with potentially small adaptions to optimize the combustion process. The phases of the combustion are depicted in Figure 9. The start of injection (A) is followed by a period of ignition delay (B). Dependent on in-cylinder and injection conditions a bigger or smaller part of the pilot undergoes a premixed auto-ignition diesel combustion (C). The rest of the pilot can combust as a diffusive flame, at the same time consuming a part of the high-octane fuel (D). This is followed by a flame propagation combustion of the premixed high-octane fuel (E).

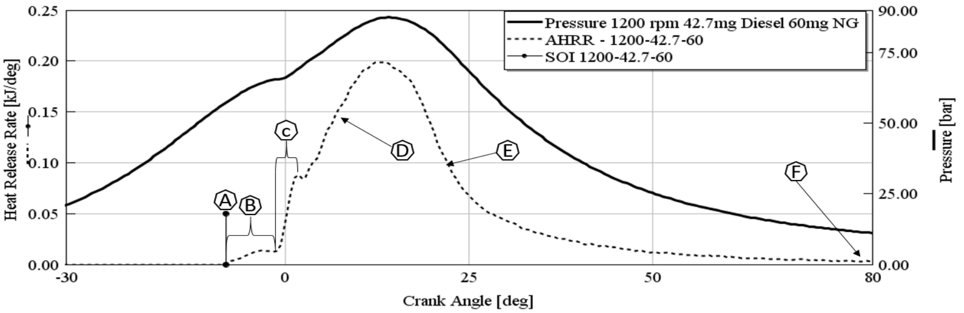

Figure 9 *Pressure trace and heat release of typical dual fuel combustion, indicating separate phases of the combustion process.*

The Conventional Dual Fuel approach is used in several real world applications, both on dedicated dual fuel engines [35] and in aftermarket conversions of diesel engines [36]. Starting from the base diesel engine, the most important modification is the addition of an extra fuel system for the high-octane fuel. In this PhD work we focus on natural gas as high-octane fuel, so this addition consists of a gaseous fuel supply system.

RCCI

Reactivity controlled compression ignition [37] has another background than the ability to apply a high-octane fuel in a CI engine. RCCI originated from the search for a controllable way of Low-Temperature Combustion (LTC) [27], aiming at extremely low NO_x emissions. Although RCCI probably is the LTC concept that is closest to market introduction, it is currently still in a research and development phase.

When using the same fuels as CDF, the distinguishing feature of RCCI compared to CDF is the significantly earlier injection of the pilot fuel. The earlier injection creates more time for premixing of the diesel injection. As a result, the combustion process is no longer a combination of a diffusive diesel combustion and a flame propagation combustion, but moves towards a kinetically controlled combustion of a mixture of air, diesel and methane.

Dual DI

A promising approach in improving dual fuel engines is the application of direct injection for both fuels used. Here also the high-octane fuel is injected directly into the cylinder, which requires extra injection hardware. For natural gas dual fuel applications this can be done by adding an extra injector into the cylinder head [38], or by using a dedicated injector which contains two separate injection systems [39], one for diesel and one for natural gas. In both cases it requires cylinder head modifications, which make this approach not feasible for conversion of existing engines. Another complication is that this approach needs a high-pressure supply of the gaseous fuel. The biggest advantage is that the fuel can be injected after the intake and exhaust valves have closed. As explained in the next section, this can give a significant reduction of the emission of uncombusted hydrocarbons (uHC). The gas injection can be timed early, just after closing of the intake valves, creating a premixed intake charge. In this case the combustion behaviour is comparable to that of an engine with indirect gas injection. Another option, if injection hardware allows it, is to inject the gaseous fuel directly after the diesel fuel. This aims at creating not a premixed but a diffusive gas combustion. This could result in a better controllability of the combustion process, but the sensitivity for NO_X emissions is very comparable to that of regular diesel engines. The fact that the Dual DI approach has a significant impact on the hardware of the base diesel engine has placed it outside of the scope of this PhD work.

Limitations of dual fuel

As with any engine concept, there are specific limitations and trade-offs with dual fuel combustion. The following section will be focussed on the dual fuel limitation topics that were addressed during this thesis. Most limitations are strongly load dependent, and have impact on emissions and/or efficiency. In dual fuel engines also the ratio between low-reactivity and high-reactivity fuel, which is preferred to be as high as possible, is likely to be reduced because of the experienced limitations.

Knock.

A dual fuel engine makes use of auto ignition of high-reactivity fuel, which requires a significant compression temperature. Commonly it is based on a diesel engine, which has a high compression ratio to reach the required compression end-temperature. To achieve a satisfying power density, it is very common to apply a significant charge pressure in such engines. As known from SI engines, these parameters are creating favourable conditions for knocking combustion, in the sense of end-gas autoignition [40] in the premixed charge. The high-octane rating of the premixed fuel and the lean combustion conditions are helping to prevent knock, but knock still is a realistic risk under high load conditions in this engine concept.

To guarantee engine integrity, knock should be prevented at all costs. An upfront safe parameter choice can be supported by a real time knock controller. After detecting knocking combustion, the controller has to take an action which has fast response. A very common approach is to retard the combustion phasing. This can be achieved quickly by retarding the start of injection. Another option is to increase the quantity of pilot fuel [41]. Keeping engine output constant this has to be combined with a reduction of the amount of low-reactivity fuel. As a consequence it results in a reduction of low-reactivity/high-reactivity fuel ratio. This conflicts with the objective of the dual fuel engine, to run on low-reactivity fuel. Finally, a very fundamental method of knock prevention could be achieved with the Dual DI concept. The change of knocking combustion in the premixed air/fuel charge can be eliminated when the low-reactivity fuel is not premixed. This is the case when diffusive combustion is applied, which can be done with a Dual DI system that allows late cycle injection under high pressure.

High uHC emissions

The concentration of hydrocarbons plays a role in local air quality. In the case of natural gas dual fuel, the emission of uncombusted fuel also has a strong greenhouse gas impact, because of the high GWP of methane. At the same time the effect of uncombusted hydrocarbon (uHC) emission on engine efficiency cannot be neglected. A typical methane emission of 6 g/kWh, often mentioned as break-even point for greenhouse gas reduction in gas engines [42], represents over 3% of fuel not taking part in the combustion.

One of the causes of high uHC emissions is the so-called methane-slip. In load cases where intake pressure is higher than exhaust pressure, the intake mixture can flow from intake manifold to exhaust manifold during valve overlap. It is common that the diesel engine on which a dual fuel engine often is based, has a significant amount of valve overlap. This makes methane-slip very likely on most dual fuel engines. It can be partly reduced by optimizing the gas injection timing. More intrusive are optimizing of valve timing and pressure ratio over the cylinder head. In the Dual DI concept methane slip can be completely prevented, by injecting the gas outside of the valve overlap window.

Also a poor combustion quality can be a significant source for uHC emissions in a dual fuel engine [43]. The combination of lean conditions and a combustion chamber not optimized for premixed combustion [44], can result in flame quenching and incomplete combustion. This especially takes place during the latest phase of the combustion, where temperature is already dropping because of expansion. For this reason the phasing of the combustion process can play a significant role in the limitation of uHC emissions [45]. Also the chosen air-fuel ratio plays a significant role in the combustion quality in dual fuel engines.

NO_x emissions.

The most dominant parameters for NO_x formation are the availability of oxygen, time, and a high temperature in the combustion chamber [46]. Compared to diesel combustion the local peak temperature during combustion is lower for dual fuel operation, and thus lower NO_x emissions are commonly reported. Since dual fuel is always operating under lean conditions, and the pilot injection can still create a high local temperature, NO_x emissions are not completely eliminated. In the same way as in diesel engines, EGR can be used to reduce NO_x formation. Also optimization of the main combustion parameters can be used to bring down NO_x to a desirable level. The dominant mechanism is to reduce peak pressure and temperature, by placing the combustion later in the engine process [47]. This requires a proper control of the combustion phasing.

Cylinder to cylinder variation

A potential dual fuel problem that is closely related to the way in which the high-octane fuel is introduced into the combustion chamber is cylinder to cylinder variation. When the fuel is not directly injected into the cylinder, its admission to the cylinder is affected by the intake flow, the design of piping and manifolds, and the valve timing of the engine [48]. A dual fuel engine is often based on a diesel engine, which has fairly limited requirements on equal quantity and quality of the intake charge for all cylinders. The air-path design is usually optimized for low pumping work, compact engine packaging, and cooling by scavenging. In the diesel engine a variation in induced air amount can be accepted, because its diffusive combustion is not very sensitive to a limited change in global in-cylinder lambda. When the same configuration is used in a dual fuel engine, differences in quantity and quality of the intake charge do have a significant impact on flame propagation or kinetically controlled combustion. The caused variation in combustion profile can alter uHC and NO_x emissions, and knock sensitivity. The fact that each cylinder does not have the same behaviour makes it very complex to optimize control of the combustion process.

Optimizing the application

During the development phase of a dual fuel application, the before mentioned limitations have to be taken into account. Cylinder to cylinder variations are strongly related to the hardware configuration of the base diesel engine, and will often not be open to modifications. Especially in aftermarket conversions, only the capacity and timing of the secondary fuel system are parameters that can be optimized to improve cylinder to cylinder variations.

To achieve low engine-out NO_x and uHC emissions without knock, the combustion process has to be optimized. With given hardware, a dominant parameter to adapt is the phasing of the combustion process, which also has a significant impact on engine efficiency [49]. The relation between combustion phasing and emissions and knock is known from SI and CI engines, and not fundamentally different for dual fuel engines, as discussed in the previous section. To achieve a desired combustion phasing, it is needed to have proper control over the start of combustion. This can be done by controlling the start of injection (SOI) timing. This leaves the question if controlling the start of injection has the same impact on the combustion behaviour for RCCI and CDF operation, leading us to our research motivation explained next.

2.4. Research motivation

CDF and RCCI timing

The phasing of the combustion process in a compression ignited engine is largely defined by the timing of the main diesel injection or the pilot injection. Retarding the combustion process can be achieved by retarding the diesel injection, while advancing the injection results in an advance of the combustion. This behaviour is seen in both Conventional Diesel Combustion (CDC) and Conventional Dual Fuel (CDF) engines. Both combustion modes also show the same trend for NO_x emissions with respect to injection timing, where advancing increases the NO_x output. Besides the increasing NO_x output, advancing the pilot injection too much can also result in reduced efficiency caused by too early combustion. For both reasons it is common to limit the advancing of the injection timing.

In dual fuel research with a further advancing of the injection, a change in behaviour was observed. Doosje [50] shows a set of experiments on a heavy duty engine where going from 6 CAD until 30 CAD bTDC results in a continuous advance of combustion. Further advancing from 30 CAD until 56 CAD bTDC subsequently retards the combustion. In [51] Yousefi observes the same behaviour in experiments, and combines it with CFD simulations. A relation with in-cylinder temperature, dilution and ignition delay is noted. At Lund University this inversing of the relation between start of injection and start of combustion is also observed in dual fuel research by Garcia [52], as shown in Figure 10. Measurements on a medium speed marine engine show that for a specific load case, advancing the injection beyond 30 CAD bTDC results in retarding of the start of combustion.

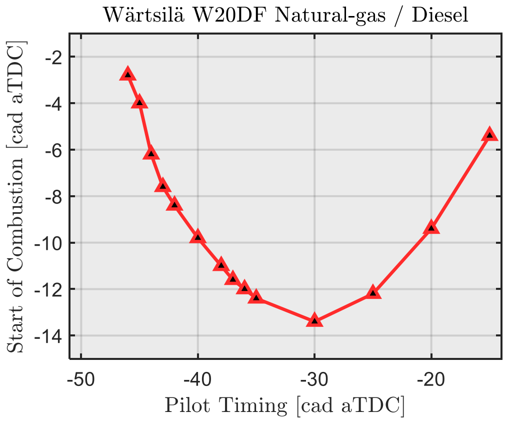

Figure 10 *Start of combustion, medium speed engine experiments. Reproduced from [52]*

This area with a very early injection timing is where the combustion behaviour moves into an RCCI operation mode. In research at TU Eindhoven [50], [53] it was shown that this can result in a strong reduction of NO_x, but too much advancing of the injection leads to an increase in uHC emissions. An extensive classification of (dual fuel) combustion modes is given by Martin [54], [55] with the MELT concept (Manifold, Early DI, Late DI), paying attention to promising intermediate combustion modes in between CDF and RCCI. Also in work done in this PhD study, on the Wärtsilä engine [56], it was shown that optima on emissions and efficiency can be found close to the transition range from RCCI to CDF. The results obtained from the experimental campaign and conclusions on preferred injection timing can be found in chapter 3.4 and paper V in the appendix.

The fact that preferred operation is close to the transition area, and the observation that the control of combustion phasing fundamentally differs between the two ranges, makes it relevant to provide a proper understanding of this transition. Detailed CFD explanations are found in literature separately for RCCI [57] and CDF [58] operation, but work where the coherence between the behaviour in both modes is addressed is only very limited available. To create a clear understanding of the SOI control-related differences between both modes, a more elementary clarification of the ignition behaviour is desired.

Towards an understanding of the relation between SOI and SOC over the operating range from RCCI until CDF

A proper conceptual understanding of the changing relation between injection timing (SOI) and start of combustion (SOC) in CDF and RCCI operation is essential when setting up a dual fuel engine. Not only does this play a role for the calibration engineer while optimizing emissions and performance at the testbench; also for controller algorithms that modulate combustion phasing through injection timing, like knock or NO_x control, this is of significance. Where in the CDF case the controller should give out an earlier start of injection when an earlier combustion phasing is required [59], it should advance injection timing in RCCI mode to reach the same goal [60]. Instead of mapping out all possible solutions in calibration tables at the engine testbench, which is expensive and time consuming, it is desired to have a conceptual understanding of this behaviour. Instead of creating detailed CFD models for each operating point separately, it is desirable to create a single model that gives insight in the behaviour of the start of combustion, over the full range from RCCI to CDF. A conceptual model, that creates insights into the main drivers for the observed SOC behaviour can help to set up the engine controller in an effective way. It can be used for model based calibration [61], or when the required computational power of the model is limited, for model-based control.

An overview of modelling approaches existing in literature for dual fuel combustion was given in a paper written during this PhD [62], and included as paper II in the appendix. Here three different modelling approaches were distinguished:

- Zero dimensional
- Multi zone
- 3D CFD

In total 7 separate steps in modelling the engine process were recognized, as shown in Table 2.

Table 2 *Combustion simulation approaches and their particular steps.*

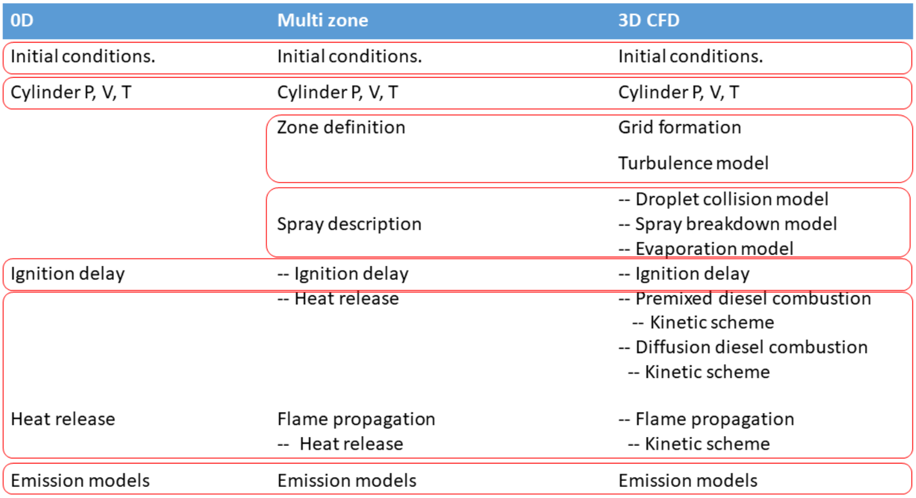

0D	Multi zone	3D CFD
Initial conditions.	Initial conditions.	Initial conditions.
Cylinder P, V, T	Cylinder P, V, T	Cylinder P, V, T
	Zone definition	Grid formation Turbulence model
	Spray description	-- Droplet collision model -- Spray breakdown model -- Evaporation model
Ignition delay	-- Ignition delay	-- Ignition delay
Heat release	-- Heat release Flame propagation -- Heat release	-- Premixed diesel combustion -- Kinetic scheme -- Diffusion diesel combustion -- Kinetic scheme -- Flame propagation -- Kinetic scheme
Emission models	Emission models	Emission models

Being interested in the relation between start of injection and start of combustion, the ignition delay is the most important step of the modelling chain. The ignition delay is defined as the time between Start of Injection and Start of Combustion. The literature review revealed that the most common approach is to describe this phase by making use of an Arrhenius equation [63]. A typical example, as presented by Assanis [64] is given in Equation *(1)*.

$$\tau_{id} = A\Phi^{-K}P^{-n}exp\left(\frac{E_a}{R_uT}\right) \tag{1}$$

Here P, T and Φ are pressure, temperature, and equivalence ratio inside the combustion chamber. R_u is the universal gas constant and E_a represents the required activation energy for the used fuel. The equation can be fitted to actual engine measurements and its operating conditions, making use of the tuning factors A, K and n. Variants of this equation are adding specific details and sensitivities for dual fuel combustion. Although an appropriate representation of the ignition delay can be achieved with this approach, it can only indirectly take the injection timing into account. This would require inputting the appropriate temperature and pressure (trajectory) for the investigated injection timing. Also on a conceptual level, the equation does not create much insight in the behaviour of a dual fuel engine when moving from CDF to RCCI operating mode.

Another approach is possible by using a kinetic scheme, which can in detail describe the start of combustion. To describe the actual in-cylinder conditions, needed to run the kinetic scheme, it is common to use a CFD simulation. The combination of a detailed scheme and CFD make that this approach comes at high computational cost. It also makes the model very specific for one application.

It can be concluded that both an ignition delay equation and a CDF model with a kinetic scheme can be used to calculate the timing of the start of combustion. Both approaches are not, in one go, giving an elementary insight on the changing relation between SOI and SOC when moving from CDF to RCCI operation. To create that insight, a new phenomenological description will be developed. This model describes on a conceptual level, for a given operation point and its in-cylinder conditions, the start of combustion in relation to pilot injection timing. The model should have limited computational requirements, to ensure it can be used for real time control purposes. After going in Chapter 3 through the experimental studies conducted in this PhD work to generate insights and data, Chapter 4 elaborates on the development of the conceptual model based on this.

3. Experimental studies

To substantiate the understanding of dual fuel and its complications, and to create insight in the ignition, combustion, and emissions of both RCCI and CDF, various experiments have been performed. The first campaign was performed on a DAF heavy duty engine at HAN University of Applied Sciences. The second part of the work was done on a Wärtsilä medium speed marine engine at Lund University. This chapter will elaborate on these experimental studies and their main conclusions.

3.1. Dual fuel on a heavy-duty engine

As preparation for this PhD work, a heavy-duty engine was converted to natural gas/diesel dual fuel operation. This was done within the Interreg project LNG Pilots [65], with the goal to better understand the behaviour of a dual fuel engine, and find room for improvement. The focus was on minimizing emissions and maximizing the replacement of diesel by natural gas. A more detailed description of this work can be found in [66]. In the following section the setup and the most important parameters for dual fuel operation for heavy duty will be illustrated. Next, a typical problem with cylinder to cylinder variation will be analysed in more detail.

Test setup

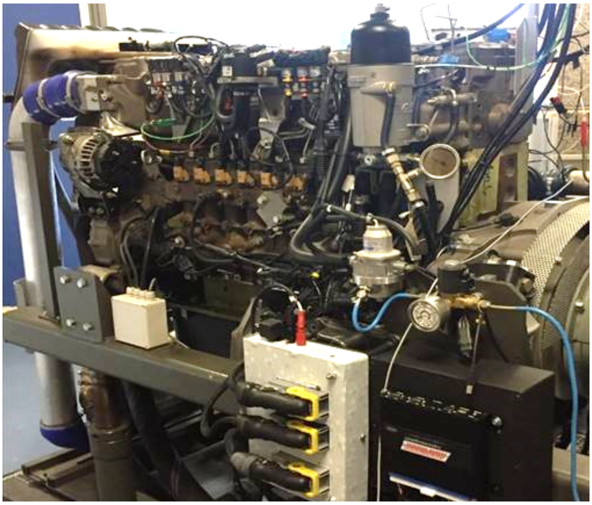

***Figure 11** DAF PR 6-cylinder engine in test cell, intake side.*

The heavy-duty campaign was performed on a Paccar DAF PR9-265 truck engine at HAN Automotive, shown in Figure 11. This engine was previously installed in cooperation with DAF Eindhoven, to instruct students during lab assignments. The specifications of this 6-cylinder engine are given in Table 3. A LabVIEW application controls the engine in constant speed mode using an Eddy current brake. The engine is equipped with Dewetron pressure indicating on cylinder 6.

***Table 3** Specifications heavy-duty engine.*

Engine configuration	*6 cylinder 4 stroke, DI, CI*
Block construction	*Cast iron.*
Head construction	*Cast iron, 4 valves.*
Fuel system	*Delphi Electronic Unit Pumps, Electronic injectors*
Emission class	*EU IV. With SCR: EU V.*
Bore x stroke [mm]	*118x140 mm*
Displacement [l]	*9.2 litres*
Compression ratio	*17.4:1*
Max power [kW]	*265 @ 2200 rpm*
Max torque [Nm]	*1450 @1100-1700 rpm*

A Prins Westport gas injection system was used to convert the engine to dual fuel operation. It was installed as a multipoint injection system, where each injector delivers the gas to its cylinder through a pipe into the intake port, shown in Figure 12. The injectors are controlled by a dedicated engine control unit (ECU), allowing the independent adjustment of injection length and timing. The base testing and calibration of the engine was done on natural gas from the Dutch grid, buffered as CNG.

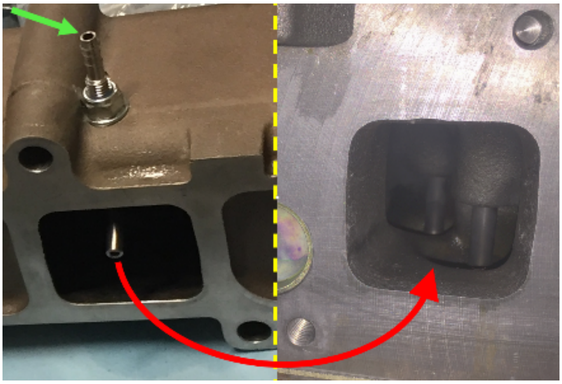

Figure 12 *Manifold pipe to dose injected gas into the intake port.*

A schematic overview of the setup is shown in Figure 13. For diesel control the stock ECU was used, where the desired pilot diesel amount was achieved by adjusting the driver's torque request accordingly. For specific tests an experimental Adaptronic FPGA-based ECU could be embedded.

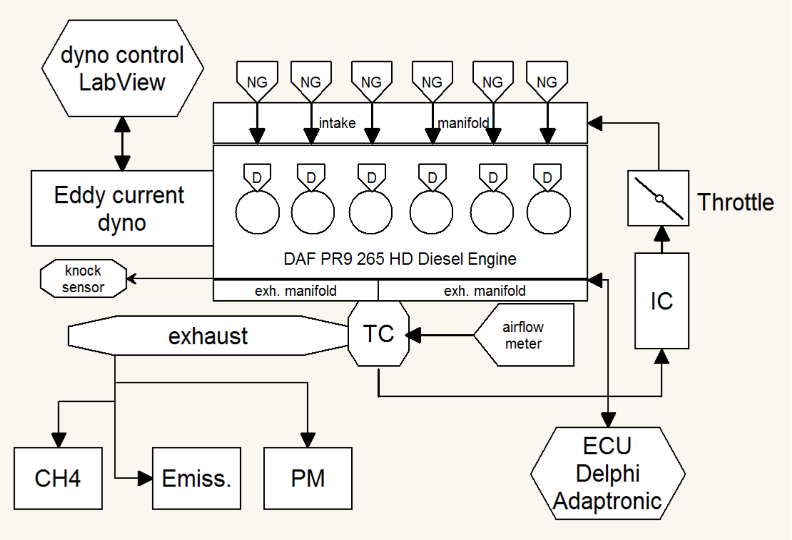
dyno control
LabView
NG
NG
NG
NG
NG
NG
intake
manifold
Eddy current
dyno
D
D
D
D
D
D
Throttle
DAF PR9 265 HD Diesel Engine
knock
sensor
exh. manifold
exh. manifold
IC
exhaust
TC
airflow
meter
CH4
Emiss.
PM
ECU
Delphi
Adaptronic

Figure 13 *Engine measurement and control overview.*

During the experiments the gaseous emissions were tested with a Siemens Ultramat analyser for methane and a Testo 350 for NO_x, O_2, uHC, CO and CO_2. Particle mass emission was measured with a Pegasus Mi3 analyser. Continuous sampling was used for all devices.

To be able to detect knock, three different information sources were applied in parallel. The instantaneous derivative of measured cylinder pressure was used during testing to have a quantitative knock limit. A maximum pressure rise rate of 8 bar/CAD was used for this. Separately a Plex knock detection system provided information based on a knock sensor bolted to the engine block. This system shows real-time intensity of the sensor signal. Based on the bore diameter of 118mm, a band-pass filter around 5.5kHz was applied in the knock detection system. When reaching the allowed pressure rise rate limit, a significant increase in signal intensity could be observed. At the same time a change of the engine sound signature could be observed. This operator assessment of combustion noise was used as the third indicator, to safeguard engine integrity.

Results

After commissioning the test set-up and methods, a set of tests was performed to create a generic indication of dual fuel performance on a truck engine. This test was done at 1200rpm and had the goal to find the maximum amount of diesel replacement by natural gas. This replacement is expressed by the Gas Energy Replacement (GER) percentage, as expressed by Equation *(2)*.

$$GER = \frac{E(gas)}{E(gas + diesel)} * 100\% \tag{2}$$

The maximum achievable GER value was based on two limiting parameters. A maximum emission of 6g/kWh of unburned methane was allowed, and combustion had to be without knock. The results are presented in Figure 14, where the emission limit was dictating the maximum gas amount at low load, while at high load the knock limit became the determining factor.

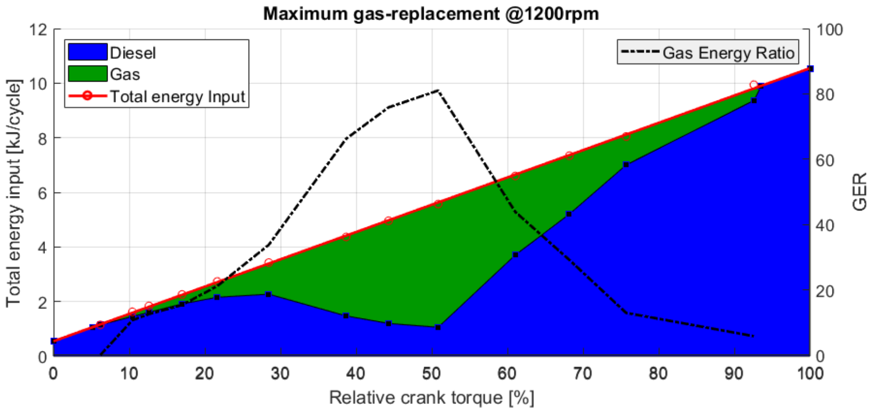

Figure 14 *Gas energy replacement on dual fuel truck engine.*

At medium load a high replacement could be achieved, peaking at 83% at 50% torque. Although high values are only seen in a relatively small operating range of the engine, it is this medium load range that is the typical load-case for highway operation of trucks. For this reason, it represents a significant replacement of energy over the truck's lifetime usage.

3.2. Cylinder to cylinder variations in a heavy-duty dual fuel engine

During attempts to increase the achievable GER value, observations were made that indicated an uneven mixture quality over all cylinders. Initially this became apparent by a temperature difference between both inlets of the twin scroll turbine, at high GER values. Also rough engine running, not indicated as knock, was observed. Combined with market questions on what the preferable gas admission system for heavy duty engines would be, this led to research on equal gaseous fuel distribution over all cylinders of a dual fuel engine. That these variations have impact on the emission of unburned methane, a strong GHG, makes it a very relevant topic in relation to the goal of improving the sustainability of powertrains. The principal research method and the main findings are given in the following section. Details of the campaign can be found in ref. [67] (paper I in the appendix).

Methodology

The investigated phenomenon of cylinder to cylinder variations is related to the amount of trapped gas and air per cylinder. Since both parameters cannot be measured separately on the engine directly, the experiments were supported by 1D simulations in GT-Power. The modelling was done to create insight in flow phenomena in the engine under different conditions. Based on this priority it was chosen to use a non-predictive combustion model. By setting modelled combustion efficiency to 100%, the observed methane emissions in the model can be attributed to slip.

For simulation, and for testing, a suitable operating point was required. The operating point should have a duration of gas injection that would fit within the intake stroke, giving sufficient room for experiments with gas injection timing during, before, and after the intake stroke. Achieving proper combustion quality during testing requires a suitable lambda value. The diesel to gas ratio was chosen such that a safe margin to the knock limit was kept. Finally, mid-range torque was preferred to make the test case representative for road use. Taking all these aspects into consideration, a load point of 600Nm (8.2 bar BMEP) was chosen for testing. This was created by a 63.5mg diesel injection and 20mg gas injection, resulting in 22% GER. The gas injection timing was varied in 5 steps from 280 till 610 CAD aTDC-F, as shown in Figure 15. Lambda values of 1.3 and 1.6 were chosen as test cases, achieved by setting the air amount by means of intake pressure adjustment. To reach the desired intake pressure, a throttle valve was added to the test setup. At the same time this reduction of intake pressure ensured a negative pressure ratio over the cylinder head, eliminating methane slip. The other hardware change was the addition of emission sample points in the exhaust ports of cylinder one and six. These were situated as close to the exhaust port as possible, preventing influence from other cylinders in the measurements.

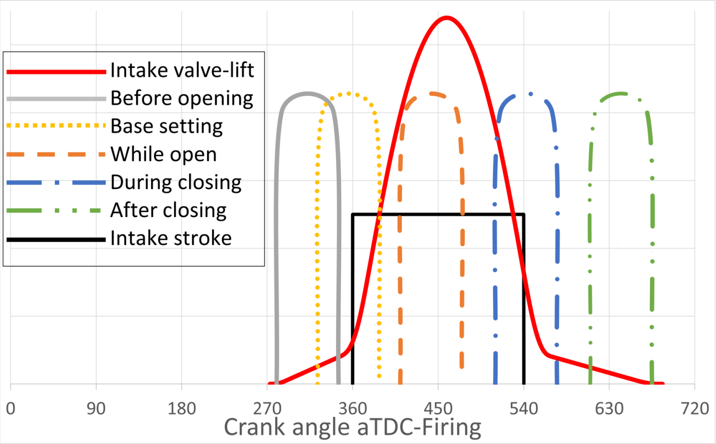

Figure 15 *Tested and simulated cases of gas injection window, SOI from 280 to 610 deg.*

Results

The measured lambda values during the experimental campaign are shown in Figure 16. The first observation is that cylinder to cylinder variations are found in all measurements. This is investigated more in detail and reported in ref. [67] (paper I in the appendix). The measurements show that for the first three timings a constant deviation between cylinder 1 and 6 is seen. Injecting during or after the closing of the intake valve results in enrichment of cylinder 6 and leaning out of cylinder 1, for both tested lambda cases.

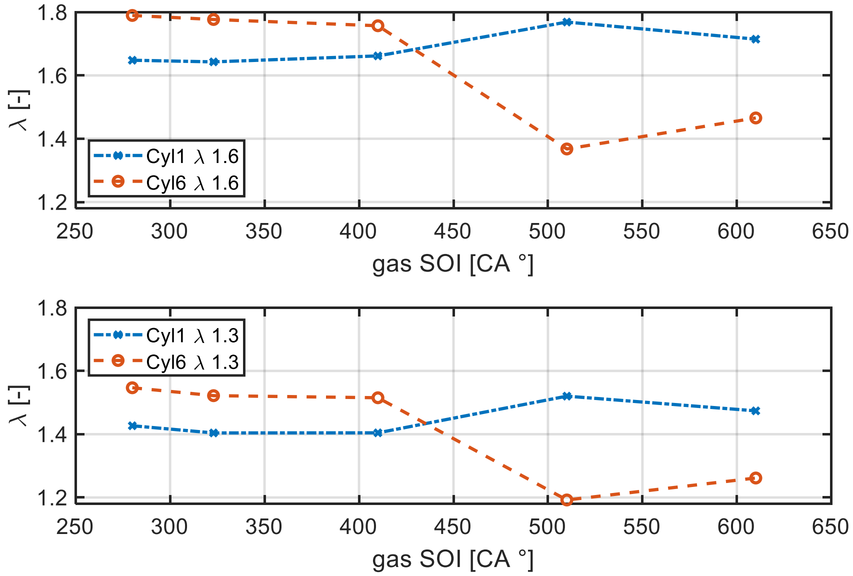

Figure 16 *Measured lambda values at cylinder 1 and 6, for a sweep of gas injection timings. Tested at two different mean lambda levels, created by variation in boost level.*

The measured lambda variations could theoretically also be influenced by variation in the diesel injectors, and trapped air amount per cylinder. Since these variations could not be included in a model in a way enabling validation, it was chosen to focus the numerical experiments solely on the variation of trapped gas mass in relation to gas injection timing. The results are shown in Figure 17. The upper part can be related to the engine measurements on cylinder 1 and 6. A qualitative match was found, where cases with a richer measurement showed an increase in the modelled trapped gas mass. The lower part of the graph shows that at 323 CAD aTDC-F all cylinders are trapping an equal gas amount, while at 510 CAD the amount monotonously increases towards the rear of the engine.

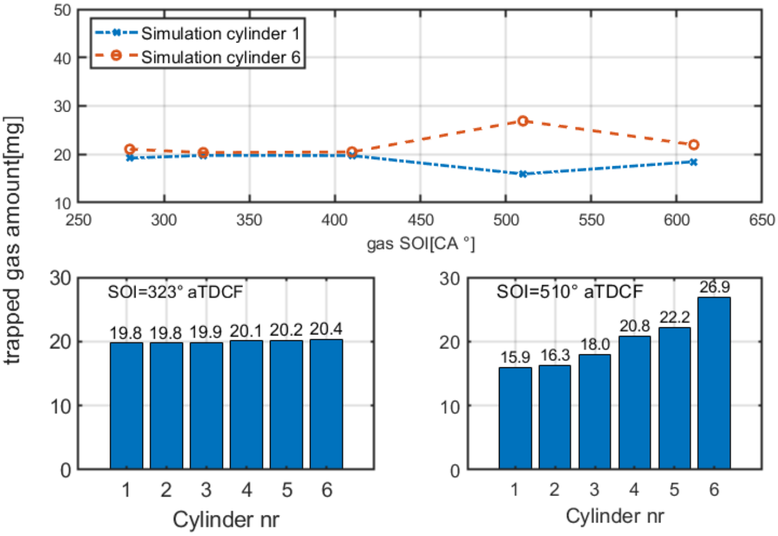

Figure 17 *Simulated lambda value at cylinder 1 and 6, for a sweep of gas injection timings. Trapped gas mass per cylinder, for gas injection during and after the intake stroke.*

Discussion

The GT-Power model was further used to investigate the mechanism behind the cylinder differences that were observed in measurement and simulation. For this, the fuel flow between intake runner and manifold plenum was analysed. This intersection is located upstream of the gas injection location, so ideally no fuel would be observed here.

In Figure 18 (I) and (II), cylinder 1 and 6 are shown with an injection during the intake stroke. A small mass of natural gas is observed at the crank angle interval indicated in the figure by (a), flowing back from the runner of cylinder 1 into the plenum. This backflow is caused by a still upwards moving piston, while the intake valve is already opened. A part of the mass available in the intake port, in which the gas injection just started, is backflowing. About 1 percent of the injected gaseous fuel flows into the manifold, and is drafted downstream in the intake manifold. As a result, cylinder 1 becomes slightly leaner. At the beginning of intake valve opening at cylinder 6 also a small backflow into the manifold is observed, (b). Remarkable is that this backflow is followed by an inflow of fuel into the intake manifold (c). Initially this is the same mass that was just forced into the plenum. Because this is the last cylinder in line, the gas was not drafted away from the plenum. Also during the rest of the intake stroke, a small inflow of natural gas can be seen (c). This is the gas that was pushed back at the other cylinders.

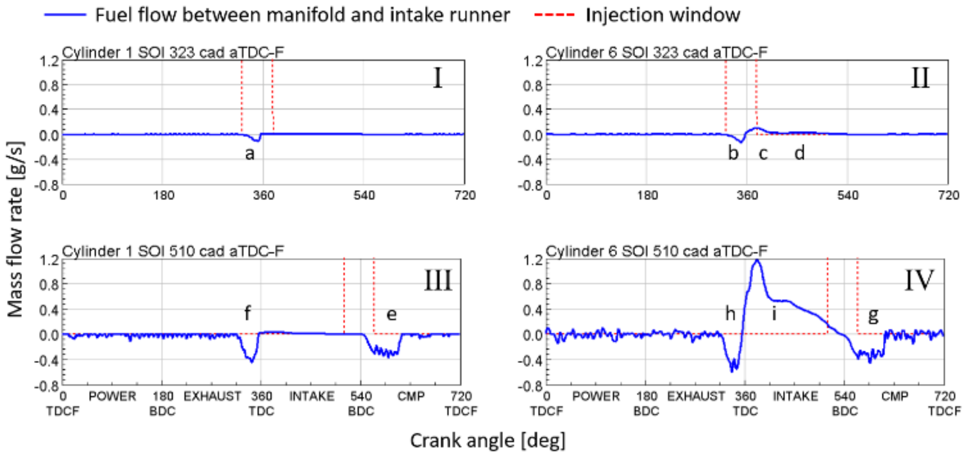

Figure 18 *Flow of natural gas between intake manifold plenum and intake port at cylinder 1 and 6 for two different gas injection timings. Positive flow denotes flow from plenum to intake port.*

In Figure 18 (III) and (IV), the situation is presented for an injection at the end of the intake stroke. At cylinder 1 a small backflow can be observed after the second BDC at (e), caused by the piston moving upwards again while the intake valve is still opened. The mass is higher than the previous case, because the intake stroke is already almost finished. As a consequence, the late injection is mainly ending up in the charge in the intake port. Ideally this fuel mass waits in the port for the next engine cycle, but a fraction is pushed into the plenum. The same happens just before TDC at (f), where the piston pushes back mixture in the intake port which still contains fuel from the previous injection. The same two peaks can be seen in cylinder 6 (g, h). The big difference here is that during the main part of the intake stroke fuel is flowing from the plenum to the intake port (i). This is the fuel that was pushed away at the upstream cylinders, and results in the richer mixture in downstream cylinders.

The analysis shows that a gas injection on a typical heavy-duty engine with very short runners should be phased in the middle of the intake stroke, preventing backflow into the plenum. Injecting before or after this phase is not per definition the result of badly chosen timing, but is inevitable if much longer injections are requested. This will be the case for higher loads and higher GER values. So next to an optimized timing, a high-capacity gas injection system, enabling a high fuel flow in short injections, is required to prevent the observed cylinder to cylinder variations.

3.3. Optical campaign on Wärtsilä W20DF

To improve our understanding of dual fuel combustion and the role of the pilot injection in a medium speed engine, research on the Wärtsilä W20DF marine engine at Lund University was performed. A former PhD student worked on the conversion of this engine into an optical engine [68]. In the present PhD work this engine was used to do optical research, in order to literally see how the pilot injection starts the combustion in RCCI and CDF mode.

The following section explains the used experimental equipment and methods of the optical campaign, followed by the main findings. More in-detail information on the results of this campaign can be found in ref. [69] (paper III in the appendix).

Methodology – equipment

Equipment

The base engine used in this campaign is a Wärtsilä W20DF, a 6 cylinder dual fuel engine with a 200mm bore diameter. Details of the engine can be found in Table 4. To increase controllability while reducing test complexity and costs, the engine runs as a single cylinder. To achieve this, the cylinder heads are removed from cylinder 2 till 6. These cylinders are blocked off, and holes in the piston crowns prevents compression and expansion of air. Cylinder 1, on the flywheel side, remains operating.

Table 4 *Medium speed engine specifications.*

Engine identification	Wärtsilä W20DF
Displaced volume	8.8 litre / cylinder
Bore	200 mm
Stroke	280 mm
Compression ratio	12.7:1
Number of valves	4 / cylinder
IVO	-5 CAD aTDC
EVO	-35 CAD aBDC
IVC	-35 CAD aBDC
EVC	10 CAD aTDC
Valve lift	17 mm

Optical engine configuration

For the optical campaign, cylinder 1 has been made optically accessible by a Bowditch design [70] as represented in Figure 19. The main components for the conversion to optical mode are the 600mm piston extension A, glass piston crown B, separate upper liner C, and a mechanical structure (D) to lift the cylinder head to its extended position. To balance the weight of the piston extension and glass piston crown, all other pistons have been equipped with a balance weight. The upper liner is separately cooled and is bolted to the window holder (E) which forms the upper part of the combustion chamber. In this part, four glass windows can be used to have lateral optical access to the combustion chamber. Inside the piston extension the mirror F is placed, glued on a rigid holder, at an angle of 45 degrees. Through the opening in the piston extension, the mirror holder is fixated on the engine block. The mirror allows a camera placed in front of the engine to have optical access to the combustion chamber, through the glass piston.

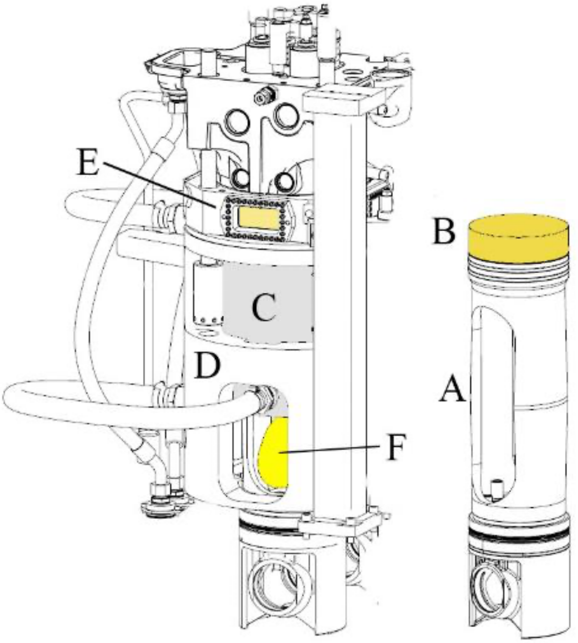

Figure 19 *Bowditch engine design, assembly and extended piston. Optical parts in yellow.*

Because of the complexity and novelty of the setup, it was chosen to start research at a safe operating point, with one of the most manageable types of optical research. Therefore, recording of natural luminescence with a high-speed camera was opted for. By using a non-laser-based method, it is not yet required to install a laser setup at the combustion chamber windows.

For the recording of natural luminescence from combustion, a Photron high-speed camera was used. The specifications and chosen settings can be found in Table 5. Camera settings were chosen such, that the complete piston window area was covered, at the highest possible frame rate. To prevent camera damage, the light sensitivity was chosen such, that extensive saturation of the camera's image chip by glowing soot was prevented.

Table 5 *Specifications and settings for optical recordings.*

Camera	Photron Fastcam SA5
Lens	Nikon 105mm / 2.8
Aperture	f#11
Shutter-speed	1/102000 sec
Frame-rate	15kHz
CAD/image	0.36 deg/frame
Resolution	576x584 pixels
Image size	533x533 pixels
Pixel density	4.1 pixel/mm
Pixel depth	$2^{12} = 4096$

In a Bowditch design the lower piston still has to be lubricated, but does not form a part of a closed volume. Because of this, attention has to be paid to maintaining the lubricating oil inside the engine. During design and implementation of the optical setup care has been taken to cover the lower piston and cylinder liner, and separate it from the area with optical components as much as possible. By creating a separate and enclosed volume above the lower piston, vacuum can be applied to prevent oil escaping into the optical area, which would limit visibility.

The engine and test cell set-up

To be able to do reliable measurements the test cell is equipped with a wide range of subsystems. All supporting periphery for the engine will be described in the following section. A complete overview of the test set-up is shown in Figure 20.

For reliable operation at constant conditions, the engine is equipped with an electrical preheating and an electrical pre-lubrication system. Since the engine is only running on one cylinder, warming up would take excessive time when it would be done by engine operation only. Thermostats ensure a constant operating temperature once warmed up. Cooling is done with tap water through a heat exchanger.

Since the engine is running as single cylinder, the original turbocharger could not be used. To mimic the compressor side of the turbocharger, pressurized air from the high-capacity workshop compressor system is used. The compressed air is admitted through a control valve. Although the initial goal was to run this valve on pressure control, better results were achieved with position control. The reason for this can be found in the high supply pressure of 10 bar. At boost levels common for this engine, the pressure ratio over the control valve is far beyond the ratio of 0.53 needed to reach choked flow. Reaching sonic conditions makes the mass flow only dependent on the supply pressure, which is constant, and the opened-up area of the control valve. This makes the position of the control valve directly proportional to the mass admitted to the engine. Being able to directly set the entering air-mass, independent of valve timing and lift, which is variable on this engine, makes testing more convenient, reliable, and precise.

After this control valve, the air is filtered and dried, and the mass flow is measured with a Coriolis flow meter. Next in line is a 70kW electric heater, to reach a realistic intake temperature. After removing pulsations by means of a 2000 litre buffer vessel, the air is supplied to the engine through its intake manifold.

To mimic the turbine, two butterfly valves were placed parallel in the exhaust system. A large valve allows coarse adjustment of the backpressure, while a smaller valve enables fine-tuning to exactly achieve the desired exhaust gas pressure.

The engine is equipped with an experimental Electro Hydraulic Valve Actuation (EHVA) system [71]. Two hydraulic pistons are directly actuating the intake and exhaust valves. The supply pressure comes from an engine-driven hydraulic pump. By means of two fast electronically controlled hydraulic valves, the desired valve timings and valve profiles can be created.

Instead of an individual plunger pump per cylinder, for research purposes the engine has been equipped with a common rail system. The system is based on an XPI system, originating from Scania. In the actual set-up it is driven by an external electric motor and can supply pressure up to 2200bar. The pilot injection is made by the full-size diesel injector, which is located centrally and is mounted perpendicularly in the cylinder head. The injector nozzle consists of 9 holes with a diameter of 295 µm and a spray angle of 156˚. Properties of the used pilot fuel, Swedish MK1 Diesel, are shown in Table 6.

The natural gas from the South Swedish gas grid was used as high-octane fuel. It is supplied through a pressure controller and flow meter, to a gas injector located in the intake port. The gas supply pressure was chosen such that sonic conditions were reached in the injector, making the system insensitive to pulsations in the engine's intake port.

Table 6 *Fuel specifications for the used high-reactivity and high-octane fuel.*

Diesel MK1	
Cetane number	51-54
H/C ratio [-]	1.87
Boiling point [˚C]	160-380
Density [kg/m^3]	810-820
LHV [MJ/kg]	43.15
Swedish Natural Gas	
Methane [mol-%]	88.91
Ethane [mol-%]	6.00
Propane [mol-%]	2.46
i-Butane [mol-%]	0.39
n-Butane [mol-%]	0.60
i-Pentane [mol-%]	0.13
n-Pentane [mol-%]	0.10
Hexane [mol-%]	0.05
Nitrogen [mol-%]	0.32
Carbon Dioxde [mol-%]	1.04
Methane Number [-]	71.70
LHV [MJ/kg]	47.90
Density [kg/m^3]	0.827

Control

The test cell control and engine control consists of multiple stages. The core of the control system is a LabVIEW application in the control room. This system has both monitoring and control tasks. For these purposes, it has an Ethernet connection with an Agilent data logger near the engine, an Ethernet connection with a LabVIEW real-time FPGA system, and USB connections with a diesel fuel scale and a Horiba emissions system.

The monitoring task provides the test cell operator with all relevant statuses, flows, temperatures, and pressures. Besides averaged values, it includes a graphical representation of crank-angle-resolved cylinder, intake, exhaust, and common-rail pressure. Based on the cylinder pressure measured and processed at the FPGA system, an apparent heat release is shown. It includes the derived parameters like IMEP, combustion phasing (CA50), and Start of Combustion. The monitoring part of the system also takes care of data storage. When a measurement is started, data can be stored for the desired number of cycles. The recorded data consists of three sets; a set of fast-recorded data sampled every 0.2 crank angle, the average values per engine cycle from the slower sensors, and all setpoint values per engine cycle.

A part of the functional control is done directly by the LabVIEW application. It actuates the air supply valve, the exhaust backpressure valves, and sends setpoints to the gas supply pressure regulator and the intake air heater. Control of the diesel and gas injection timing and duration; and the common rail pressure, is operated by the Wärtsilä CCM20 control unit. This is the OEM engine control unit, as used in marine applications. For research purposes it receives its setpoints from the LabVIEW FPGA application over a CAN connection.

The EHVA system is controlled by a dSpace MicroAutoBox, which can be initialized, set and real-time monitored with a dSpace dashboard on a separate pc in the control room.

To be able to control engine speed and absorb the delivered torque, the engine is direct coupled to a 355kW ABB electric motor. The invertor is placed in a separate electro powerhouse, and operated through a remote control in the engine control room. This is used to start and stop the system and give in the desired rpm set point.

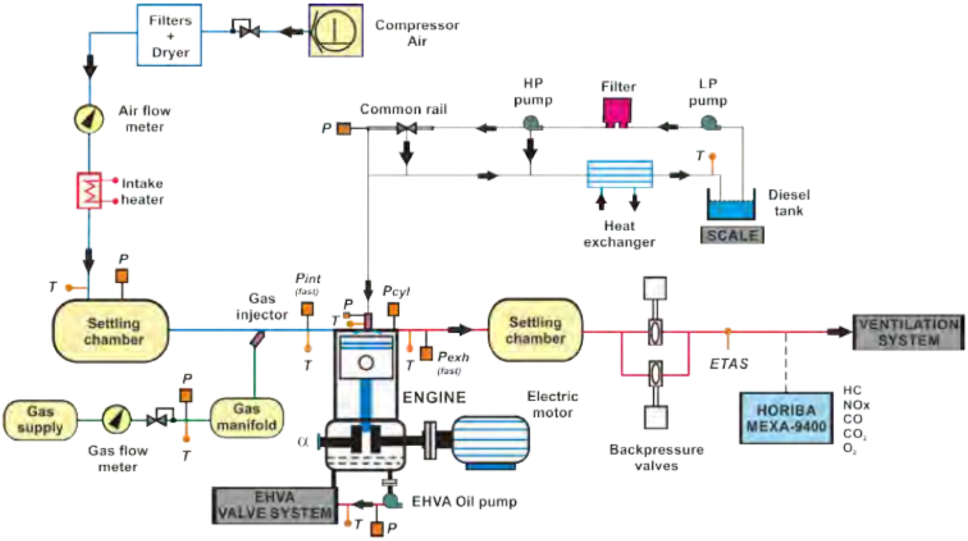
Filters
+
Dryer
Compressor
Air
Air flow
meter
Common rail
HP
pump
Filter
LP
pump
P
T
Intake
heater
Heat
exchanger
Diesel
tank
SCALE
P
T
Settling
chamber
Gas
injector
Pint
(fast)
P
T
Pcyl
T
Pexh
(fast)
T
Settling
chamber
ETAS
VENTILATION
SYSTEM
P
Gas
supply
Gas flow
meter
T
Gas
manifold
α
ENGINE
Electric
motor
Backpressure
valves
HORIBA
MEXA-9400
HC
NOx
CO
CO₂
O₂
EHVA
VALVE SYSTEM
EHVA Oil pump
T
P

Figure 20 *Schematic overview of W20DF test cell. [68]*

Operating points

All measurements were performed at 900 rpm. This is the lowest nominal speed at which this engine is used in applications. A limited speed is relevant because of possible elongation of the piston extension because of mass-forces. Also, it was decided to start with medium load tests, for a safety margin against the design limits of the optical setup. In total 10 different pilot injections were examined, with a rail pressure ranging from 1200 till 2000 bar, and injection duration of 300, 340 and 390 µs. All optical measurements were performed in skip-fire mode, which make emission measurements impossible. Skip-fire mode was applied to prevent thermal overloading of the glass piston. A sequence of 6 fired and 6 unfired cycles was used.

Methodology - post processing

For a proper analysis of the results from this campaign, specific post-processing was required. Because of the large data amount, post-processing was automated through Matlab scripts. Measurements consisted of two separate data streams: the LabVIEW data and the optical data. Both will be elaborated separately.

LabVIEW engine test data

The first step was to convert and organize all recorded LabVIEW data from all performed tests into one single Matlab structure per test. The most important part of the processing of this data is converting the raw measured cylinder pressure sensor data into a heat release analysis. The process contains the following steps:

- TDC correction. A motoring cycle is used to find the exact position of top dead centre. The motoring cycle is also used to determine the exact compression ratio of the engine. An adjustment on the known geometrical value is done, to indicate zero heat release during motoring.
- Pressure pegging. To correct for drift of the piezo-electric cylinder pressure sensor, the sensor measurement is shifted to match with the measured absolute intake pressure at bottom dead centre, obtained from a separate sensor.
- Estimation of the polytropic exponents, γ. This is done by iteratively finding the best fit between a polytropic and the measured in-cylinder process, outside of the combustion process. According to [72] a separate value is estimated for the compression and the expansion stroke.
- Heat release rate. Based on Equation *(3)*, the apparent heat release rate can be calculated as an indicator for the combustion intensity. The obtained values are the basis for the integrated heat release.
- Heat release indicators. By normalizing the integrated heat release, the crank angle positions for 5%, 10%, 50% and 90% combustion progress can be found. The found values are used as indicator for respectively start of combustion, combustion phasing and end of combustion

$$\frac{dQ_{hr}}{d\theta}=\frac{\gamma}{\gamma-1}P\frac{dV}{d\theta}+\frac{1}{\gamma-1}V\frac{dP}{d\theta} \tag{3}$$

Optical data

Data processing of optical data is challenging because of the large amount of data that is involved. Besides the required storage space, it results in time consuming file transfers and data processing. In the performed optical campaign, a single test resulted in 8 Gb of data. For this reason data is cut where allowed, before starting with the actual post-processing. The following steps were taken:

Frame cutting

Although the camera position and frame size were optimized to have as much useful area as possible, the recorded image is still slightly larger than the maximum available piston window. The recorded images had a frame size of 576*584 pixels, and were reduced to a circle with a diameter of 533 pixels. Besides limiting data size it also ensures that reflections on the piston extension, outside of the glass piston window, are not influencing the analyses. This step reduced the data size per test to 5 Gb.

Frame selection

During all tests, the trigger for camera recording was set at the start of injection. Although it is known that it takes at least the time of the ignition delay before visible light can be observed, it was seen as a risk and unnecessary addition of complexity to add a case-sensitive delay on this trigger. As a result, all recordings start with a significant amount of black images. Since images can contain artefacts or noise, and because of cycle-to-cycle variations, it was not sufficient to simply search for black images and delete them. As a solution, the sum of pixel intensities was calculated per image. Per cycle of each test the first image exceeding the noise limit was found, and the earliest of all cycles was selected. Adding a safety margin of 4 images, the start image of the selection was defined. To increase file handling speed, all remaining images were stored in one single Matlab array per test. This resulted in a file size of around 1,5 Gb. At this stage it was important to do proper book-keeping, and store which image belongs to which crank angle position. At the same time the camera-settings were retrieved from a camera-specific file and stored in the same Matlab dataset.

Image analysis

Since it was not known in detail upfront which information could be retrieved from the images, the analysis was started with extensive viewing sessions of the recorded images. Looking at pixel data and images at the same time, it was observed that very dark images contained much more information than the human eye could recognize. This was solved by applying a gamma filter, where a gamma value of 0.4 gave satisfying results. The results of this non-linear filtering can be seen in Figure 21.

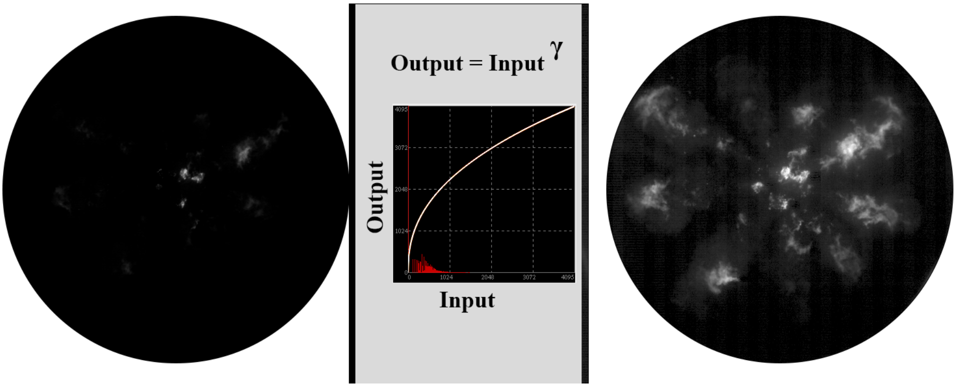

Figure 21 *Combustion image before and after gamma filtering.*

To be able to go through the images in a convenient way, the images from every test were converted into a movie.

Images with different colour mappings were tried, and also analytic attempts were made to distinguish between gas and diesel combustion based on a simple pixel intensity threshold, but without satisfying results. The next section lists which indicators could be retrieved successfully from the images.

Parameter calculations

Amount of light

To create an indication for how intensely the combustion is visible during the cycle, the integrated amount of light per image can be calculated over an engine cycle. This analysis is shown in Figure 22, combined with individual combustion images from an RCCI and a CDF case. No absolute analytics can be taken from such results, but it can be used for comparative purposes.

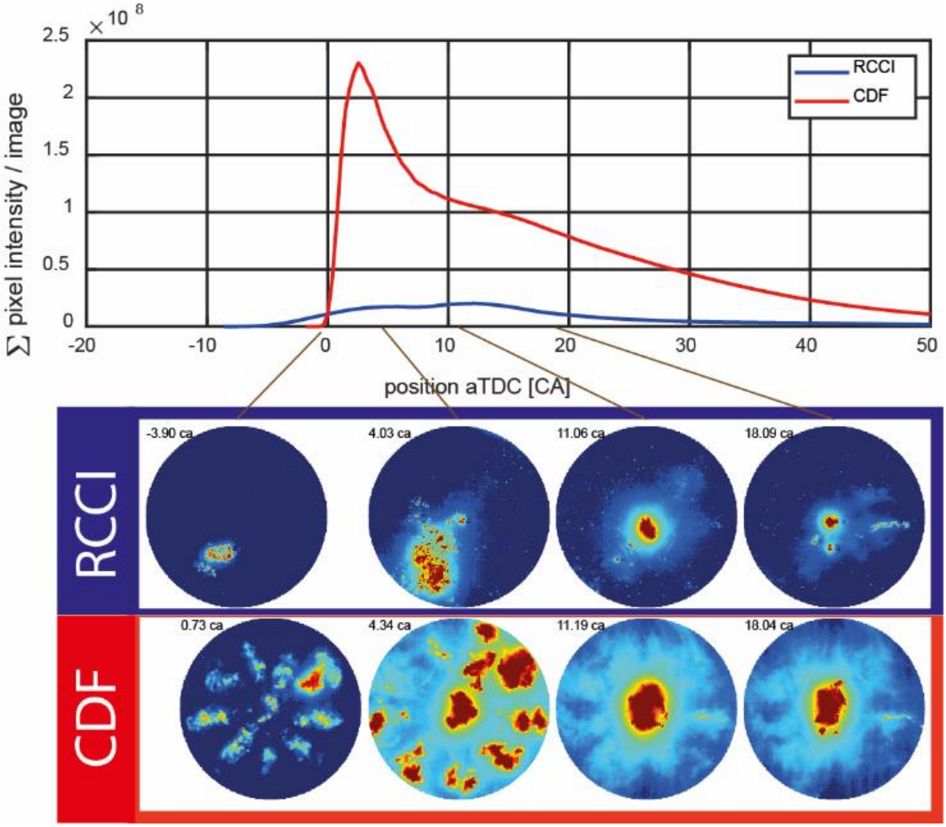

Figure 22 *Sum of emitted light during combustion, for RCCI and CDF combustion mode, with colour-mapped combustion images.*

Start of combustion position

By finding, per cycle, the first pictures above a carefully chosen noise threshold, the position where the first combustion occurred could be identified. This position was expressed as a function of radius from the centre and azimuth angle inside the cylinder. An azimuth angle of zero is positioned between exhaust and intake valves, where a positive angle rotates towards the exhaust valves and a negative angle towards the intake valves. When multiple pixels above the noise threshold were found at the same time, the radial position could be averaged. For the angular position this would not give a realistic result in cases with multiple ignition kernels, and was for that reason not done.

Development of light profile inside the combustion chamber

Although the movies created much insight into how the combustion develops under different conditions, this type of data is very difficult to use in printed material. Showing a selection of stills from a movie did not give a satisfying result. A solution was found in creating a 3D surface graph, representing the development of combustion light during the cycle. The chosen method of presentation can be seen in Figure 23 for pure diesel operation at medium load as reference. For every consecutive image of the combustion process an integration of pixel intensities is made along radial lines, anti-clockwise through the combustion chamber. The development of the combustion process over time can be followed along the crank angle position axis. The angular position in the cylinder is represented by the azimuth angle. In Figure 23, the nine separate jets of the diesel injector can be clearly recognized. Also the increase and decrease of combustion intensity during the combustion process can be identified.

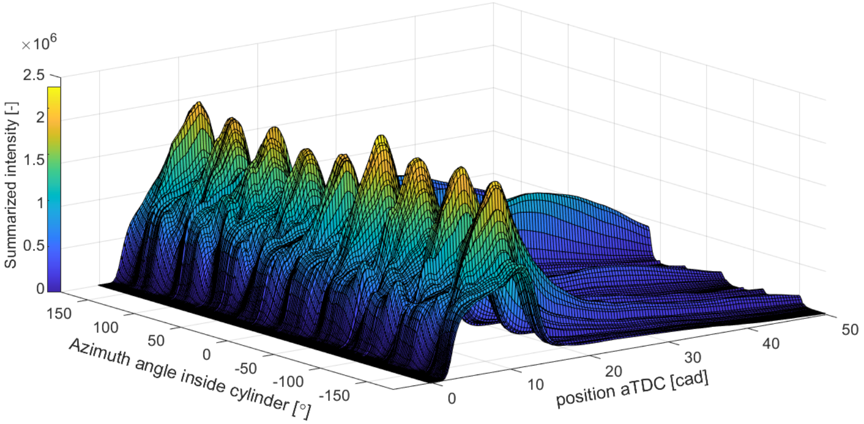

Figure 23 *Combustion light intensity, radially integrated per time-step. Medium load diesel-only combustion.*

Results, conclusions and outlook

During the campaign ten different fuel pressure / injection duration combinations were tested, resulting in six different pilot masses. All ten different pilots were tested with an early injection timing – representing RCCI combustion, and a late timing – representing CDF. Within its early (70-30 CAD bTDC) or late (5-20 CAD bTDC) timing domain, the timing of every pilot case was optimized to reach a reasonable combustion phasing.

As expected, the RCCI cases resulted in a significantly longer ignition delay. This can be seen in Figure 24. During this longer ignition delay, the fuel has more time to dilute, and to move away from the injector. This phenomenon can be clearly identified by the start of combustion taking place at a larger radius for RCCI cases, compared to CDF. This is shown in Figure 25, which was created from an analysis of the combustion images. Not only the start of combustion is different, also the progress varies significantly between RCCI and CDF. A series of images along the combustion progress for both modes was shown in Figure 22. From these images it can be concluded that in CDF mode the combustion is following the shape of the pilot and shows a high light intensity. RCCI combustion is not controlled by the shape of the diesel jet and takes place at varying places at varying intensity levels.

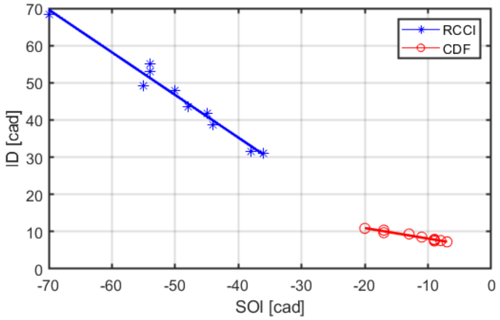

***Figure 24** Observed ignition delay for all tested pilots end their timing, in RCCI and CDF mode.*

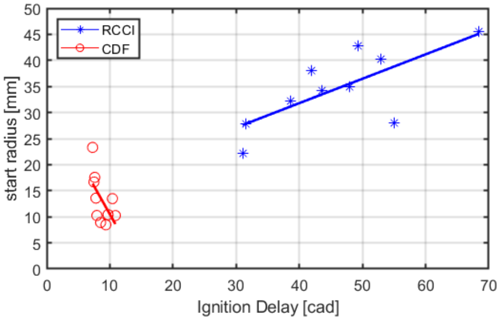

***Figure 25** Optically determined position for start of combustion, related to observed ignition delay.*

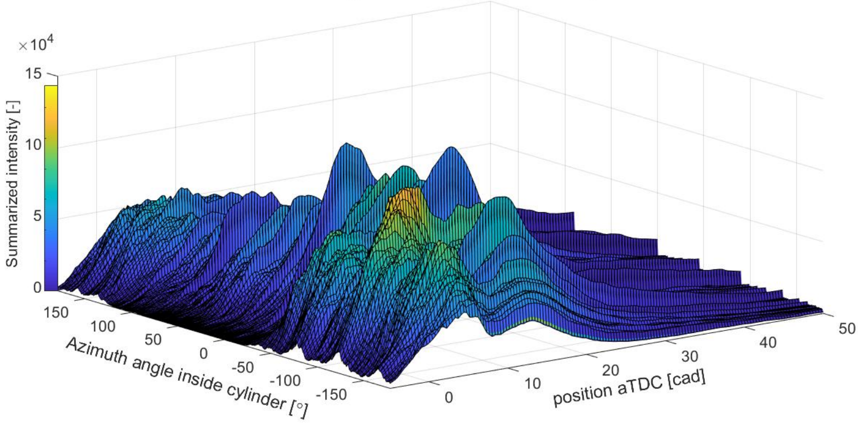

***Figure 26** Development of combustion, based on intensity of emitted light, radially integrated in the combustion chamber. RCCI case*

To give a better indication of the recognition of the jet shape in combustion images, Figure 26 and Figure 27 are created conform the method already explained for Figure 23. Although less clear than in the pure diesel case, in the CDF case the individual jets can still be well recognized. Not all jets show the same intensity, which might be related to the very short injections or the actual condition of the injector. In RCCI mode, the location of light is much more random, and recognition of the presence of nine jets is not possible. Also, a more gradual increase and decrease of intensity is seen, while in CDF mode, intense peaks are seen. It is this high intensity of combustion, as a rich diffusive flame around the diesel jet, that is correlated to NO_x formation.

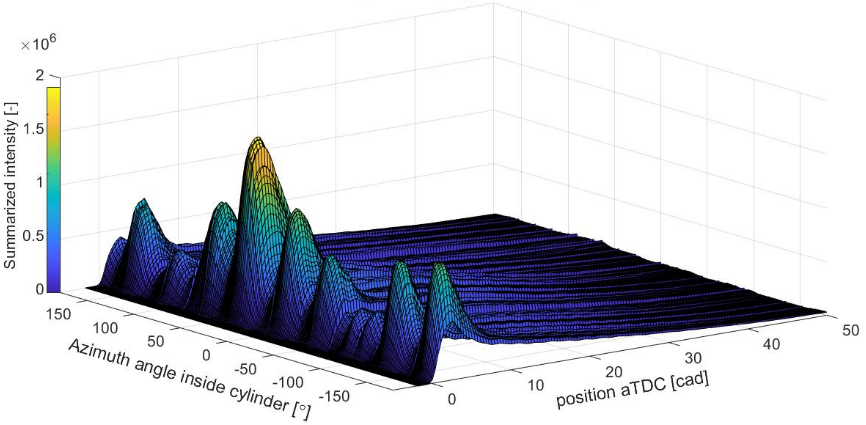

Figure 27 *Development of combustion, based on intensity of emitted light, radially integrated in the combustion chamber. CDF case*

Limitations

During a previous PhD project on the Wärtsilä engine [68] an excellent effort was delivered to prepare the test cell for optical diagnostics. Because of limited time and the wide scope of that project, the test set-up was not completely validated. As a result, a fair list of issues showed up during preparation for this optical campaign. Most of them were solved, but one of them was persistent; oil contamination on the mirror and on the glass piston. This oil is leaking around the lower piston rings and can enter the area inside the piston extension and create visibility problems. Several improvements had already been tried during a previous campaign, like reducing oil supply through the con-rod, and optimizing the piston rings. Unfortunately this did not give the desired results. Also covering up the open area and connecting it to multiple vacuum pumps to flow away oil vapour did not improve the situation. The work-around that was applied during the described optical campaign was to test in very short runs, alternated with repetitive extensive cleaning of the mirror and piston crown. Although far from ideal, it at least allowed to acquire optical results. During a separate test without piston extension, the high-speed camera was placed inside the cylinder in an attempt to identify and better understand the origin of the oil contamination. A result of this investigation can be seen in Figure 28, which clearly shows that the oil does not show up as vapour as was assumed, but as clear droplets. From this it can be concluded that more rigorous measures are needed to prevent oil passing the piston rings. The next step considered is to add a significant spring force to the piston rings, replacing the missing combustion pressure on the rings.

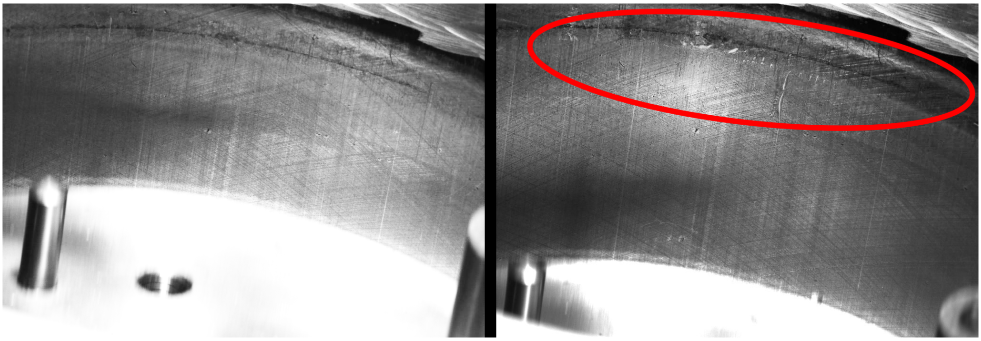

Figure 28 *High-speed recording of cylinder liner on running engine, at start and after 30sec running. Encircled the occurring oil droplets and traces.*

For optical campaigns dual fuel is a challenging concept. It requires a high range of optical sensitivity since it contains both rich combustion with strongly emitting soot, and the faint light of natural gas combustion. This limitation became apparent in attempts to calculate a flame propagation speed based on the recorded images. With the current set-up it was not possible to do this correctly. Especially in RCCI operation the recorded light is too close to the noise level, to come to a reliable result. The calculations showed to be very sensitive to the chosen noise threshold level, and no relation between flame propagation speed and heat release could be assigned. When in a next campaign the soot luminescence would be taken out with an optical band-pass filter, more camera sensitivity can be applied on the natural gas combustion. In a subsequent research phase, laser spectroscopy could be used to analyse the start and progress of the combustion more in detail.

It also has to be noted that this campaign was only the starting point. It consisted of one load case with limited knowledge on parameter optimization while only making use of natural luminescence as optical diagnostics methodology. However, it was an important step that was taken: all hardware is now up and running, and the required improvements are known. As follow-up, a metal campaign was executed to get more insight into desired combustion parameters (as detailed in the next section). Parts were designed to solve the oil problem. Based on the optical results it was concluded how the optical diagnostics can be improved.

3.4. Metal campaign on W20DF

This section describes the experimental campaign, executed on the “metal configuration” of the Wärtsilä W20DF set-up, as follow-up on the optical campaign that was explained in the previous section. It serves to create a better understanding of the differences between RCCI and CDF operation than were seen in the optical analysis of combustion. The found data will serve the development of the conceptual model as described in Chapter 4, and can be used for the definition of operating conditions for a future optical campaign. The main conclusions will be given in the following paragraph, while more details on the campaign can be found in ref. [56] (paper V in the appendix).

Methodology

The same engine as for the optical campaign was used to perform the metal campaign. Metal mode means all optical components are removed, and the original piston is fitted, with the cylinder head mounted directly on the engine block again, as shown in Figure 29. The metal single cylinder configuration is equipped with the same EHVA system and injector hardware and can run on the same parameter sets as used in the optical campaign.

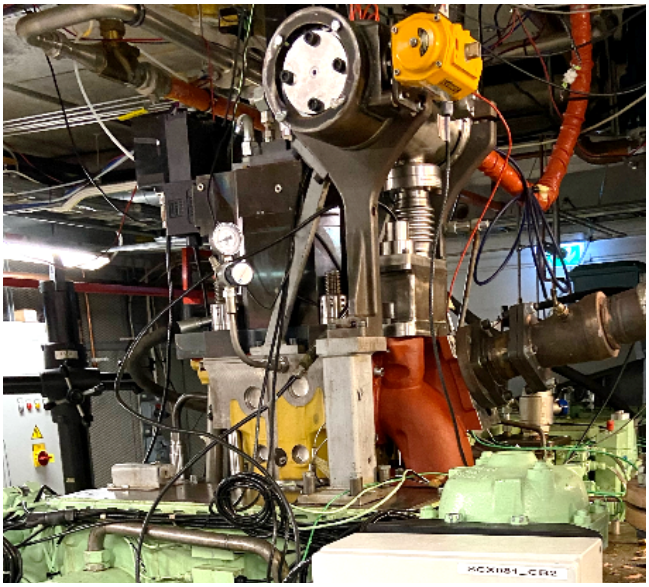

Figure 29 *Wärtsilä W20DF in metal configuration.*

All tests were run on diesel and natural gas as described in Table 6. Instead of the skip-fire mode needed for optical operation, in metal mode the engine can run in continuous-firing mode, allowing reliable emission measurements.

Emissions are sampled at the end of the exhaust pipe, and continuously analysed with a Horiba MEXA system. To take care of sampling delay, measurements are only started after all measurement values have stabilized. For fast NO_x measurements during set-up, the engine is equipped with a uniNO_x sensor in the exhaust system. Each measurement was recorded for 300 combustion cycles, over which the results were averaged.

Operating points

The campaign was performed at 900 rpm, at three different loads. For these loads the required gas amount was determined, and kept constant during all tests. Running with a constant fuel input while varying the conditions, results in a variation of engine output. The measured reference IMEP values for the three load cases were 10, 14 and 18 bar.

Experiments were performed using several pilot injection settings, with a rail pressure ranging from 1100 to 2000 bar and an injection duration from 300 till 620 µs. The caused change in energy input was taken into account during analysis and calculation of results.

***Table** 7 Base operating conditions during metal campaign*

Engine speed	900 rpm
Lambda	1.95
Diesel railpressure	1700 bar
Diesel injection duration	300 µs
Reference IMEP	14 bar – medium load

The tests performed at the conditions presented in Table 7 will be elaborated in the next paragraph. With rather limited complications caused by knock and misfire, this set allowed to do a wide and reliable collection of data. This makes the set suitable to create insights, under representative conditions that can also be run safely in the optical configuration. The core of the experiments was the variation of the pilot injection timing over the range from early RCCI till late CDF operation.

The sweep over SOI for the selected medium load case consisted of 9 individual tests, with an SOI ranging from 52 till 18 CAD bTDC. Outside of this range a too strong increase in misfire was observed. No measurements were taken in the range from 38 till 25 degrees bTDC, because of knock limitations. Operating points earlier than this range are identified as RCCI mode, the points later than this range are representing CDF mode.

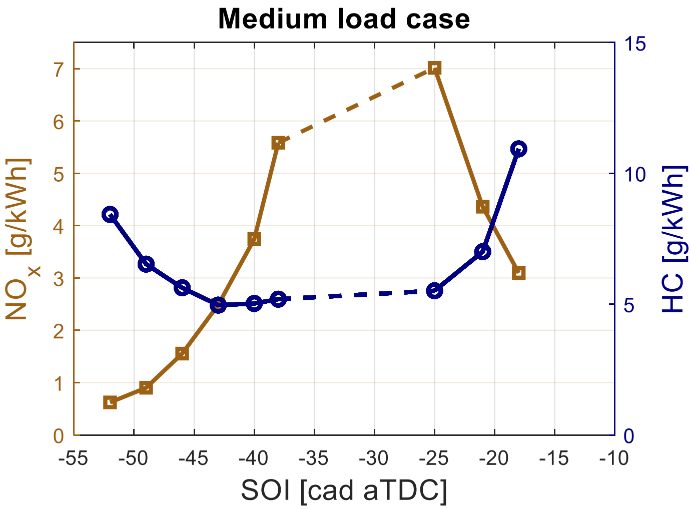

Figure 30 *Specific emission of NO$_x$ and uHC over a sweep of injection timings.*

In Figure 30 the specific NO$_x$ and uHC emissions are shown. In the CDF range a typical diesel behaviour is seen, where a later SOI results in a lower emission of oxides of nitrogen. In RCCI mode the opposite is seen, where further advancing from 38 degrees before TDC results in a decrease of this emission.

The emissions of unburned methane show the opposite behaviour of the NO$_x$ emissions. The minimum of unburned methane can be found in the area where NO$_x$ peaks, and advancing or retarding the injection timing results in an increase of specific uHC. That uHC shows a range where it clips at a minimum value, around 2.5g/kWh, suggests that emissions are not further influenced anymore by combustion behaviour. It could be suggested that the remaining 2.5 g/kWh is coming from methane slip, or flame quenching above the piston rings, but this was not investigated or proven in this work.

The indicated efficiency is shown in Figure 31. Two important factors influencing the efficiency are the completeness and the phasing of the combustion. Completeness of combustion is related to uHC emissions, as shown in Figure 30. The combustion phasing is shown in Figure 31, represented by the crank angle at which 50% of heat is released from combustion.

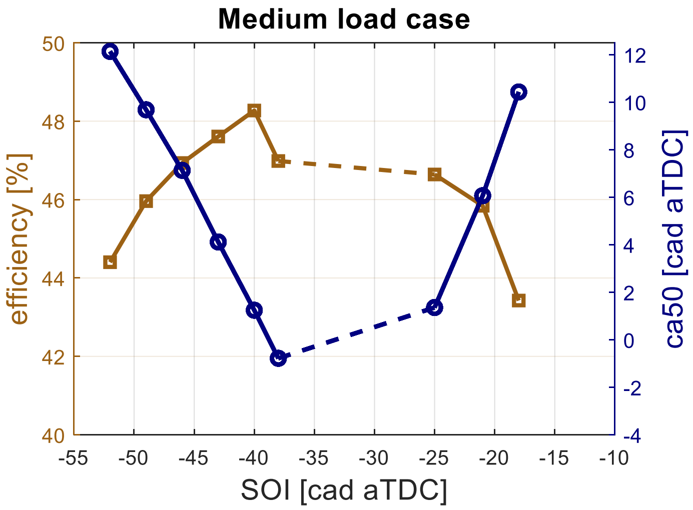

Figure 31 *Indicated efficiency and combustion phasing over a sweep of injection timings.*

The highest efficiencies can be found at late RCCI and early CDF combustion. These are the cases with lowest uHC emission. The better combustion quality helps to increase engine efficiency: more of the injected fuel is effectively used in the combustion process. The variation of combustion quality makes it impossible to strongly assess the separate influence of combustion phasing. An indication that can be drawn from Figure 31 is that late combustion phasing goes with a reduction in efficiency. Only a clear conclusion can be drawn from two measured points in RCCI mode, with a SOI of 40 CAD and 38 CAD bTDC. With 5 g/kWh uHC emission, their combustion quality can be considered equal. Shifting CA50 to 0.8 CAD bTDC is obviously too early, leading to an efficiency reduction of 1%.

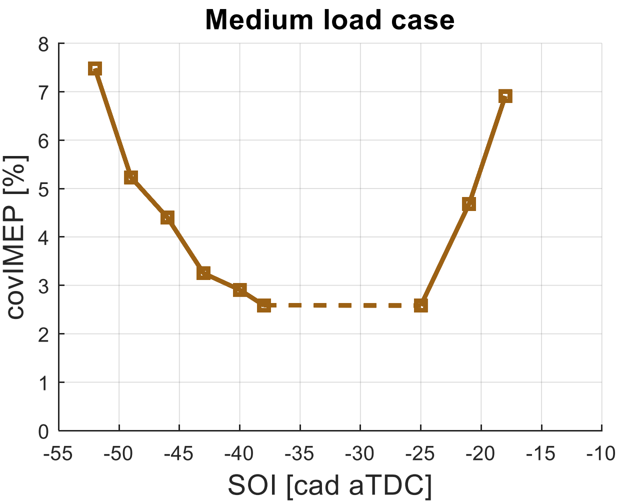

Figure 32 *Coefficient of variation of measured IMEP, for a sweep of injection timings.*

The last limiting aspect for dual fuel combustion that was investigated is the cycle-to-cycle variation, represented by the coefficient of variation on IMEP. It is calculated on the measured cycles from each single test conform Equation *(4)*. The results are shown in Figure 32.

$$cov_{IMEP} = \frac{\sigma_{IMEP}}{IMEP} * 100\%$$

(4)

The trends shown are highly comparable to the behaviour seen for uHC emissions. The lowest variations are found at late RCCI and early CDF SOI, which are the cases with the earliest combustion phasing. Further retarding of the combustion increases the cycle-to-cycle variation. Although COV_{IMEP} can be related to variability of external operating parameters [73], in this case it is mainly induced by the conditions during combustion. The later phasing of the combustion process means this takes place at a lower pressure and temperature. This limits the fast and steady propagation of combustion in the lean natural gas mixture, resulting in an increase in COV_{IMEP}.

Main findings

The Start of Injection timing sweep has shown there is a trade-off between NO_x versus efficiency, uHC and COV_{IMEP}. Which injection timing within this compromise should be preferred is strongly dependent on the requirements and legislation of the engine's application. For marine applications there is a strong focus on NO_x legislation, which makes the RCCI combustion mode most interesting for the tested conditions. The shown NO_X reduction in this mode suggests that LTC is actually achieved, where enough dilution of the pilot fuel prevents the initially high-intensity premixed combustion. A comparison of heat release rates between RCCI and CDF mode from the described campaign is shown in Figure 33, which endorses this LTC assumption.

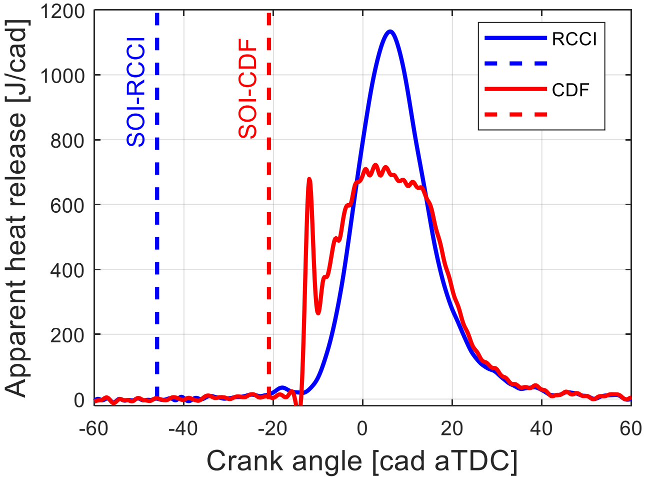

Figure 33 *Heat release for RCCI and CDF timing cases, recorded at medium load in the metal campaign.*

To achieve low NO_x while not strongly deteriorating the other relevant indicators, the injection should not be placed too early in the RCCI range. In the shown data an optimum can be found at an SOI in the range from 40 to 45 CAD bTDC. Here a NO_x value below 2 g/kWh is combined with an efficiency close to the achievable maximum and uHC close to the achievable minimum. Only the COV_{IMEP} that is reached at this point is rather high at 4%. Although dependent on the application, commonly a range of 3 to 5% is mentioned, above which the variation becomes noticeable in a driveline [74].

The emission results show that when running at the suggested timing of 40 to 45 CAD bTDC, a further advance is needed if a lower NO_x output is required. The opposite direction is required when the engine is running at a timing later than 25 CAD bTDC. This can be related to the reversing relationship with SOI and CA50 that was presented in Figure 31. This matches with the behaviour of SOC that was shown in Figure 10.

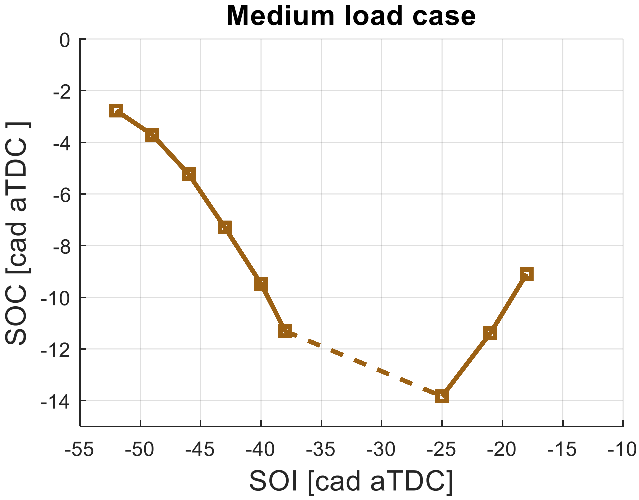

Figure 34 *Start of combustion resulting from variation of pilot timing in the range from RCCI till CDF.*

The same representation can be made for this actual dataset, which is shown in Figure 34. Here it can be seen that before 38 CAD bTDC an advancement in pilot timing results in a later start of combustion. After 25 CAD bTDC, retarding the pilot timing is required to create a later start of combustion. A conceptual explanation of this difference will be given in Chapter 4.

4. Conceptual model

As seen in previous campaigns, optimizing the dual fuel engine for emissions and performance requires a proper control of combustion phasing. One of the most obvious and fastest means to control this, is by adjusting the start of combustion through the timing of the pilot injection. The fact that for CDF and RCCI operation the relation between the start of injection and the start of combustion is opposite, can complicate this control.

To be able to properly operate a dual fuel engine in both modes, and in operating points at or close to the transition area between the two modes, a clear understanding of this changing relationship is desired. In this chapter an explanation will be developed based on the physics taking place in the combustion chamber. The focus will be on the conceptual difference between CDF and RCCI. This will be done by means of a white box model. By limiting the level of detail in favour of a conceptual understanding, the computational cost of the model is limited to make it suitable for future application in an engine controller.

The first paragraph of this chapter explains the basic assumptions from which the conceptual model will be constructed. In the second paragraph a verification of the model will be done, by combining measurement data and existing numerical tools. In the third paragraph the conceptual model will be used to create insight in the effect of parameter variations in dual fuel engines. A more detailed elaboration on the model can be found in ref. [75], paper IV in the appendix.

4.1. From assumption to concept

In a dual fuel engine two fuels with a different reactivity are combined in one cylinder. The fuel of the pilot injection, which has the higher reactivity, will be the fuel that ignites earliest. The moment at which this fuel starts to react, is dependent on its local temperature and equivalence ratio. As such, the ignitability is the result of both the thermodynamic conditions in the cylinder, and the progress of the spray formation of the pilot injection. To come to a description of the moment at which these conditions are reached, we start with listing the following sets of basic assumptions on temperature, mixture formation and ignitability:

Temperature

A1. Diesel fuel has a minimum ignition temperature $T_{ignition}$ of 210°C, 483K [76].
A2. Diesel is injected, heated up by the Fuel Injection Equipment (FIE), at a temperature T_{diesel}, slightly above ambient temperature.
A3. The diesel fuel warms up from T_{diesel} till $T_{cylinder}$, which will be described as a first order system.

Mixture formation

B1. Diesel fuel is injected at SOI, having an initial lambda (λ) value λ_{start} of 0.
B2. The final amount of trapped air, methane and injected diesel in the cylinder combine to λ_{global} as end value.
B3. The injected diesel fuel undergoes a trajectory from λ_{start} till λ_{global}. Although the detailed steps from liquid fuel till fully mixed vapour are known [77] and will initially show a distribution profile, it will be described here as a basic first order system [78].

Ignitability

C1. SOC takes place when the diesel fuel has reached the required T and λ.
C2. Combustion locally takes place under stoichiometric conditions, concluding $T_{ignition}$ is valid for λ=1.
C3. Increasing temperature above $T_{ignition}$ increases λ-ignitability limits.

Step by step we will elaborate on the basic assumptions, and place them in the perspective of the observations during engine measurements, discussed in the previous chapter. Two specific test cases will be used for this, one RCCI and one CDF case. Their most relevant data is listed in Table 8.

Many physical processes like heating, cooling [79] and mixing, which have an exponential response on a step input can be described as first order system. When assuming that the warm-up of the injected fuel can also be seen as a first order system that starts at the fuel supply temperature, and will end at $T_{cylinder}$, it can be described with Equation *(5)*.

$$T_{fuel}(t) = T_{diesel} + (T_{cylinder} - T_{diesel}) * (1 - e^{-\frac{t}{\tau 1}}) \tag{5}$$

Table 8 *Test data of a CDF and RCCI case, for setup up the conceptual model.*

Engine speed	900	[rpm]
IMEP, RCCI | CDF	13.5 | 10.5	[bar]
Intake pressure	2.3	[bar]
Gas amount	507	[mg]
Diesel amount	18	[mg]
Lambda global	2.2	[-]
Gas/diesel energy ratio	96.8	[%]
Rail pressure	1705	[bar]
Injection duration	300	[µs]
SOI, RCCI | CDF	46 | 9	[ca BTDC]
Start of combustion, RCCI | CDF	5.2 | 1.5	[ca BTDC]
CA 50, RCCI | CDF	7.1 |16.4	[ca ATDC]
Ignition delay, RCCI | CDF	40.8 | 7.5	[ca]

To fulfil assumption A1, time constant τ1 can be fitted such, that at the SOC for CDF, the required temperature of 483K is achieved. This results in a time constant of 4.1 ms for warming up. At each time step the actual cylinder temperature is applied, which enables the same time constant to be applied for warming up in the RCCI case. The warm-up curves for CDF and RCCI are shown in Figure 35. Since mixing and warming up are transient processes evolving in time, the corresponding graphs are created with a time-axis instead of a crank angle-axis. Time zero represents top dead centre of the engine.

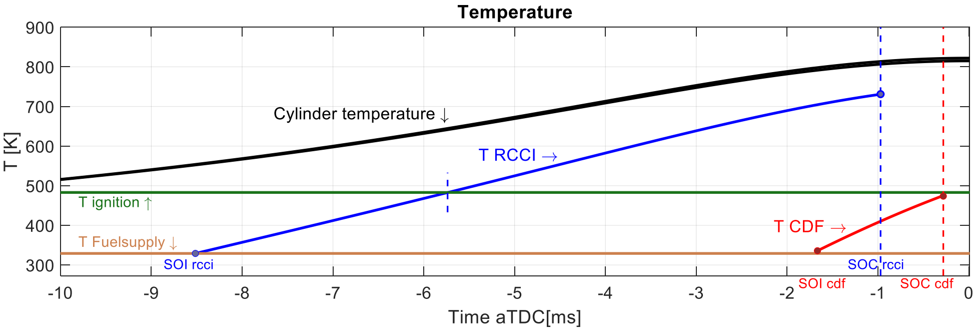

Figure 35 *Warming up of injected fuel under CDF and RCCI conditions.*

The warm-up curve for RCCI operation shows that the minimum ignition temperature for diesel fuel is reached at 5.8 ms before TDC. The engine experiments, however, have shown that combustion is not starting at this moment, but it takes until 0.5 ms before TDC until the RCCI combustion starts.

Since ignitability is not only dependant on temperature but also on air-fuel ratio, the second set of assumptions will now be processed. They describe how the injected fuel mixes with the air-gas mixture in the cylinder. Although the mixing of the diesel injection can be described in detailed steps, we will start here with a simple approximation. In the same way as done with the temperature of the injected fuel, we will describe its mixing as a first order system represented by Equation *(6)*. A more detailed representation by a spray model will follow later.

$$\lambda = \lambda_{final} * (1 - e^{-\frac{t}{\tau 2}}) \tag{6}$$

Taking into consideration that combustion locally takes place under lambda = 1 conditions, τ2 will be fitted such that this mixture condition is reached at SOC for the CDF case. This is depicted by the dilution curve shown in Figure 36. In the same figure the dilution curve for RCCI is shown, making use of the same time constant of 2.3 ms.

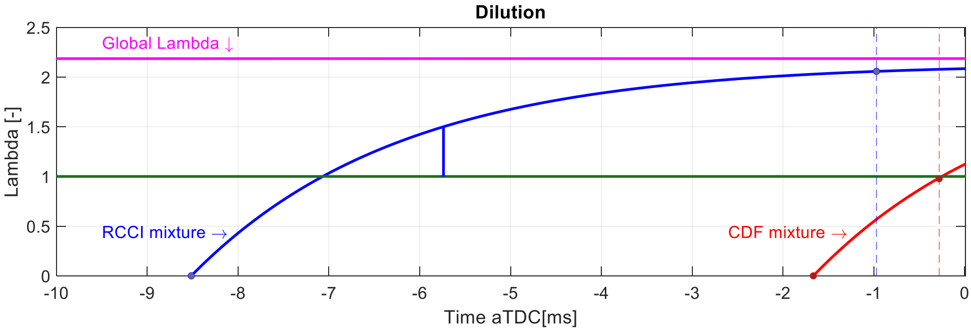

Figure 36 *Dilution of injected fuel towards global lambda, for CDF and RCCI operation.*

Based on the made assumptions, for CDF operation the conditions required to start the combustion are met at SOC. For RCCI operation this conclusion cannot be drawn. At t=-5.8 ms the stated minimum required temperature is reached, but at this moment the mixture is already leaner than lambda = 1. This explains why combustion is not starting at t=-5.8 ms. To explain how ignitable conditions are reached in RCCI mode, we need to include assumption C3, on how increasing temperature increases the lambda-ignitability limits. An expansion of the ignitable lambda value will be created, based on the difference between the actual fuel temperature and the minimum ignition temperature of diesel fuel. This is parametrized such, that the RCCI dilution curve will reach the ignitability limit at SOC_RCCI. This can be seen in Figure 37, where the green island represents the area where conditions to start combustion are met. The same expansion could be expected in the fuel rich area, but is left out here for simplicity.

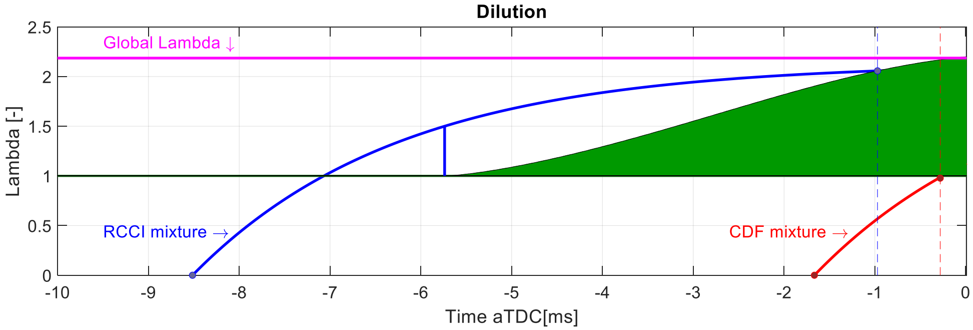

Figure 37 *Ignitability island, indicating the required lambda at the actual temperature, to achieve ignition.*

The shown concept at this stage has no quantitative predictive value to describe the start of combustion for CDF and RCCI, because the parameters were exactly tuned to match the upfront known start of combustion. But despite this parameter tuning it can still be used to explain the difference between CDF and RCCI in the way their ignitable conditions are met. For CDF, the temperature criterion inside the cylinder is already met at the start of injection, so the ignition delay boils down to the time required for spray formation and dilution from pure fuel towards an ignitable mixture. Graphically it can be summarized as approaching the green ignitability island from the rich side. For RCCI operation, an ignitable temperature is not available yet at the start of injection, giving much time for dilution. The ignition delay is the time needed for reaching a sufficiently high temperature, to ignite the diluted mixture. Graphically this can be seen as approaching the ignitability limit from the lean side.

The two graphical observations can be used to explain the relation between start of injection and start of combustion. For the CDF case it is clear that a shift of injection timing would lead to an almost equal shift of the moment at which combustion starts. When injection timing is retarded for RCCI, and we represent it with a shift of the dilution curve to the right in Figure 38, it can be concluded that the ignitability island will be hit earlier in time. Physically this can be explained by the fact that a later injection reduces the time available for dilution, and thus requires a lower temperature before combustion can start. In the same way the concept of the ignitability island can explain how an earlier injection will result in a later start of combustion. With this, the behaviour as shown in Figure 10 and Figure 34 can be explained.

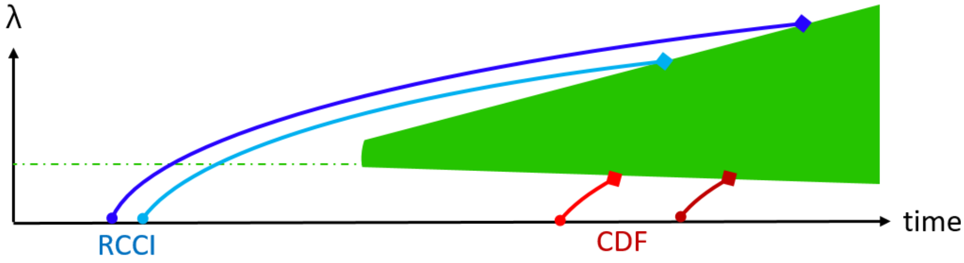

Figure 38 *Effect of SOI change, for CDF and RCCI operation.*

In the next section this concept based on assumptions will be verified in more detail, making use of a combination of experimental data, 1D spray simulation and performed detailed kinetic calculations.

4.2. Verification of the assumptions

A conceptual model has been composed, which can be used to explain the relation between start of injection and start of combustion both in CDF and RCCI mode. As a next step, the assumptions on which the model was built will be replaced by combinations of simulation and measurement data. This serves the goal to increase the reliability of the conceptual model, and get more insights in its benefits and limitations.

The model is based on three different phenomena, which will be detailed in this paragraph. Insight in the behaviour of the spray and its dilution will be created making use of a 1D spray simulation tool. To get more insight on the ignitability of the mixture, a chemical kinetic scheme will be used. Finally, the in-cylinder conditions will be addressed.

Spray modelling

To describe the dilution of the pilot fuel from start of injection until start of combustion the 1D spray modelling software DICOM is used. This tool is developed and validated by the CMT Motores Termicos institute from the Polytechnic University of Valencia. A detailed description can be found in [80] and [81]. The spray simulations described were performed by Alvaro Fogué Robles from CMT.

Based on the injection parameters an injection profile is constructed, conform the method described in [82]. Making use of this spray profile and a crank-angle-resolved pressure and density inside the cylinder, DICOM is able to calculate the evolution over time of the equivalence ratio distribution. This is based on the conservation of mass, species, and momentum within the spray. The integrated distribution for RCCI operation at the final time-step is shown in Figure 39.

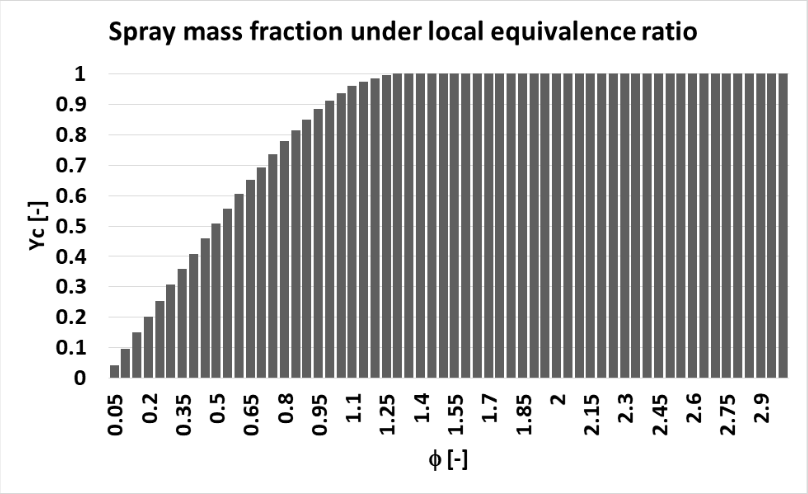

Figure 39 *Integrated distribution of RCCI mixture strength below each equivalence ratio at the final time step. Inflection point at $\phi = 1.25$ represents the richest mixture available.*

From this distribution profile, one can track over time what the richest available section is. For both RCCI and CDF operation this is shown in Figure 40.

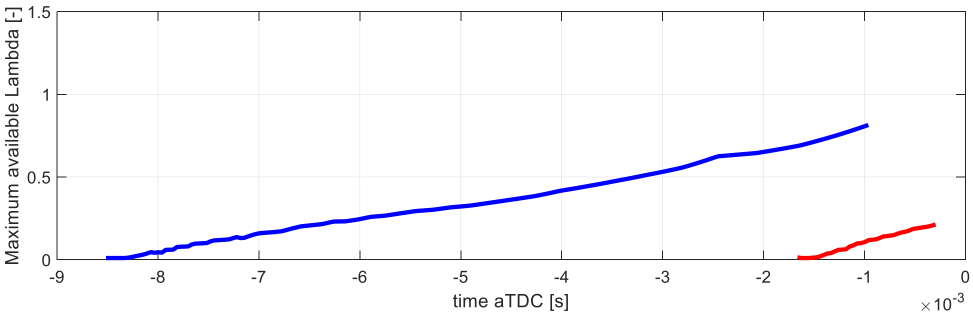

Figure 40 *Richest mixture available, simulated by 1D spray model.*

When comparing these curves with the assumed curves as shown in Figure 36, the most noticeable difference is that the even the RCCI case is still far from reaching its final mixture value. Apparently, the mixing process takes place with a much longer time constant than initially assumed.

Ignitability from kinetic scheme

In the initial description of the conceptual model, the area in which the air-fuel mixture would ignite was sketched. The parameters used to define this behaviour were lambda and temperature. In this section the ignitability will be determined, by performing detailed kinetic calculations. For this the scheme of Seidel [83] was used, since it contains the desired fuels, and includes a wide range of equivalence ratios. It contains 349 species and 3986 reactions. Loge Research [84] was used as software to evaluate the kinetic scheme. This was done in a constant volume reactor, with separate simulations for a range of initial conditions. These conditions are defined by temperature, pressure, equivalence ratio and mass ratio of low-reactive to total amount of fuel. The equivalence ratio ϕ is defined as 1/lambda. The mass ratio is defined conform Equation *(7)* for dual fuel operation.

$$Mass\ ratio = \frac{Mass_{CNG}}{Mass_{CNG} + Mass_{DIESEL}} \tag{7}$$

After estimating a realistic range that could occur during engine operation, and performing a sensitivity analysis, the parameter ranges shown in Table 9 were chosen to run the simulations. This resulted in 4928 individual simulations to run.

Table 9 *Range and steps for simulation conditions of the detailed kinetic scheme in a constant volume reactor.*

	Minimum	Maximum	Steps
P [bar]	10	80	8
T [K]	550	850	7
ϕ [-]	0.1	7.1	8
Mass ratio [-]	0.01	0.99	11

Although the simulation requires four separate inputs, it has to be realized that they are actually two sets of two coupled parameters. In-cylinder pressure and temperature cannot be separately changed for a given engine operating condition, and are both dependent on initial conditions and an engine crank position. Also the air-fuel ratio and gas-diesel mass ratio are coupled. Considering a constant volume with premixed air-gas mixture at a known equivalence ratio, the diesel fuel gradually mixing into this volume alters both the total air-fuel ratio and the gas-diesel mass ratio. Their relation can be described by equation *(8)*, based on the stoichiometry of both fuels, the equivalence ratio of the premixed natural gas, and the equivalence ratio at the actual state of diesel dilution.

$$Mass\ Ratio = \frac{1}{\frac{L_{stoichCNG}}{L_{stoichDIESEL}} * \left(\frac{\phi_{actual}}{\phi_{CNG}} - 1\right) + 1} \qquad (8)$$

For every simulated condition, the output of the simulation is the evolution of chemical species, heat release and reaction temperature in the volume. A small selection for an example condition is shown in Figure 41. The reaction simulation gives insight on how favourable a set of conditions is to achieve combustion, but it does not give a discrete indicator whether the conditions are ignitable or not, which was chosen as basis for the previously constructed ignitability island. What was chosen instead was the duration of the ignition delay, as indicator for the ignitability of a mixture under given conditions.

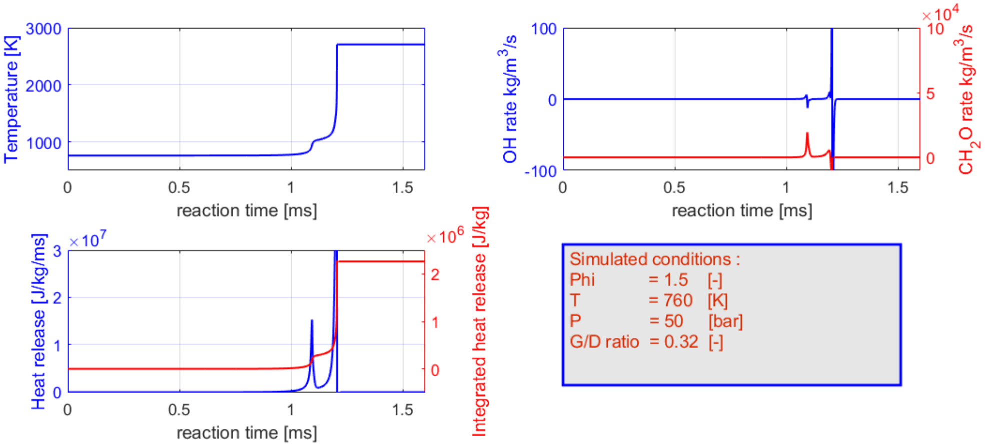

Figure 41 *Example of simulated chemical reaction in a constant volume reactor.*

Within the simulation tool multiple options are available to use as indicator for the onset of combustion, to calculate the ignition delay. An increase in the temperature can be used, but this requires a rather subjective choice of threshold value. The same goes for the first increase in heat release as indicator. A better indicator was found in the formation of formaldehyde, CH_2O, indicating the start of the cool flame phase. This was used to calculate the ignition delay. The result of the simulation was a 4-dimensional table, giving the ignition delay for all simulated parameters shown in Table 9.

In-cylinder conditions

The in-cylinder conditions are described by a crank-angle-resolved pressure and temperature in the cylinder. The pressure is measured with the cylinder pressure sensor. Since this pressure is one of the parameters used to describe whether combustion could take place, it is required that this pressure trace does not contain a pressure-increase caused by combustion itself. This could be done by using a motoring curve, but it was chosen not to use such measurement, because it was measured under different thermodynamic conditions. Instead, it was chosen to take a combustion cycle, and replace the measurement values from -60 till 0 CAD aTDC with a polytrope. The result can be seen in Figure 42. The shown temperature is also a calculated value, using the polytropic relation between cylinder volume and temperature. The calculation of this temperature trace starts with the temperature of the intake charge at BDC, which is measured in the intake port.

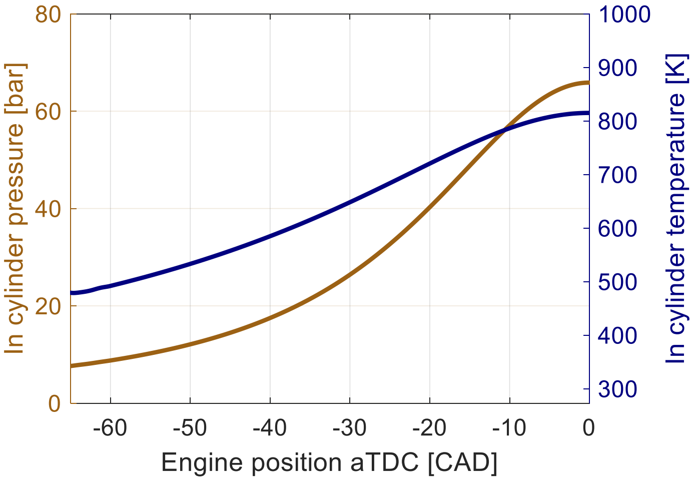

Figure 42 *Cylinder pressure and temperature curve for both operating conditions. Measured pressure till -60CAD, polytropic calculation from -60 till 0 CAD.*

Synthesis

Now that the dilution of the spray is known, the conditions in the cylinder are known, and a kinetic scheme is used to indicate how reactive the air / dual fuel mixture is under any possible condition, all this information can be combined, to come to the conceptual description. The graphical representation is shown in Figure 43. Here we see the dilution curve for both RCCI and CDF. They start as pure fuel at lambda 0, and gradually get leaner. The green ignitability island is based on the described kinetic simulation and represents which lambda values are ignitable for the in-cylinder pressure and temperature occurring at the engine position indicated on the x-axis. Ignitability is defined as conditions having an ignition delay of 0.5 ms or lower. For RCCI operation we can see that the dilution curve is hitting the ignitability on what could be called the lean side. Although richer than stoichiometric, it is the side of the island where the ignitability increases towards leaner mixtures, because of increasing temperature and pressure. This increase is required to ignite the mixture that is already significantly leaner than in case of the much later injected CDF case. In this representation it can also be recognized that an earlier RCCI injection would hit the ignitability island on a higher lambda value, and thus ignites later. A later RCCI injection would ignite earlier.

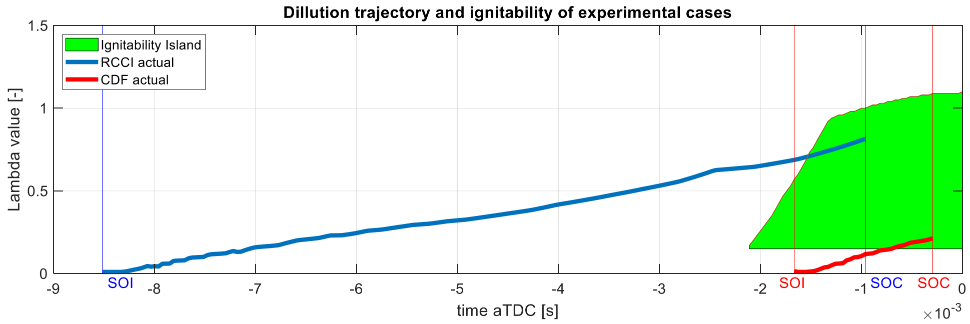

Figure 43 *Conceptual model to describe start of combustion for CDF and RCCI mode, based on actual simulations.*

The results on the rich side of the island, as applicable for the CDF case, do not show a clear limitation of ignitability caused by excessively rich mixture. Such limit is expected, as known from literature. Dec [25] mentions a required Phi in the range from 2 till 4, to come to realistic ignition delay, which is in line with Higgins [85], mentioning the occurring of ignition in a diesel spray at a local lambda value between 0.25 and 0.65. The richest simulation is shown as the lower limit of the ignitability island at lambda = 0.14 in Figure 43. The crossing of this limit of the CDF curve matches with an ignition delay of 0.5 ms. This part of the simulation does not give a clear indication of the detailed behaviour of ignition delay for CDF. From measurements as shown in Figure 24 it is known that the variation in ignition delay for CDF is relatively small, for that reason the observed limitation of ignition delay prediction on the rich side is acceptable. The principles from the initially assumed simplified conceptual model, as shown in Figure 37, match with what can be demonstrated with a more detailed model based on measurements, spray simulations and kinetic simulations.

4.3. Expanding on the conceptual model

Based on the conceptual model, a prediction can be done on what the influence of parameter variations will be, on the start of combustion. At first the results as shown in Figure 10 and Figure 34 will be explained making use of the conceptual model.

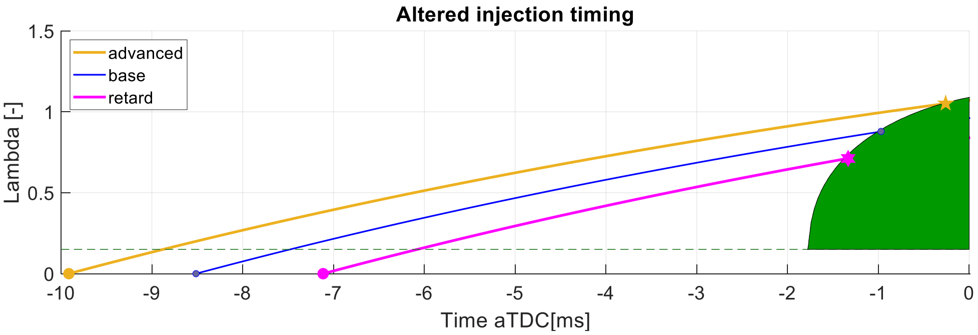

Figure 44 *Explaining the effect of RCCI pilot timing making use of the conceptual model.*

A variation of pilot injection timing is shown in Figure 44. The start of combustion is represented by the moment at which the dilution curve hits the ignitability island. This can explain the inverse relation between a change of injection timing and the resulting start of combustion in RCCI mode. An earlier injection creates more time for dilution. The resulting leaner mixture requires a higher temperature to start combustion. This higher temperature takes place later in the engine cycle. Also the opposite is shown for retarded pilot timing. This will hit the ignitability island at a richer value, which occurs earlier in time.

Not only the impact of injection timing, but also the effect of injection pressure can be simply explained making use of the conceptual model. In the work of Garcia [52] it was experimentally shown that an increase in rail pressure, in the range from 1300 till 2100 bar resulted in a later start of combustion in RCCI operation. From diesel and conventional dual fuel engines it is known that an increase in injection pressure results in a faster mixing process. This creates a shorter ignition delay, and thus an earlier start of combustion can be expected in these modes. The effect of pressure variation is depicted in Figure 45.

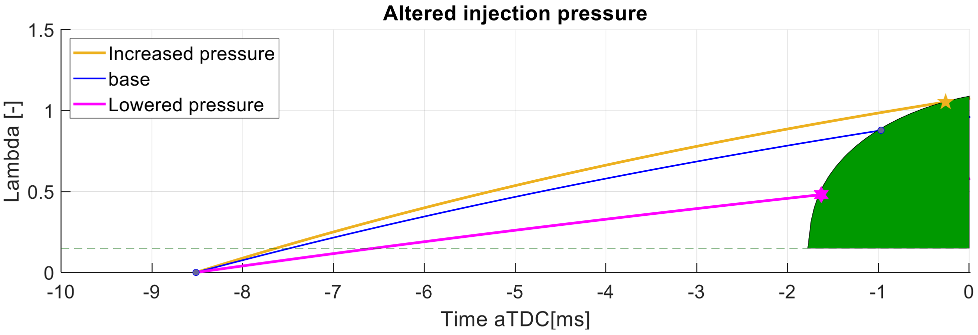

Figure 45 *Conceptual explanation of the influence of injection pressure variation on start of combustion timing in RCCI mode.*

A higher injection pressure creates a faster mixing process, which can be represented by a shorter time constant in the conceptual model. This creates a dilution curve that goes faster towards its end value. As a consequence the ignitability island will be hit at a leaner value, which takes place later in time. Injecting at a lower pressure slows down the dilution process, resulting in a richer mixture. Hitting the ignitability island at a richer value will take place earlier in time, as can be seen in the figure. This explains how a decrease in injection pressure advances the start of combustion in RCCI mode, while a higher pressure retards the combustion process.

Besides altering the dilution curve by changing ignition timing or pressure, one could also think of the influence of parameters that alter the shape and position of the ignitability island. This island was created making use of in-cylinder pressure, temperature, φ and fuel mass ratio, being the parameters of direct influence. Besides these parameters, also the combination of applied fuels and the presence of EGR will play a role. Instead of probing the impact of each individual parameter change, consideration will be made on what a desirable ignitability island would look like. This will be done from the perspective of controllability and predictability of the combustion process timing, with start of injection as desired control parameter. SOI is chosen, because it can be changed in a fast and precise manner.

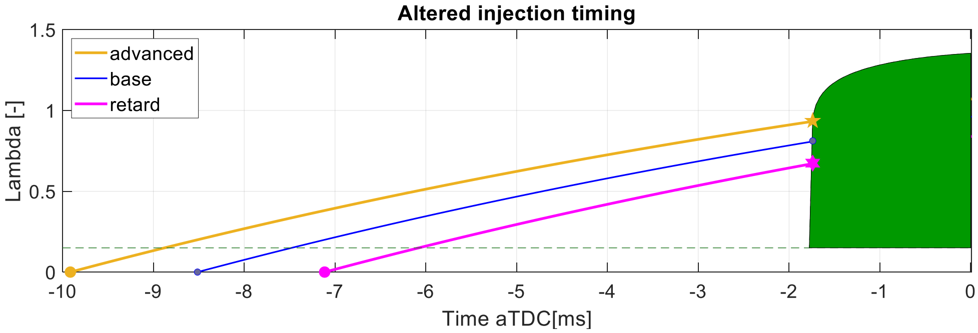

Figure 46 *Fictional case, with a vertical edged ignitability island.*

What would happen if the ignitability would only be dependent on in-cylinder temperature, and not on mixture dilution, is depicted in Figure 46 by a vertical edge of the ignitability island (representing the required temperature being reached). In this case the start of combustion could not be controlled anymore by adjusting the start of injection. On the other hand a too large dependency of ignitability on mixture dilution is also not very desirable, as depicted in Figure 47.

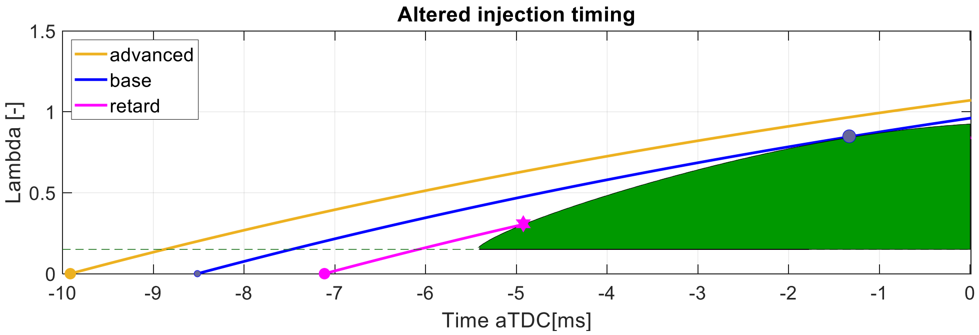

Figure 47 *Fictional case, where ignitability is very strongly related to mixture dilution.*

Here the injection timing can have a significant impact on the start of combustion. But the fact that the dilution curve develops almost parallel to the ignitability island, makes it very hard to predict when exactly combustion takes off. A small variation in parameter settings can have a large impact on the combustion phasing, which is highly undesirable.

From the two suggested representations of the ignitability island it can be concluded that a preferable RCCI configuration has a predictable and gradual relation between temperature, mixture dilution and ignitability. Making use of simulations of injection spray formation and reaction kinetics, a suitable parameter choice can be designed upfront. If the application allows, also a choice of fuels with favourable sensitivity [86] can be used to achieve the desired behaviour of the ignitability island.

5. Summary and conclusions

This chapter contains a brief summary of the main contributions and observations of the work covered in this thesis. Finally, suggestions for future work are given.

5.1. Contributions

Studies on dual fuel have been performed on a heavy-duty engine and a medium speed marine engine. The large bore engine was operated both in optical and in metal configuration. Combining the experimental observations with theoretical reasoning, a 1D spray model and chemical kinetic calculations, a conceptual model was deduced that can support control and understanding of conventional dual fuel and RCCI combustion. Specifically, the following contributions were made:

- It was discussed how a sustainable world needs renewable fuels. Most renewable fuels are high-octane fuels, and most energy-intense applications use diesel engines. The combination of such fuels and engines can be achieved through dual fuel operation.
- A synthesis was presented on the literature on modelling approaches for dual fuel combustion. A well matching non-predictive model can be created with a combination of multiple Wiebe functions. 3D CFD models using a detailed kinetic scheme can give a good prediction of heat release and emissions, but come at high computational costs. Fast running models with strong predictive capacities would be very useful but are scarce.
- On a dual fuel truck engine, a problem with cylinder to cylinder variations was discovered. The cause for this was found through gas dynamic simulations of the engine. The base diesel engine was converted to dual fuel, making use of multipoint gas injection. The gas is injected into the intake port. Requiring a gas injection that takes longer than the intake stroke, and the absence of a significant intake runner length, resulted in an exchange of air and premixed fuel through the intake manifold. The cylinder closest to the entrance of the manifold thus ended up leaning out because of backflow, while the cylinder furthest away enriched by collecting this fuel-containing flow.

- Dual fuel can be implemented as Conventional Dual Fuel or RCCI. The main parameter that can be modulated to achieve a specific mode is the SOI timing. RCCI uses a much earlier pilot injection timing. In an optical campaign on the medium speed marine engine it was shown that this results in a stronger dilution of the pilot fuel. By high-speed recording of natural luminosity it was observed that combustion takes place at a lower intensity, and starts at a location not related to the shape of the diesel jet. It was expected that this observed lower intensity of combustion results in lower NO_x emissions and higher efficiency. This was proven in a metal campaign on the same engine.
- In an experimental campaign on the metal medium speed marine engine the operating point preferred for low emissions and high efficiency was found in RCCI mode, close to the transition towards CDF. The best results were achieved with a global lambda around 2, as a compromise between emissions, efficiency, and knock-safety.
- In CDF operation, an earlier SOI results in an earlier start of combustion, while in RCCI mode it gives a later start of combustion. For control purposes this opposition creates a complexity.
- For control purposes, and to create insight in the phenomenon, a conceptual model was developed. Based on ignition delay times calculated with a kinetic scheme, an ignitability island was defined in the lambda/crank angle domain. When a mixture reaches the temperature and lambda boundaries of this island, combustion will start. The dilution trajectory of the pilot diesel fuel was described by a 1D spray model.

The developed conceptual model explains how in CDF mode the combustion starts when the conditions of the spray hit the ignitability island from the rich side. In RCCI mode combustion starts when the diluted fuel conditions enter the ignitability island from the lean side. The model can be used to explain the influence of control parameters on the start of combustion in a quantitative and qualitative way.

5.2. Outlook

A wide range of activities was employed during this PhD work to advance our understanding of dual fuel combustion. Most attention and effort went into the optical campaign and the conceptual model. More value can be added to both topics by expanding them. The following activities are suggested as worthwhile extensions of this work:

- The optical campaign was strongly restricted by problems with oil contamination on the optical components. All solutions tried until now were aimed at preventing and venting oil vapour. During separate high-speed recordings, it was found out that the oil was mainly entering the optical area of the engine in the form of droplets instead of vapour. This requires a different approach for this to be prevented and mitigated. Putting additional spring pressure on the lower piston rings to compensate for the lack of combustion pressure is seen as the most promising solution.
- The recording of dual fuel combustion showed a wide range of light intensity coming from different types of combustion. The camera sensitivity was chosen to prevent saturation by luminosity coming from rich flame kernels. This limits the capability to record the faint light of lean methane combustion. It is suggested to apply an optical filter, having the wavelength of the rich glowing kernels. This allows an increase in camera sensitivity, so more insight on the lean combustion can be created. This should be a first step, before moving into active, laser induced, optic technologies on this engine.
- The conceptual model was tested on its prediction of the start of combustion within a limited range of conditions. Expanding the range of conditions, such as engine load, fuel ratios and temperature, is suggested. Also the expansion towards other high-reactivity fuels is seen as beneficial for further development of RCCI and CDF engines.
- The model was set up in a conceptual way, to provide principal understanding without distraction by details. As a consequence, the model comes at low computational cost. This makes it suitable to be applied as a control-oriented model. The achievable precision and required effort have to be further explored. Especially the parametrization of dilution curves has to be investigated.

References

[1] K. Steentjes *et al.*, *European Perceptions of Climate Change (EPCC): Topline findings of a survey conducted in four European countries in 2016*. Cardiff: Cardiff University, 2017.

[2] P. Forster *et al.*, “Changes in Atmospheric Constituents and in Radiative Forcing Chapter 2,” in *Climate Change 2007: The Physical Science Basis. Contribution of Working Group I to the Fourth Assessment Report of the Intergovernmental Panel on Climate Change.*, United Kingdom: Cambridge University Press, 2007.

[3] R. K. Pachauri, L. Mayer, and Intergovernmental Panel on Climate Change, Eds., *Climate change 2014: synthesis report*. Geneva, Switzerland: Intergovernmental Panel on Climate Change, 2015.

[4] S. Dale, “BP statistical review of world energy,” *BP Plc, London, United Kingdom*, pp. 14–16, 2021.

[5] W. CAIT, “World Resources Institute, Climate Analysis Indicators Tool (WRI, CAIT),” *WRI CAIT, Washington, DC*, 2012.

[6] T. A. Hansen, “Stranded assets and reduced profits: Analyzing the economic underpinnings of the fossil fuel industry’s resistance to climate stabilization,” *Renewable and Sustainable Energy Reviews*, vol. 158, p. 112144, Apr. 2022, doi: 10.1016/j.rser.2022.112144.

[7] *REGULATION (EU) 2021/1119 OF THE EUROPEAN PARLIAMENT AND OF THE COUNCIL of 30 June 2021 establishing the framework for achieving climate neutrality and amending Regulations (EC) No 401/2009 and (EU) 2018/1999 (‘European Climate Law’)*. 2021. doi: 10.5040/9781782258674.

[8] IEA, “World gross electricity production by source, 2019 – Charts – Data & Statistics,” Paris, 2019. Accessed: Feb. 21, 2022. [Online]. Available: https://www.iea.org/data-and-statistics/charts/world-gross-electricity-production-by-source-2019

[9] S. Verhelst, “Future vehicles will be driven by electricity, but not as you think [Point of View],” *Proc. IEEE*, vol. 102, no. 10, pp. 1399–1403, Oct. 2014, doi: 10.1109/JPROC.2014.2351191.

[10] C. Panoutsou *et al.*, “Advanced biofuels to decarbonise European transport by 2030: Markets, challenges, and policies that impact their successful market uptake,” *Energy Strategy Reviews*, vol. 34, p. 100633, Mar. 2021, doi: 10.1016/j.esr.2021.100633.

[11] D. M. Wall, S. McDonagh, and J. D. Murphy, “Cascading biomethane energy systems for sustainable green gas production in a circular economy,”

Bioresource Technology, vol. 243, pp. 1207–1215, Nov. 2017, doi: 10.1016/j.biortech.2017.07.115.

[12] Y. Bicer and I. Dincer, "Clean fuel options with hydrogen for sea transportation: A life cycle approach," *International Journal of Hydrogen Energy*, vol. 43, no. 2, pp. 1179–1193, Jan. 2018, doi: 10.1016/j.ijhydene.2017.10.157.

[13] J. Hansson, S. Brynolf, E. Fridell, and M. Lehtveer, "The Potential Role of Ammonia as Marine Fuel—Based on Energy Systems Modeling and Multi-Criteria Decision Analysis," *Sustainability*, vol. 12, no. 8, p. 3265, Apr. 2020, doi: 10.3390/su12083265.

[14] J. Dierickx *et al.*, "Strategies for introducing methanol as an alternative fuel for shipping," in *7th Transport Research Arena TRA 2018 (TRA 2018)*, 2018, pp. 1–10. doi: 10.5281/ZENODO.1456425.

[15] I. Fraunhofer, "PTX-ATLAS: Weltweite potenziale für die erzeugung von grünem wasserstoff und klimaneutralen synthetischen kraft- und brennstoffen.," *https://maps. iee. fraunhofer. de/ptx-atlas*, p. 28, 2021.

[16] A. Tremel, *Electricity-based Fuels*. Cham: Springer International Publishing, 2018. doi: 10.1007/978-3-319-72459-1.

[17] H. S. Eggleston *et al.*, "2006 IPCC guidelines for national greenhouse gas inventories," 2006. http://www.ipcc-nggip.iges.or.jp/public/2006gl/index.htm

[18] K. MacKay *et al.*, "Methane emissions from upstream oil and gas production in Canada are underestimated," *Sci Rep*, vol. 11, no. 1, p. 8041, Dec. 2021, doi: 10.1038/s41598-021-87610-3.

[19] U. Albrecht, P. Schmidt, W. Weindorf, R. Wurster, and W. Zittel, "Zukünftige Kraftstoffe für Verbrennungsmotoren und Gasturbinen," p. 209.

[20] J. L. Jiménez, J. Valido, and N. Molden, "The drivers behind differences between official and actual vehicle efficiency and CO2 emissions," *Transportation Research Part D: Transport and Environment*, vol. 67, pp. 628–641, Feb. 2019, doi: 10.1016/j.trd.2019.01.016.

[21] J. C. Mankins, "Technology readiness levels," *NASA White Paper*, 1995.

[22] G. P. Merker, C. Schwarz, and R. Teichmann, Eds., *Combustion engines development: mixture formation, combustion, emissions and simulation*. Heidelberg: Springer, 2012.

[23] John B. Heywood, *Internal Combustion Engine Fundamentals, Second Edition*, 2nd edition. New York: McGraw-Hill Education, 2018.

[24] S. S. Shy, C. C. Liu, J. Y. Lin, L. L. Chen, A. N. Lipatnikov, and S. I. Yang, "Correlations of high-pressure lean methane and syngas turbulent burning velocities: Effects of turbulent Reynolds, Damköhler, and Karlovitz numbers," *Proceedings of the Combustion Institute*, vol. 35, no. 2, pp. 1509–1516, 2015, doi: 10.1016/j.proci.2014.07.026.

[25] J. E. Dec, "Advanced compression-ignition engines—understanding the in-cylinder processes," *Proceedings of the Combustion Institute*, vol. 32, no. 2, pp. 2727–2742, 2009, doi: 10.1016/j.proci.2008.08.008.

[26] P. M. Najt and D. E. Foster, "Compression-Ignited Homogeneous Charge Combustion," Feb. 1983. doi: https://doi.org/10.4271/830264.

[27] R. K. Maurya, *Characteristics and Control of Low Temperature Combustion Engines*. Cham: Springer International Publishing, 2018. doi: 10.1007/978-3-319-68508-3.

[28] G. Kalghatgi, “Petroleum-Based Fuels for Transport,” *Journal of Automobile Safety and Energy Saving*, vol. 6, no. 1, p. 16, 2015, doi: 10.3969/j.issn.1674-8484.2015.01.001.

[29] J. Bosklopper *et al.*, “Experimental study on a retrofitted marine size spark-ignition engine running on port-injected 100% methanol,” presented at the INEC, 2020.

[30] J. Liu and C. E. Dumitrescu, “Lean-Burn Characteristics of a Heavy-Duty Diesel Engine Retrofitted to Natural-Gas Spark Ignition,” *Journal of Engineering for Gas Turbines and Power*, vol. 141, no. 7, p. 071013, Jul. 2019, doi: 10.1115/1.4042501.

[31] D. Janecek, D. Rothamer, and J. Ghandhi, “Investigation of cetane number and octane number correlation under homogenous-charge compression-ignition engine operation,” *Proceedings of the Combustion Institute*, vol. 36, no. 3, pp. 3651–3657, 2017, doi: 10.1016/j.proci.2016.08.015.

[32] P. T. Aakko-Saksa *et al.*, “Renewable Methanol with Ignition Improver Additive for Diesel Engines,” *Energy Fuels*, vol. 34, no. 1, pp. 379–388, Jan. 2020, doi: 10.1021/acs.energyfuels.9b02654.

[33] G. A. Karim, *Dual-fuel diesel engines (1st ed.)*. CRC Press, 2015.

[34] F. L. Dryer, “Chemical kinetic and combustion characteristics of transportation fuels,” *Proceedings of the Combustion Institute*, vol. 35, no. 1, pp. 117–144, 2015, doi: 10.1016/j.proci.2014.09.008.

[35] S. Grzesiak, “Alternative Propulsion Plants for Modern LNG Carriers,” *New Trends in Production Engineering*, vol. 1, no. 1, pp. 399–407, Oct. 2018, doi: 10.2478/ntpe-2018-0050.

[36] M. E. J. Stettler, W. J. B. Midgley, J. J. Swanson, D. Cebon, and A. M. Boies, “Greenhouse Gas and Noxious Emissions from Dual Fuel Diesel and Natural Gas Heavy Goods Vehicles,” *Environ. Sci. Technol.*, vol. 50, no. 4, pp. 2018–2026, Feb. 2016, doi: 10.1021/acs.est.5b04240.

[37] R. D. Reitz and G. Duraisamy, “Review of high efficiency and clean reactivity controlled compression ignition (RCCI) combustion in internal combustion engines,” *Progress in Energy and Combustion Science*, vol. 46, pp. 12–71, Feb. 2015, doi: 10.1016/j.pecs.2014.05.003.

[38] H. Liu *et al.*, “Effects of injection strategies on low-speed marine engines using the dual fuel of high-pressure direct-injection natural gas and diesel,” *Energy Science & Engineering*, vol. 7, no. 5, pp. 1994–2010, 2019, doi: https://doi.org/10.1002/ese3.406.

[39] D. Mumford, D. Goudie, and J. Saunders, “Potential and Challenges of HPDI,” May 2017, pp. 2017-01–1928. doi: 10.4271/2017-01-1928.

[40] Z. Wang, H. Liu, and R. D. Reitz, “Knocking combustion in spark-ignition engines,” *Progress in Energy and Combustion Science*, vol. 61, pp. 78–112, Jul. 2017, doi: 10.1016/j.pecs.2017.03.004.

[41] M. S. Lounici, M. A. Benbellil, K. Loubar, D. C. Niculescu, and M. Tazerout, "Knock characterization and development of a new knock indicator for dual-fuel engines," *Energy*, vol. 141, pp. 2351–2361, Dec. 2017, doi: 10.1016/j.energy.2017.11.138.

[42] R. P. Verbeek and M. M. J. F. Verbeek, "LNG for trucks and ships: fact analysis Review of pollutant and GHG emissions Final," TNO 2014 R11668, 2015. [Online]. Available: http://resolver.tudelft.nl/uuid:63cff506-a4da-47ef-a9e4-27da8b04c5e6

[43] CIMAC WG17 - Gas Engines, "CIMAC Position Paper WG17 Methane and Formaldehyde Emissions." Apr. 2014.

[44] F. Königsson, J. Kuyper, P. Stalhammar, and H.-E. Angstrom, "The Influence of Crevices on Hydrocarbon Emissions from a Diesel-Methane Dual Fuel Engine," *SAE International Journal of Engines*, vol. 6, no. 2, pp. 751–765, Apr. 2013, doi: 10.4271/2013-01-0848.

[45] W. Kim, C. Park, and C. Bae, "Characterization of combustion process and emissions in a natural gas/diesel dual-fuel compression-ignition engine," *Fuel*, vol. 291, p. 120043, May 2021, doi: 10.1016/j.fuel.2020.120043.

[46] Y. A. Zeldovich, D. Frank-Kamenetskii, and P. Sadovnikov, *Oxidation of nitrogen in combustion*. Publishing House of the Acad of Sciences of USSR, 1947.

[47] G. Belgiorno, G. Di Blasio, and C. Beatrice, "Parametric study and optimization of the main engine calibration parameters and compression ratio of a methane-diesel dual fuel engine," *Fuel*, vol. 222, pp. 821–840, Jun. 2018, doi: 10.1016/j.fuel.2018.02.038.

[48] M. Kassa, C. Hall, A. Ickes, and T. Wallner, "Cylinder-to-Cylinder Variations in Power Production in a Dual Fuel Internal Combustion Engine Leveraging Late Intake Valve Closings," *SAE International Journal of Engines*, vol. 9, no. 2, Apr. 2016, doi: 10.4271/2016-01-0776.

[49] J. A. Caton, "Combustion phasing for maximum efficiency for conventional and high efficiency engines," *Energy Conversion and Management*, vol. 77, pp. 564–576, Jan. 2014, doi: 10.1016/j.enconman.2013.09.060.

[50] E. Doosje, F. Willems, and R. Baert, "Experimental Demonstration of RCCI in Heavy-Duty Engines using Diesel and Natural Gas," Apr. 2014, pp. 2014-01–1318. doi: 10.4271/2014-01-1318.

[51] A. Yousefi, M. Birouk, and H. Guo, "An experimental and numerical study of the effect of diesel injection timing on natural gas/diesel dual-fuel combustion at low load," *Fuel*, vol. 203, pp. 642–657, Sep. 2017, doi: 10.1016/j.fuel.2017.05.009.

[52] P. García Valladolid, P. Tunestål, J. Monsalve-Serrano, A. García, and J. Hyvönen, "Impact of diesel pilot distribution on the ignition process of a dual fuel medium speed marine engine," *Energy Conversion and Management*, vol. 149, pp. 192–205, Oct. 2017, doi: 10.1016/j.enconman.2017.07.023.

[53] C. Bekdemir, R. Baert, F. Willems, and B. Somers, "Towards Control-Oriented Modeling of Natural Gas-Diesel RCCI Combustion," Apr. 2015, pp. 2015-01–1745. doi: 10.4271/2015-01-1745.

[54] J. Martin, A. Boehman, R. Topkar, S. Chopra, U. Subramaniam, and H. Chen, "Intermediate Combustion Modes between Conventional Diesel and RCCI," *SAE International Journal of Engines*, vol. 11, no. 6, pp. 835–860, Apr. 2018, doi: https://doi.org/10.4271/2018-01-0249.

[55] J. Martin and A. Boehman, "Mapping the combustion modes of a dual-fuel compression ignition engine," *International Journal of Engine Research*, p. 146808742110183, May 2021, doi: 10.1177/14680874211018376.

[56] M. Merts, B. Veenhuizen, M. Lundgren, and S. Verhelst, "Experimental optimization of a medium speed Dual Fuel engine towards RCCI operation.," presented at the Thiesel 2022, Valencia, Spain, Sep. 2022.

[57] M. Nazemi and M. Shahbakhti, "Modeling and analysis of fuel injection parameters for combustion and performance of an RCCI engine," *Applied Energy*, vol. 165, pp. 135–150, Mar. 2016, doi: 10.1016/j.apenergy.2015.11.093.

[58] L. Eder, M. Ban, G. Pirker, M. Vujanovic, P. Priesching, and A. Wimmer, "Development and Validation of 3D-CFD Injection and Combustion Models for Dual Fuel Combustion in Diesel Ignited Large Gas Engines," *Energies*, vol. 11, no. 3, p. 643, Mar. 2018, doi: 10.3390/en11030643.

[59] P. Napolitano, V. Fraioli, C. Guido, and C. Beatrice, "Assessment of optimized calibrations in minimizing GHG emissions from a Dual Fuel NG/Diesel automotive engine," *Fuel*, vol. 258, p. 115997, Dec. 2019, doi: 10.1016/j.fuel.2019.115997.

[60] Y. Wang, M. Yao, T. Li, W. Zhang, and Z. Zheng, "A parametric study for enabling reactivity controlled compression ignition (RCCI) operation in diesel engines at various engine loads," *Applied Energy*, vol. 175, pp. 389–402, Aug. 2016, doi: 10.1016/j.apenergy.2016.04.095.

[61] S. Grasreiner, J. Neumann, M. Wensing, and C. Hasse, "Model-based virtual engine calibration with the help of phenomenological methods for spark-ignited engines," *Applied Thermal Engineering*, vol. 121, pp. 190–199, Jul. 2017, doi: 10.1016/j.applthermaleng.2017.04.046.

[62] M. Merts and S. Verhelst, "Literature Review on Dual-Fuel Combustion Modelling," Sep. 2019, pp. 2019-24–0120. doi: 10.4271/2019-24-0120.

[63] Arrhenius Svante, "Über die Dissociationswärme und den Einfluss der Temperatur auf den Dissociationsgrad der Elektrolyte," *zpch*, vol. 4U, no. 1, p. 96, 1889, doi: 10.1515/zpch-1889-0408.

[64] D. N. Assanis, Z. S. Filipi, S. B. Fiveland, and M. Syrimis, "A Predictive Ignition Delay Correlation Under Steady-State and Transient Operation of a Direct Injection Diesel Engine," *Journal of Engineering for Gas Turbines and Power*, vol. 125, no. 2, p. 450, 2003, doi: 10.1115/1.1563238.

[65] "LNG PILOTS," *CMSX*. https://lngpilots.eu/?lang=DE (accessed Feb. 26, 2022).

[66] M. Merts, Pet, Quintin, and Mesman, Peter, "A comparison of dual fuel engine simulation and dyno testing," in *EAEC 2017*, Madrid, 2017, vol. 15th.

[67] M. Merts, Q. Pet, P. Mesman, and S. Verhelst, “Cylinder to Cylinder Variation Related to Gas Injection Timing on a Dual-Fuel Engine,” Detroit, Nov. 2019, vol. 2019.

[68] P. Garcia, “Experimental Investigations on Natural Gas-Diesel Dual Fuel Combustion,” PhD Thesis, Department of Energy Sciences, Lund University, 2018.

[69] M. Merts, S. Derafshzan, J. Hyvönen, M. Richter, M. Lundgren, and S. Verhelst, “An optical investigation of dual fuel and RCCI pilot ignition in a medium speed engine,” *Fuel Communications*, vol. 9, p. 100037, Dec. 2021, doi: 10.1016/j.jfueco.2021.100037.

[70] F. W. Bowditch, “A New Tool for Combustion Research A Quartz Piston Engine,” 1961. doi: 10.4271/610002.

[71] M. Herranen, K. Huhtala, M. Vilenius, and G. Liljenfeldt, “The Electro-Hydraulic Valve Actuation (EHVA) for Medium Speed Diesel Engines - Development Steps with Simulations and Measurements,” Apr. 2007, pp. 2007-01–1289. doi: 10.4271/2007-01-1289.

[72] P. Tunestål, “Self tuning cylinder pressure based heat release computation,” *IFAC Proceedings Volumes*, vol. 40, no. 10, pp. 183–189, 2007, doi: 10.3182/20070820-3-US-2918.00026.

[73] R. S. Jupudi *et al.*, “Application of High Performance Computing for Simulating Cycle-to-Cycle Variation in Dual-Fuel Combustion Engines,” Apr. 2016, pp. 2016-01–0798. doi: 10.4271/2016-01-0798.

[74] R. D. Atkins, *An Introduction to Engine Testing and Development*. Warrendale, PA: SAE International, 2009. doi: 10.4271/R-344.

[75] M. Merts, “Conceptual model for the start of combustion timing in the range from RCCI to conventional dual fuel.,” presented at the SAE WCX 2022, Detroit, Apr. 2022.

[76] S. Sarıkoç, “Fuels of the Diesel-Gasoline Engines and Their Properties,” *Diesel and Gasoline Engines*, p. 31, 2020, doi: 10.5772/intechopen.75259.

[77] G. Stiesch, *Modeling Engine Spray and Combustion Processes*. Berlin, Heidelberg: Springer Berlin Heidelberg, 2003. doi: 10.1007/978-3-662-08790-9.

[78] N. S. Nise, *Control systems engineering /*, 6th ed. Hoboken, NJ : Wiley, 2011.

[79] Isaac Newton, “VII. Scala graduum caloris,” *Philosophical Transactions of the Royal Society of London*, vol. 22, no. 270, pp. 824–829, Apr. 1701, doi: 10.1098/rstl.1700.0082.

[80] J. M. Desantes, R. Payri, J. M. Pastor, and J. Gimeno, “Experimental characterization of internal nozzle flow and diesel spray behavior. Part I: Nonevaporative conditions,” *Atomization and sprays*, vol. 15, no. 5, 2005.

[81] J. M. Desantes, J. V. Pastor, R. Payri, and J. M. Pastor, “Experimental characterization of internal nozzle flow and diesel spray behavior. Part II: evaporative conditions,” *Atomization and sprays*, vol. 15, no. 5, 2005.

[82] L. Xu, X.-S. Bai, M. Jia, Y. Qian, X. Qiao, and X. Lu, “Experimental and modeling study of liquid fuel injection and combustion in diesel engines with a

common rail injection system," *Applied Energy*, vol. 230, pp. 287–304, Nov. 2018, doi: 10.1016/j.apenergy.2018.08.104.

[83] L. Seidel, K. Moshammer, X. Wang, T. Zeuch, K. Kohse-Höinghaus, and F. Mauss, "Comprehensive kinetic modeling and experimental study of a fuel-rich, premixed n-heptane flame," *Combustion and Flame*, vol. 162, no. 5, pp. 2045–2058, May 2015, doi: 10.1016/j.combustflame.2015.01.002.

[84] "Products – LOGEsoft." https://logesoft.com/loge-software/

[85] D. L. Siebers and B. Higgins, "Flame Lift-Off on Direct-Injection Diesel Sprays Under Quiescent Conditions," Mar. 2001, pp. 2001-01–0530. doi: 10.4271/2001-01-0530.

[86] N. Alemahdi, A. García, E. Boufaim, G. Aferiat, and M. Tunér, "Development of an empirical test method to quantify the ϕ-sensitivity of liquid fuels," *Energy Conversion and Management*, vol. 254, p. 115257, 2022, doi: https://doi.org/10.1016/j.enconman.2022.115257.

Scientific publications

Paper I Cylinder to Cylinder Variation Related to Gas Injection Timing on a Dual-Fuel Engine

M. Merts, Q. Pet, P. Mesman, and S. Verhelst
Published: SAE Technical Paper, 2019-01-1162

This paper presents an experimental and simulation study on the cylinder to cylinder variations occurring in a heavy duty engine converted to dual fuel operation. It investigates how the variations are caused by an unequal distribution of the injected fuel over the six cylinders. It is found how this is related to injection timing in an MPI setup and air flow to runners and the intake manifold plenum.

The study was designed by me. I prepared the test setup and performed the measurements together with a Quintin Pet. I did the analysis of the experimental results and combined it with simulation results performed by Quintin Pet. I wrote the draft paper, and processed the peer-reviews. This paper was presented by me at SAE World Congress in Detroit, in April 2019.

Paper II Literature Review on Dual-Fuel Combustion Modelling

M. Merts and S. Verhelst
Published: SAE Technical Paper 2019-24-0120

This paper gives an overview of the state of art on dual fuel combustion modelling. It is explained how the engine process can be divided in separate steps, and which approaches are feasible to simulate the individual steps. The approaches are assessed on computational costs and their predictive capabilities.

I did the categorization of the dual-fuel process into its separate steps. Based on these steps I did the search and selection of relevant literature, performed a synthesis, and wrote the paper. This paper was presented by me at SAENA ICE2019 on Capri, in September 2019.

Paper III An optical investigation of dual fuel and RCCI pilot ignition in a medium speed engine

M. Merts, S. Derafshzan, J. Hyvönen, M. Richter, M. Lundgren, and S. Verhelst
Published: Fuel Communications, vol. 9, p. 100037, 2021

This paper covers the differences between early and late pilot injection timing, observed in an optical campaign. The medium speed engine experiments show how a strong dilution of the pilot injection, caused by early injection, results in a longer injection delay and a start of combustion more outwards in the combustion chamber. Late injection shows an ignition of pilot fuel concentrated around the fuel jets.

For the optical campaign I made the engine setup ready for testing. Together with a co-author I performed the optical measurements. I did the analysis of optical and measurement data, and organized the sessions to discuss the results. Based on these outcomes I wrote the paper and processed the feedback on it.

Paper IV Conceptual model for the start of combustion timing in the range from RCCI to conventional dual fuel

M. Merts, A. Fogué Robles, J. Monsalve-Serrano, A. Garcia, M. Lundgren, and S. Verhelst
Published: SAE Technical Paper 2022-01-0468

This paper presents a conceptual model that explains the difference in the relation between start of injection and start of combustion for CDF and RCCI operation. In the engine process an area is sketched where fuel is able to ignite. The model can explain the observed behaviour by showing how this so called ignitability island is approached from the rich side in CDF mode, and from the lean side in RCCI mode. A verification is done making use of spray and kinetic simulations.

The conceptual model was designed by me. I created the results from my kinetic simulations with the spray simulations of the co-author. Based on the concept and the simulations I wrote the paper, and corrected it based on the peer review. This paper was presented by me at SAE World Congress in Detroit, in April 2022.

Paper V Experimental optimization of a medium speed Dual Fuel engine towards RCCI operation

M. Merts, J. Hyvönen, B. Veenhuizen, M. Lundgren, and S. Verhelst,
Paper accepted for publication at Thiesel 2022, Valencia, Spain

In this paper an experimental campaign the Wärtsilä W20DF dual fuel engine is reported, to give insight in the combustion process and find optima for a future optical campaign. At medium load the engine was tested over a range of pilot timings, to achieve the best possible emissions, efficiency, and stability. It shows how the relation between pilot timing and start of combustion inverses between CDF and RCCI mode.

For this paper I structured the experimental campaign and performed the engine measurements. I post-processed the results, analysed them, and wrote the paper about it. To be presented at Thiesel 2022 in Valencia, in September 2022.

Printed by Media-Tryck, Lund 2022 NORDIC SWAN ECOLABEL 3041 0903

LUND
UNIVERSITY

Division of Combustion Engines
Department of Energy Sciences

Lund University, Faculty of Engineering
ISBN 978-91-8039-258-7
LUTMDN/TMHP-22/1168-SE
ISSN: 0282-1990

9 789180 392587